Ultrawideband IEEE802.15.4a Cognitive Localization Methods for the 5G Environment

AKEEM ADERIBIGBE ADEBOMEHIN

A thesis submitted for the

degree of Doctor of Philosophy

Department of Computing and Electronic Systems Engineering

University of Essex

Date of submission: July 2017

DEDICATION

This work is dedicated to the whole of humanity;

Indeed all the peace loving people in the quest to make the world a better place for all.

Abstract

This thesis focuses on utilization of ultra-wideband (UWB) technology for cognitive localization in the fifth generation (5G) wireless environment that envisages seamless global connection of ubiquitous devices. This suggests the need for cognitive high-definition location-aware networks and devices devoid of the drawbacks of current positioning systems.

The thesis therefore models a cognitive UWB IEEE802.15.4a LOS sufficient technique (ULOSTECH); with a framework for optimal UWB localization channel that utilizes combined cluster decay rate and mistiming probability method that achieves over 90% realizations. Moreover, the ULOSTECH NLOS mitigation method achieves about 0.257 improvement ratio on the accuracy of cellular network localization methods. An impulse radio (IR)-UWB device-to-device (D2D) WWAN is further proposed with channel time partitioned into discrete micro-channel slots (DMCS) along with a cluster formation scheme that achieves above 350Mbps network throughput in comparison with 100Mbps cellular and 250Mbps wi-fi standards respectively. Additionally, the cluster cooperation method achieves multi-user access rate of over 485% above cellular network standards.

Also proposed is the ULOSTECH D2D-propagation-based combined localization and communication scheme (UD-CLOCS) for ultra-dense networks. This utilizes cooperative D2D data hoping localization technique that achieves a mean distance error of 0.54 – 3.32 shorter than trilateration and multi-dimensional scaling (MDS) methods respectively. Finally, the thesis proposes an overall IR-UWB network layout for the 5G setting. This comprises an all-IP D2D UWB network overlay of concurrent multi-layered super-core architecture (5G-COMUSA). This is significant as the proposed solutions could serve to decongest the licensed spectrums in the 5G environment.

ACKNOWLEDGEMENTS

I wish to acknowledge the support of my Supervisor, Professor Stuart Walker for his guidance throughout the period of my research. This also goes for other support staff in my Department as well as the University.

May I also acknowledge the unwavering support of my family during this period.

Contents

CHAPTER TWO:- ***LITERATURE REVIEW*** *11-55*

LIST OF FIGURES

LIST OF TABLES

LIST OF SIMULATION EXPERIMENTS

LIST OF ACRONYMS

5G	Fifth Generation
5G-COMUSA	5G Concurrent Overlay Multilayered Supercore Architecture
AMTS	Advanced Mobile Telephone System
ARS	Address Resolution System
BEFY	Best Experience Follows You
BN	Base Node
BRAN	Broadband Radio Access
C2C	Car to Car Communications
CDMA	Code Division Multiple Access
CH	Cluster Head
CLOUDNET	Cloud Networking
CNM	Cluster Normal Member
COMP	Coordinated Multipoint
C-RAN	Cloud Radio Access Network
CS	Circuit Switch
CSMA	Carrier Sense Multiple Access

CSS	Chirp Speed Spectrum
DHT	Distributed Hash Table
DOA	Direction Of Arrival
DS	Direct Sequence
DVB	Digital Voice and Video
DWMDS	Distributed Weighted Multi – Dimensional Scaling
E2E	End To End
EDGE	Enhanced Digital GSM Evolution
EPRC	Excellent Real – Time and Reliable Connections
FCC	Federal Communications Commission
FDMA	Frequency Division Multiple Access
GPRS	General Packet Radio System
GPS	Global Positioning System
GSIC / MP	Generalized Successive Interference Cancellation Matching Pursuits
GSM	Global System for Mobile
HETNA	Hierarchical Ethernet Transport Network Architecture
ICT	Information and Communication Technology
IEEE	Institute of Electrical and Electronics Engineers

IMTS	Improved Mobile Telephone System
INS	Inertial Navigator System
IoT	Internet of Things
IR	Impulse Radio
IR-UWB	Impulse Radio UWB
ITU	International Telecommunication Union
IV	Intent Value
KPI	Key Performance Indicators
L2	Layer 2
L3	Layer3
LLS	Least Likelyhood Square
LOS	Line of Sight
LPS	Local Positioning System
LTE	Long Term Evolution
M2M	Machine to Machine
MAC	Media Access Control
MB-OFDM	Multi-Band Orthogonal Frequency Division Multiplexing

MC-UWB	Multi – Carrier UWB
MHP	Modified Hermite Polynomials
MIMO	Multi-Input Multi-Output
ML	Maximum Likelyhood
mmWAVE	Millimeter Wave
MPC	Multipath Components
MT	Mobile Terminal
MTS	Mobile Telephone System
MULTI-RAT	Multi-Radio Access Technology
NFC	Near Field Communications
NFV	Network Function Virtualization
NLOS	Non Light of Sight
OOK	On – Off Keying
P2M	People to Machine
P2P	People 2 People
PAM	Pulse Amplitude Modulation
PCT	Pervasive Communication of Things

PDF	Probability Density Function
PEB	Position Error Bound
PHY	Physical Layer
POCS	Projection Onto Curvex Sets
PPM	Pulse Position Modulation
PS	Packet Switch
PSD	Power Spectral Density
PSM	Pulse Shape Modulation
PTT	Push To Talk
RAN	Radio Access Network
RFID	Radio Frequency Identification
RMSE	Root Mean Square Error
RRM	Radio Resource Management
RSS	Received Signal Strength
RSSI	Received Signal Strength Indicator
SDN	Software Defined Networks
SINR	Signal to Interference – Plus Noise Ratio

SLAAC	Stateless Address Auto Configuration
SMS	Short Message Service
SOP	Simultaneously Operating Piconet
TAU	Target Area Update
TCAS	Traffic Alert and Collision Avoidance System
TDOA	Time Different of Arrival
TF	Time Frequency
TG	Task Group
TH – PPM	Time – Hopped Pulse – Position Modulation
TH	Time Hoping
TM	Terminals
TOA	Time of Arrival
TRILL	Transparent Interconnection of Lots of Links
UAP	Universal Access Point
UBSC	Unlimited and Boundless Service in a Crowd
ULOSTECH	UWB LOS Sufficient Technique
UWB	Ultra-Wide Band

WBAN	Wireless Body Area Networks
WDM	Wavelength Division Multiplex
WIMAX	Worldwide Interoperability For Microwave Access
WLAN	Wireless Local Area Network
WLLS	Weighted Least Likelihood Square
WLPS	Wireless Local Positioning System
WLS	Weighted Least Square
WPAN	Wireless Personal Area Network
WSN	Wireless Sensor Network
WWAN	Wireless Wide Area Network
WWRF	Wireless Works Research Forum

CHAPTER ONE

Introduction

1.0. Research preamble.

1.1. Research problem.

1.2. Motivation.

1.3. Research framework.

1.4. Assumptions.

1.5. Key contributions.

1.6. Limitations.

1.7. Major constraints.

1.8. Thesis outline.

1.9. List of publications.

Introduction

1.0 Research Preamble.

The aim of this study is to provide high resolution positioning system for the 5G environment that envisions trillions of connected devices enabled for seamless global wireless everywhere connection [1]. In particular, recent announcement in the United Kingdom (UK) to provide Country-wide 5G wireless platforms by year 2020; and other efforts around the world, presents opportunities for more advanced networks including software-defined radios (SDR) [2][3]. It could be observed that new user requirements in information and communication technology (ICT) solutions and services have started to change the way mobile and wireless systems are exploited. It is expected that by the year 2018, there will exist around 10 billion mobile connections around the world along with about 15EB of mobile data traffic [4]. Moreover, the new era of always-on, always-connected and always-with-you devices is expected to shift personalized and contained systems towards cloud based solutions. This entails corresponding challenges of millisecond latency, higher network capacity requirements and spectrum shortages. The foregoing suggests new methods for high-definition systems to address the shortcomings of traditional infrastructure-based positioning systems along with the drawbacks of current network-based localization.

It is anticipated that today's scenarios of human-centric communication would in the near future be complemented by the Internet of Things (IoT), device-to-device (D2D) and machine-to-machine (M2M) communication concepts with a significant increase in the number of communication capable devices and machines. It is further envisaged that these IoT and M2M concepts would introduce more than 50 billion online devices by the year 2020, and most of them will utilize wireless connections in order to provide ease of access and cost-efficient deployments [5]. The expected coexistence of human-centric and machine-type applications imposes additional and diverse requirements on future mobile and wireless communication systems, such as rigorous reliability [6]. The current expectation therefore, is that these requirements would trigger fundamental advances in wireless systems leading to 5G networks [7]. However, questions persist at to the most appropriate architecture for the upcoming 5G wireless implementation.

CHAPTER ONE (1): - Introduction

The 5G wireless network is expected to be large-scale, dynamic and heterogeneous such that would foster seamless integration on a global scale with proposed gigabits level data capability. Considering huge investments in legacy wireless systems, it is believed that future systems should accommodate long term evolution (LTE) concepts together with newer systems [8]. Also presupposed is the presence of nodes in close spatial proximity of about 50m for cooperative and cognitive activities to prevail for which short-range wireless solutions like UWB are expected to play significant roles. It is believed that an unprecedented transformation in the design, deployment and application of short-range wireless devices and services has emerged. This trend is in line with the imminent transition to 5G radio access network (RAN) systems that could afford concurrent single protocol heterogeneous environments [9]. A key driver in this transition is the steep growth in both demand and deployment of wireless local area networks (WLAN) and wireless personal area networks (WPAN) based on the wireless standards within the Institute of Electrical and Electronics Engineers' (IEEE) - IEEE802 suite which include amongst others: IEEE802.11a, IEEE802.11b, IEEE802.11g and IEEE802.11n. It could however be observed that integration of short-range devices and networks into mainstream wireless wide-area infrastructure is still very minimal [10].

Notable short-range wireless communications technologies include radio frequency identification (RFID), Zigbee, Bluetooth, UWB and 60GHz millimetre wave (mmWave). UWB-based and 60GHz mmWave-based communications have attractive features which are suitable for future ubiquitous environments. These features include low-power, high speed, and an ability for robust location awareness. However, it is believed that the short-range wireless application space envisages novel devices and systems based on emerging technologies including UWB applications that are considered probably the most promising prospect. This has the potential to provide solutions for many of today's problems in the areas of spectrum management and radio system engineering. It is opined that heterogeneity of networks and devices for the 5G setting suggests common protocol architecture with short-range network overlay [11].

This thesis therefore investigates UWB approaches for 5G wireless implementation that entails sharing of already occupied spectrum resources by means of a network overlay that supports combined D2D communication links and localization services with a view to freeing-up the license spectrums. UWB transmission technology is particularly attractive for short to medium range localization, especially in GPS-denied environments since it has the ability to resolve sub-nanosecond delays in centimetre–level distance resolution with orders of magnitude improvement on the timing resolution compared to conventional narrowband signals [12]. Moreover, the deep wall penetration ability of UWB including its high-resolution ranging capabilities makes it a promising technology for localization applications in harsh environments and accuracy-critical applications such as would be required in 5G setting. Table1.1 shows details of some localization accuracy requirements. It could be observed that the accuracy requirements for most of the critical location-aware applications fall within the effective ranges that could be catered with UWB. This is believed to be a more promising solution compared to the search for available but possibly unsuitable new mmWave bands that have high propagation losses, as well as sensitivity to directivity and blockage. Notwithstanding the preceding view, UWB is expected to operate alongside existing RAN as well as mmWave that are in consideration for higher spectrum bands above 10GHz to leverage ultra-broadband communications [13].

Table 1.1 - Accuracy requirements of potential localization applications [14].

S/N	Applications	Accuracy
1	Automated handling	0.5 cm
2	Route-guidance for blind	1 cm
3	Tool positioning	1 cm
4	In-building robot guidance	8 cm
5	Formation flying	10 cm
6	Incidence tracking/guidance	80 cm
7	Goods and item tracking	1 m
8	Hazard warnings	1 m
9	Pedestrian route guidance	1 m
10	Precision landing	1 m
11	Location based services	3 m
12	Parolee tracking	10 m
13	Local information	30 m
14	Train/air/bus information	30 m

1.1 Research Problems

It is envisaged that the 5G environment would feature a worldwide all-IP core of always-connected self-aware devices in close spatial proximity of less than 50m that requires high accuracy positioning systems beyond the capabilities of the legacy global positioning system (GPS). Figure 1.1 is a schematic of traditional infrastructure-based positioning method that requires a link to at least three (3) satellites on the GPS constellation for accurate position determination. This legacy method however suffers drawbacks in harsh environments and dense urban scenarios such as signal blocking effects. Moreover, current wireless network positioning approaches suffers multipath effects and are characterized by detection and mitigation of NLOS paths. This explains the focus of most related works on range measurements with attendant complexity of design. This suggests the need for new methods to implement location-based services. Added to this is the challenge for combined ubiquitous communications and high definition localization that also addresses the problem of in-band multi-user interference. It is believed that impulse radio (IR)-UWB possesses features that point in the direction of solutions that could provide combined communication and localization services. Highlights of the focus, objectives and significance of the research are enumerated in sub-paragraphs 1.1.1; 1.1.2 and 1.1.3 respectively.

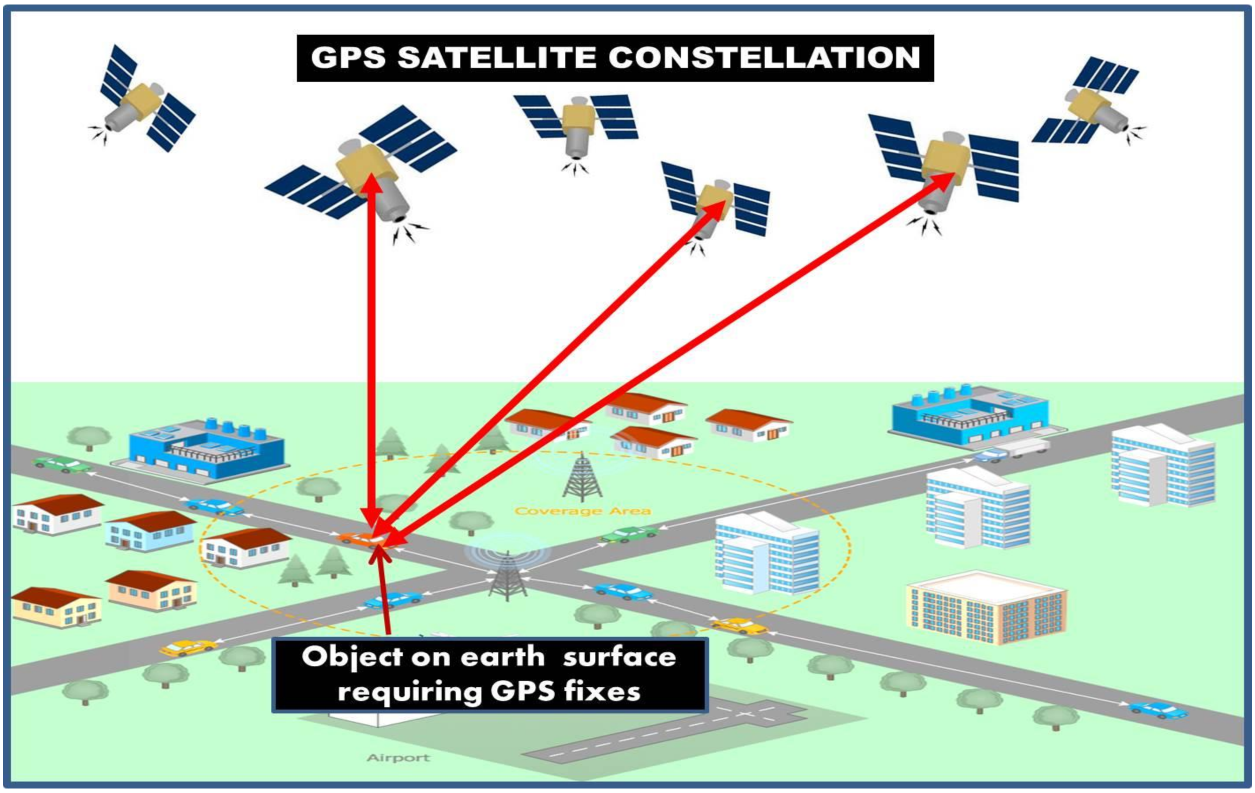

Figure 1.1. Adapted schematic of a GPS-based positioning system [16].

1.1.1. Focus

The research focuses on UWB simultaneous multiple access location estimation with successive interference cancellation for 5G wireless networks using the LOS sufficient technique and therefore proposes the *ULOSTECH.*

1.1.2. Objectives

The main objective of this research is to develop an algorithm for simultaneous multiple access D2D location estimation with capability for continuous interference cancellation suitable for use in the 5G wireless environment. It also proposes a possible 5G architecture based on UWB overlay network by way of contributing to on-going discourse regarding 5G implementation.

1.1.3. S*ignificance*

The significance of the research is founded on the need to address the inadequacies of traditional geo-positioning methods in harsh environments as well as the drawbacks of current wireless positioning systems for a desirable 5G setting for which UWB promises a better alternative.

1.2 Motivation

The motivation for this research founds on the possibility of a promising architecture for UWB in the 5G setting that affords a combined communication link and location service data flow within the same band of short range transmission technology.

1.3 Research Framework

The research investigates the prospect of improved localization accuracy and network coverage using UWB signals in a 5G setting. Various localization approaches were studied considering that earlier works concentrated on NLOS propagation mitigation with consequences on design and cost. The research therefore explores a UWB LOS sufficient technique for positioning in 5G setting along with a common protocol overlay architecture that exploits UWB capabilities. The framework also envisages decongestion of the licensed spectrums in 5G wireless environment since UWB operates in the unlicensed (FCC: part 15: 3.1-10.6 GHz) and in line with IEEE802.15.4a WPAN standard [15]. The thesis therefore models a UWB IEEE802.15.4a LOS sufficient technique with a view to an improved multi-user access compared to cellular network standards. It highlights an in-band multi-user interference mitigation method. Also explored is concurrent multi-layered super-core architecture for 5G D2D network overlay that utilizes IR-based UWB schemes for wireless wide area network (WWAN) cluster activities.

1.4 Assumptions

This research assumes that:

I. There will always be a cluster of nodes and devices in spatial proximity of not more than 50 meters.

II. Each participating relay station (RS) and devices receives either a LOS or an NLOS component of the transmitted UWB signal.

III. For any given estimation process, the instantaneous time of arrival (TOA) and the position of the node are constant.

IV. The estimator is unbiased such that equation 1.1 is true.

V. The estimation error variance can be expressed as equation 1.2.

$$\hat{\tau_b} = \arg min\ \{a_b^2(\tau)E_s - 2a_b\ (\tau) \int_0^{T_0} \Re\left(r_b^*(t)s(t-\tau)\right)dt\} \qquad (1.1)[13]$$

Where

$a_b\ (\tau) = \sqrt{K\ (d_0/c\tau)\frac{1}{2}\gamma b}$ is the path gain as a function of the time of arrival (TOA) τ,

$\Re(\cdot)$ is the real part of the transmitted signal, and:

T_0 is the observation period in which the TOA and the node position are constant.

Assuming unbiased estimator, the estimation error variance is given by equation 1.2.

$$E_{nb(t)}\{\widehat{\tau_b} - \tau_b\} = 0 \qquad (1.2)[13]$$

1.5 Key Contributions

The research contributes as follows:

I. A method for determination of UWB optimal localization channel in 5G setting.

II. ULOSTECH; a technique exploring cognitive UWB IEEE802.15.4a LOS sufficient positioning estimation for 5G environment.

III. A technique for ULOSTECH NLOS mitigation in a 5G setting.

IV. An IR-UWB D2D WWAN cluster formation scheme and cluster cooperation method.

V. The ULOSTECH UD-CLOCS; an IR-UWB combined localization and communication scheme for ultra-dense networks.

VI. The 5G-COMUSA; a concurrent multi-layered super-core architecture for 5G wireless implementation.

1.6 Limitations

The investigations and simulation experiments for which the research obtained promising results are limited to the following:

I. IR-UWB for channel realizations with cluster decay and mis-timing probability.

II. IR-UWB D2D WWAN.

1.7 Major Constraints

The major constraint of this research rests on the fact that 5G which is the core area of study is still emerging as discourse is currently on-going in both academia and industry as to the appropriate approach to implementation. Another constraint is that the IEEE 802.15.4a WPAN standard is relatively new as it was approved in the year 2007. The subject of study is therefore still an emerging area.

1.8 Thesis Outline

The remainder of this thesis is organized as follows.

Chapter 2. Chapter 2 is a literature review of the proposed area of study in this thesis. The chapter consist three sections which are (i) background study, (ii) review of related works and (iii) research overview. Background study outlines related wireless concepts and principles by way of conceptual clarification, as well as a survey of position systems and methods. The chapter thereafter reviewed related works on the subject of study and then finally gave a summary outline of research hypothesis, scenario and methodology.

Chapter 3. Chapter 3 outlines the core ULOSTECH model along with simulation experiments on LOS sufficient positioning estimation. It also discusses an optimal UWB IEEE802.15.4a localization channel as a framework that utilizes cluster decay rate and mistiming probability and a framework for the ULOSTECH NLOS mitigation.

Chapter 4. In Chapter 4, the IR-UWB D2D WWAN layout is presented along with a cluster formation scheme and ULOSTECH UD-CLOCS; a WWAN D2D-propagation-based combined communication and localization technique for ultra-dense network situations expected in the 5G environment.

Chapter 5. Chapter 5 explores 5G-COMUSA; a proposed overall architecture for 5G wireless by implementing a cognitive concurrent super-core UWB overlay network model. The chapter also discusses the envisaged 5G-COMUSA scenarios for the 5G setting.

Chapter 6. Chapter 6 presents some concluding discussion, thesis reflection and the future direction for this line of research while areas of possible further studies are suggested.

1.9. List of Publications

1.9.1. Journal papers

- **Akeem A Adebomehin**, Stuart D Walker, Adewale Abe: "Proposed 5G Roadmap:- Prospects, Challenges, Scenarios and Proposed Architecture for Ultrawideband Signals in 5G Wireless" - a paper submitted to the Journal of Electrical Engineering (ISSN: 2328-2223) USA – September 2016 (in-review).
- **Akeem A Adebomehin**, Stuart D Walker : "EULOSTECH – Ultrawideband Line-of-sight Sufficiency Positioning and Mitigation for Cognitive 5G Wireless Setting - a paper submitted to the Journal of Communications and Computer (ISSN:1548-7709) USA – August 2016 (in-review).
- **Akeem A Adebomehin**, Stuart D Walker: "5G-COMUSA – a probable architecture for cognitive UWB for positioning and network links in 5G setting" - a paper submitted to the Journal of Wireless Communications (Special Issue on Wireless Sensor Networks), ISSN2377-3308
- **Akeem A Adebomehin**, Stuart D Walker "Ultra-wideband IEEE802.15.4a simultaneous multi-access location estimation with successive interference cancellation for 5G future wireless" a paper submitted to IEEE Antennas and Wireless Propagation Letters, 2016, New York, USA. (in-review).

1.9.2. Conference/workshop papers

- **Akeem A Adebomehin**, Stuart D Walker "Enhanced ultra-wideband LOS suffiency positioning and mitigation for cognitive 5G wireless setting" in the proceedings of the 39th International Conference on Telecommunications and Signal Processing, (TSP-2016), Vienna, Austria, pages 87-93.
- **Akeem A Adebomehin**, Stuart D Walker, Adewale Abe "Cognitive High-definition Ultrawideband positioning Technique for 5G-based Emergency Networks" a paper submitted to IEEE International Workshop on Emergency Networks for Public Protection and Distracter Relief; in conjunction with Wireless and Mobile Computing, Networking and Communications Conference 2016 (WiMob'16), New York, USA. (in-review).
- **Akeem A Adebomehin**, Stuart D Walker "Impulse Radio Ultrawideband D2D-Based localization for Ultra-dense 5G Networks" in the proceedings of IEEE Wireless and Microwave Technology Conference 2017 (WAMICON 2017), Cocoa Beach, Florida -USA.

1.9.3. PhD forum

- **Akeem A Adebomehin**, Stuart D Walker: "Enhanced Ultrawideband Methods for 5G LOS Sufficient Positioning and Mitigation" in the proceedings of 17th International Symposium on a World of Wireless, Mobile and Multimedia Networks, WOWMOM2016: Coimbra, Portugal. Pages 1-4.

1.9.4. Conference posters

- **Akeem A Adebomehin**, Stuart D Walker: "Ultra-wideband Signals for High-resolution Cognitive Positioning Technique in 5G Wireless" in the proceedings of 37th IEEE Sarnoff Symposium – Newark, New Jersey, Sept 2016 (poster short paper).

CHAPTER TWO

Literature Review

2.0. Chapter overview.

BACKGROUND STUDY

2.1. The era of multivariate wireless networks.

2.2. Related wireless concepts and principles.

2.3. Survey of positioning techniques.

2.4. Cognitive cooperative wireless localization.

2.5. Overview of UWB cooperative localization.

REVIEW OF RELATED WORKS

2.6. Related works on UWB optimal localization channel.

2.7. Related works on UWB localization Techniques.

2.8. Related works on UWB localization mitigation methods.

2.9. Related works on 5G wireless architecture.

RESEARCH OVERVIEW

2.10. Research hypothesis, scenario and methodology.

2.11. Summary.

Literature Review

2.0. Chapter Overview

The Chapter comprises three sections consisting of (i) background study, (ii) review of related works and (iii) research overview. The background study gives a global view of the subject covering important topics on wireless networks along with related wireless concepts and principles. Other topics covered are positioning techniques, as well as cognitive cooperative wireless positioning and UWB cooperative localization. Thereafter, a review of related works is outlined while gaps in literature are identified. The chapter concludes with research hypothesis, scenario and methodology.

Background Study

2.1. The Era of Multivariate Wireless Networks

Wireless networks have come a long way in terms of generations and accompanying features. Figure 2.1 highlights the evolution of information delivery from the conventional direct approach to multi-hop techniques and finally through a short-range network. It is believed that the composite approach to architecture will be of significant relevance in future wireless networks. In this thesis, the term short-range network or cooperative cluster is used to denote a variety of possible network configurations, with homogeneous or heterogeneous component nodes like wireless grids, wireless sensor networks, ad-hoc broadband networks and other related devices. Considering the multiplicity of wireless networks of different capabilities, future wireless communication networks are expected to consist of two main components which are the WWAN and short-range networks; for cellular mobile and local broadband access respectively [17]. The coexistence of centralized architectures comprising licensed spectrum and distributed (ad-hoc) license exempt spectrum promises harmonization of the benefits of both approaches. It is believed that the expected high density of cognitive nodes in the 5G setting will enable a given device to be regarded as a constituent node of a short-range ad-hoc network or cooperative cluster of devices situated in its immediate neighbourhood. This offers improved communication services as well as the need for higher levels of localization for which UWB holds promise.

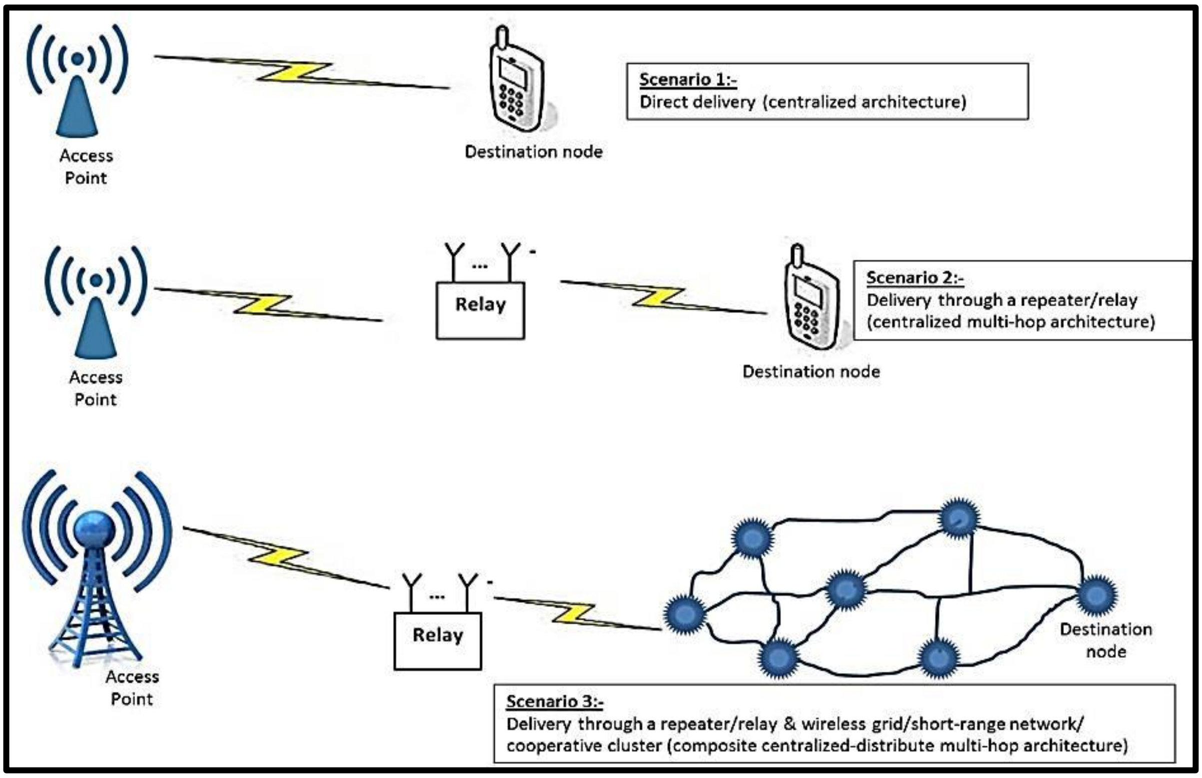

Figure 2.1. Schematics of information delivery approaches through access networks. Adapted from [18]

2.2. Related Wireless Concepts and Principles

2.2.1. Short-range Communications.

Short-range wireless communications concern a diverse array of air interface technologies, network architectures and standards. The most well-known short-range wireless network technologies include WLAN, WPAN, wireless body area networks (WBAN), wireless sensor networks (WSN), car-to-car communications (C2C), radio frequency identification (RFID) and near field communications (NFC). Figure 2.2 highlights an overview of short-range communications by typical range. According to the Wireless World Research Forum (WWRF), by year 2017, seven trillion wireless devices will serve seven billion people around the world [19]. It is believed that most of these devices will be for short-range communications and the projected average figure of about 1000 devices per person is seen by some predictions as conservative [20]. This suggests that a given wireless device will be surrounded by many other devices in a potential cluster to interact with, and likely higher data throughputs [21]. It is opined that short range systems like UWB will play a significant network access and positioning roles in the 5G environment.

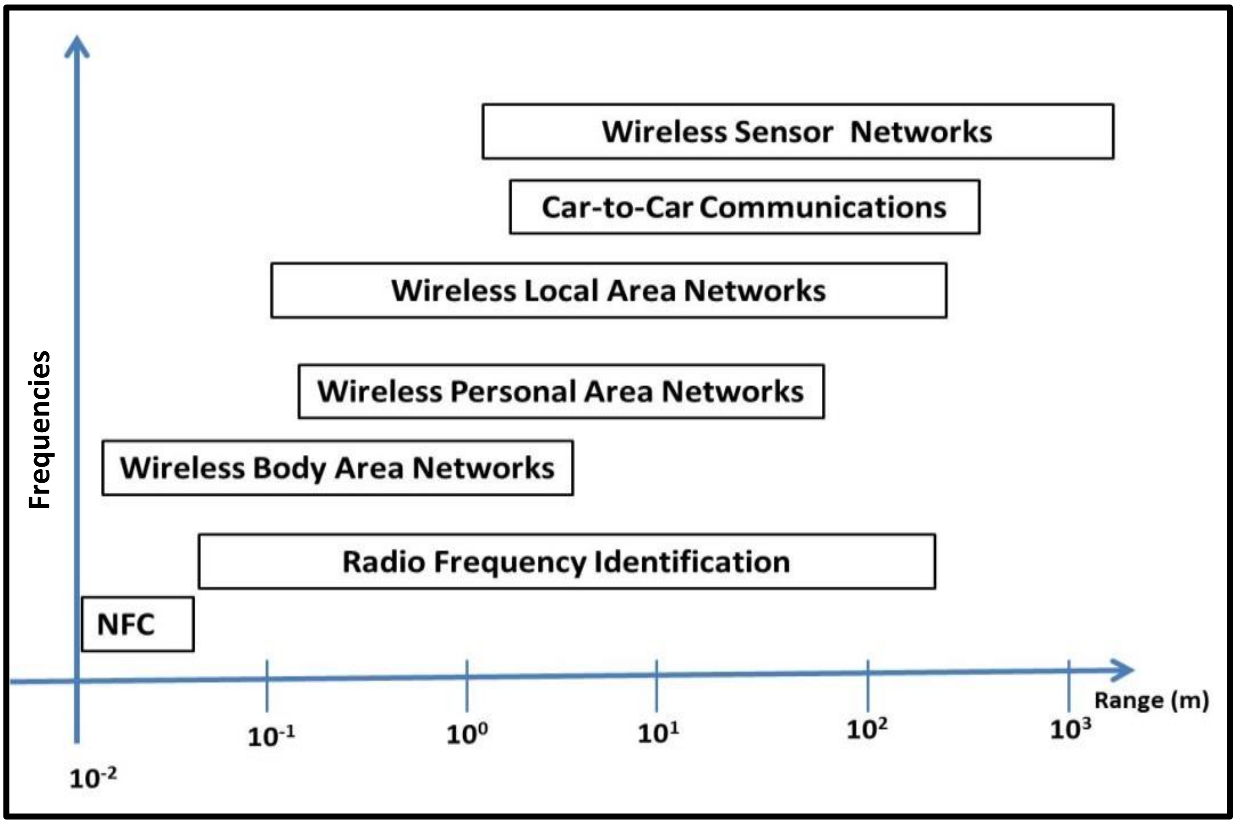

Figure 2.2. Classification of short-range communications according to the typical supported range [18].

2.2.2. Internet of Things.

The connection of devices to the Internet makes it possible to remotely access data and control the physical world. IoT is based on the vision of web-based data for new services that go beyond what an isolated embedded system can provide [22]. Essentially, a smart object is an embedded system connected to the Internet. It is believed that the novelty of the IoT is not in any new disruptive technology, but in the pervasive deployment of smart objects. This has been made possible as a result of the exponential growth of the Internet from a small research network of a few nodes, to a worldwide network that services more than a billion users [22]. Nevertheless, the prospects of IoT and the advantages that come with it, presents opportunity for improved communication services. It is suggested that future devices should have access to a domain specific knowledge-base along with capabilities to orient themselves in their specific application domains. This suggests that future devices will be activity-aware, policy-aware, and process-aware [22]. It must be noted however, that these service expectations for the 5G setting will dependent largely on high definition positioning systems that UWB technology most probably offers.

2.2.3. The Ubiquitous communication concept.

The concept of ubiquitous communications recognizes the trend that humans interact no longer with one device at a time, but rather with a dynamic set of networked devices that are often invisible and embodied in everyday objects in the environment. With the unprecedented development of wireless communication technologies, various elements of ubiquitous computing are beginning to appear as increasing numbers of devices and objects become addressable and connected. However, seamless connectivity is very important to ubiquitous communications [23]. It is believed that with the increasing demands for low-power communication, UWB has the underlying key communication and localization features that are probably suitable for implementation of the 5G wireless setting.

2.2.4. User-centric Network Approach.

One of the underlying key considerations for future wireless and mobile network designs has been the user. User-centric approach is endorsed by the International Telecommunications Union (ITU) as well as the WWRF as a driving force leading 5G wireless development [24]. However, users will not only be the sources inspiring the key requirements for future networks but, more than ever, they will also play active roles. Firstly, the user will become a source of content and more importantly as an integral part of the collaborating chain with notable impact on the operation and performance of wireless networks. Indeed, collaborative interactions among entities are expected to be embedded in system design and transparent to the users. It is however envisioned that users will have a direct participation in the cooperative scene, as ultimately users will decide whether to cooperate or not [24][25]. It is noteworthy that today's user predisposition to interact and cooperate through the Internet is certainly phenomenal and of such positive attitude.

2.2.5. Cooperative Concepts and Principles.

Cooperation is the basic principle of any communication system. In fact, cooperation is deeply embedded in wireless communication networks where, tacitly all connected or interacting entities agree on using common signal formats, protocols and behavioural rules. Clearly, without this essential principle, no communication would be possible. Such implicit form of collaboration or implicit cooperation is the key underlying assumption when designing a communication network. Indeed, cooperation has the potential to improve the most important link and network performance figures, including achievable data throughput, quality of service, network capacity and coverage while it can also in principle enhance the efficiency in the utilization of radio resources [26]. Cooperation helps to create virtual devices with scalable architecture and enhanced features.

2.2.6. Cognitive Concepts and principles.

Cognition; according to the Encyclopaedia Britannica, is: “the process involved in knowing, or the act of knowing, which in its completeness, includes awareness and judgement” [27]. Indeed, as often pointed out, perception and reasoning are also closely related to the cognitive process. Techniques like channel estimation and sensing the presence of other users, can be seen as elementary forms of applying cognition in wireless networks that is usually followed by analysis and further reaction and adaptation. Figure 2.3 is a schematic depiction of the cognitive principles in a wireless network. The schematic details the cognitive process that entails: sense, understand, decide and adapt. It could be argued that spectral efficiency is of fundamental importance since users of wireless systems are increasing while advance broadband services are becoming more popular thus putting more pressure on bandwidth demands [28]. There is thus the need for cognition schemes to enhance efficiency in the use of radio resources to improve performance figures of networks. Additionally, cognition is fundamental to heterogeneous networks as achieving end-to-end connectivity between different wireless devices operating in different networks requires awareness of the characteristics and capabilities of counterparts which also calls for location awareness.

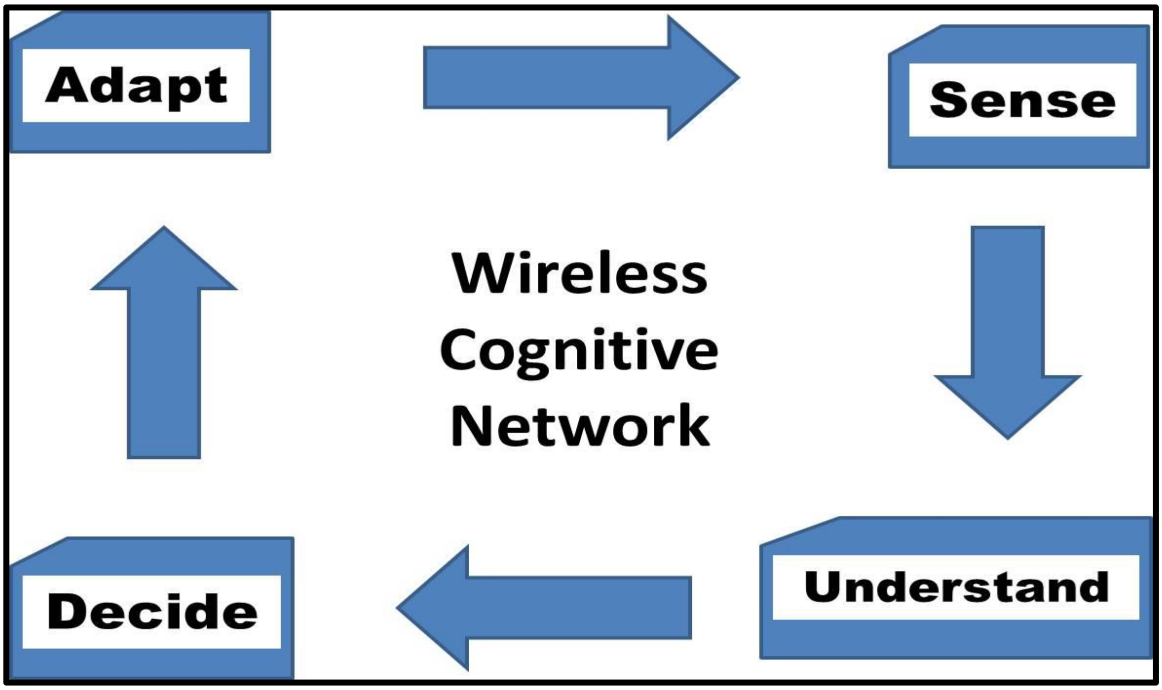

Figure 2.3. Adapted Schematic of a typical cognitive cycle in wireless networks [28].

2.2.6. Cooperation and Cognition in Wireless Networks.

Cooperative and cognitive principles are complementary to each other and thus, it appears reasonable to exploit this rational synergy by applying them jointly in future communication systems that would consist of highly heterogeneous wireless ecosystem. Moreover, technical limitations and scarcity of resources puts constraints in the design of future wireless networks. It is therefore believed that issues such as complexity, power, energy and spectral efficiency are key resources that could be traded in different ways to achieve a desired level of performance, cooperation and cognition for a promising resource trading framework for future wireless networks [29]. It could be said that efficient cooperation relies on previously obtained knowledge, while effective acquisition of knowledge and awareness could be achieved through cognition. In composite scenarios, where different wireless devices and networks coexist, fruitful interaction cannot be devised without being aware of the surrounding wireless environment. In addition, proliferation of wireless entities in close spatial proximity suggests the need for devices and networks to cooperate and be aware. This requires a robust positioning systems that could be powered with short range schemes like UWB approaches.

2.3. Survey of Positioning Techniques

2.3.1 Overview of Positioning Systems.

Positioning systems can be classified into two categories. These are the GPS and local positioning system (LPS) as detailed in Figure 2.4. GPS enables each device to find its own position on the globe while LPS is a relative positioning system classified into self and remote positioning. The self-positioning systems allow each person or object to find its own position with respect to a static point at any given time and location [17]. An example of self-positioning system is the inertial navigation system (INS) that is used majorly in the aviation industry. Conversely, remote positioning systems allow each node to find the relative position of other nodes located in its area and the nodes can either be static or dynamic. Remote positioning systems are further divided into active target remote positioning and passive target remote positioning. In the active target remote positioning systems, the target is active and cooperates in the process of positioning. Examples of active target positioning systems are RFID, wireless local positioning systems (WLPS), and traffic alert and collision avoidance systems (TCAS). In the passive remote positioning system, the target is passive and non-cooperative. Examples of passive target positioning systems are tracking radars and vision systems [17].

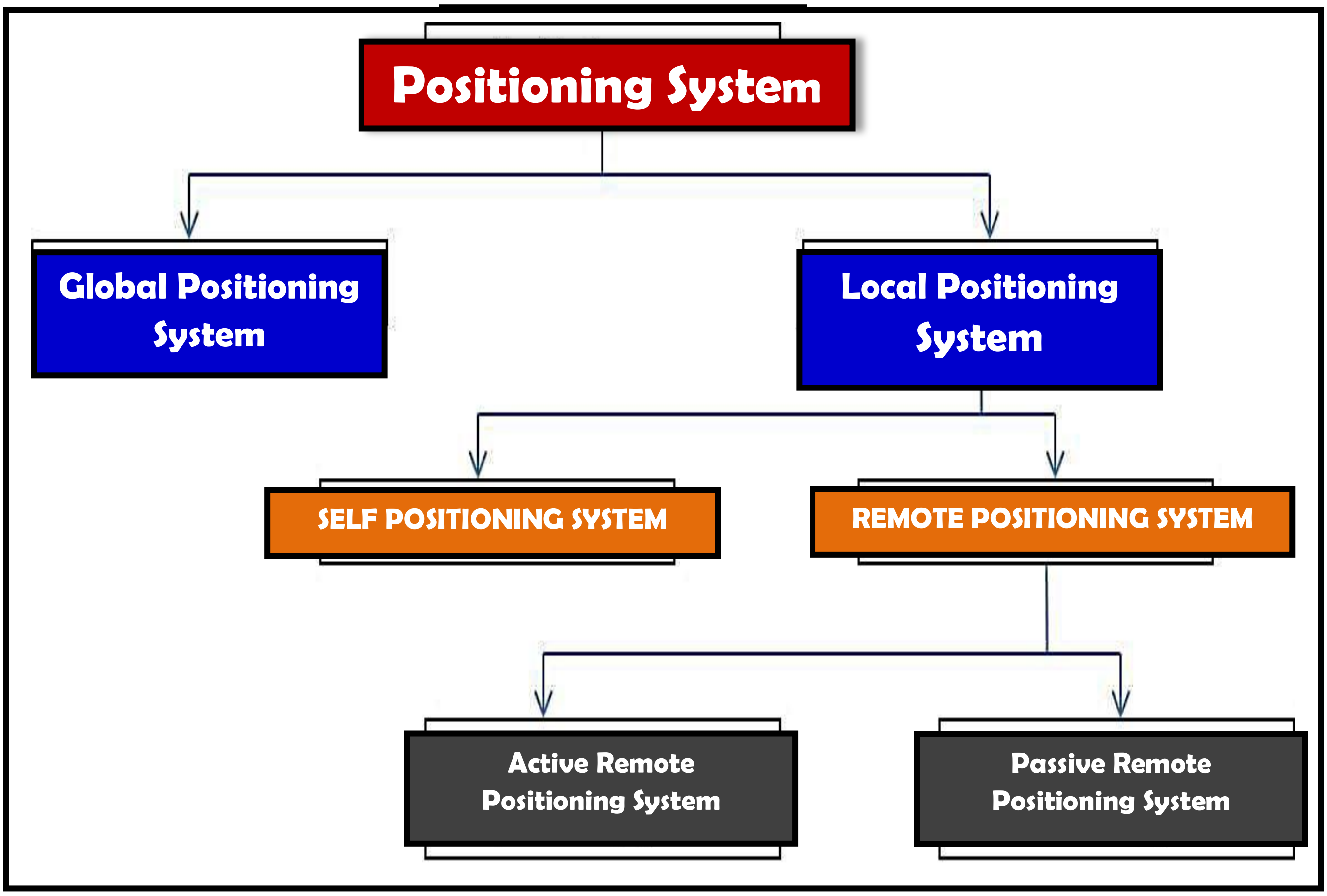

Figure 2.4. Classification of positioning systems. Adapted from [17].

2.3.2. Positioning Techniques.

Positioning techniques are based fundamentally on geometric estimation methods that form the background of all complex positioning systems. These techniques together constitute the guides used in selection and analysis of positioning systems for a particular application based on combination of parameters. The fundamental techniques adopted for position location activities are time of arrival (TOA) estimation, time difference of arrival (TDOA) estimation, direction of arrival (DOA) estimation, received signal strength (RSS) and RSS indicator (RSSI). A wide variety of positioning systems do use combinations of these techniques for positioning applications [17]. The underlying estimation principles for positioning techniques are highlighted in the following respective paragraphs: 2.3.2.1; 2.3.2.2; 2.3.2.3 and 2.3.2.4.

2.3.2.1. Time of Arrival (TOA) Positioning Estimation.

The TOA estimation technique utilizes the spherical geometry such as that of the earth to measure distances based on the fact that any object on the globe is located on a circular cross-sectional plane of the spheroid earth. The term "spheroid" used throughout this thesis refers to the circular surface circumference of the spheroid only, and not the solid spheroid For TOA localization to be realized, multiple base nodes of known spatial locations must collaborate with themselves using triangulation to determine the position of a target node. It must be noted however, that in some instances of TOA estimation, the base nodes may have to first cooperate to find their own positions before they localize a target node. Furthermore, the base nodes may be in coplanar or non-coplanar scenarios. In a coplanar scenario, three base nodes are required for TOA estimation to be achieved while the non-coplanar scenario needed four base nodes [16]. If we Assume three base nodes N_1, N_2 and N_3 of known positions in a coplanar scenario (x, y) as shown in Figure 2.5, using the measurement of distance methods, the position of a target node could be localized within a sphere of radius R_1 that has a receiver (i) at the centre of the sphere. Hence, R_1 bears direct proportionality to TOA-t_1; the time the signal is received. Therefore, the localization of the target node can be carried out either by the base nodes using a master station or by the target node itself. The TOA geometrically can be mathematically expressed as Equation 2.0 [16].

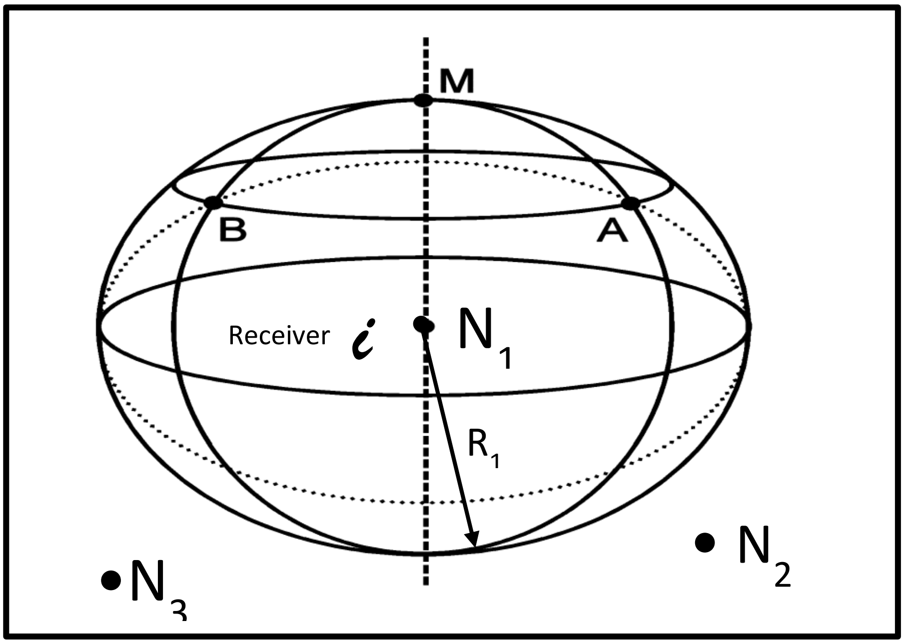

Figure 2.5. Hypothetic Three TOA Base Nodes in a Coplanar Scenario.[16]

$$\text{TOA}(t_1) = \tau_1 + t_s \tag{2.0}$$

Where: TOA($\mathbf{t}_1$) is the time the signal is received

$\mathbf{t}_s$ is the time the signal was sent

τ_1 is the time it takes the signal to travel to the receiver.

Therefore, $$\text{TOA}(t_1) - t_s = \frac{R_1}{c} \tag{2.1}$$

Where c is the speed of light (3 x 10^8 ms^{-1});

Thus, equation (2.1) could be expressed geometrically as (2.2):

$$\tau_1 = \text{TOA}(t_1) - t_s = \frac{\sqrt{(x_i - x)^2 + (y_i - y)^2}}{\text{c}} \tag{2.2}$$

If both sides of Equation 2.2 are squared and then rearranged we get (2.3)

$$(\tau_1)^2 = \frac{(x_i - x)^2 + (y_i - y)^2}{c^2} \tag{2.3}$$

Further rearrangement of Equation 2.3 results in (2.4) which is a standard circular plane equation

$$1 = \frac{(x_i - x)^2}{(c\tau_1)^2} + \frac{(y_i - y)^2}{(c\tau_1)^2} \tag{2.4}$$

It could be deduced from Equation 2.4 that it defines a circular plane with points upon which the target node must lie for TOA localization to be realized. As shown in Figure 2.6, the potential target location will be one of the two points of intersections: **a** and **b**: that are intersection points for the 2 dimensional sphere planes (circles) given as: $\mathbf{R_1} \propto \mathbf{t}_1$ and $\mathbf{R_2} \propto \mathbf{t}_2$. Therefore, the final target location is the potential target point (**a**) that intercepts the circle with radius $\mathbf{R_3}$ given by $\mathbf{R_3} \propto \mathbf{t}_3$. It must be noted however, that the foregoing scenario assumed there were no errors in the measurements which is not possible. In practical systems however, there usually occur errors due to thermal noise, multipath and possibly system errors [30]. The presence of errors makes the results to be inconsistent with the actual target location; thus the need for a method that mitigates the errors to determine the best solution. This is achieved by minimizing the squared error between the measurement and the implied values called the least square solution (LSS). To determine the value of LSS, we assume that $\mathbf{t}_1$ for i = 1,...N are the received TOA measurements and the measurement noise and N base stations located at (x_i, y_i) and is denoted as n_i, the LSS is given as expressed in Equation 2.5:

$$\widetilde{t_\iota} = \mathbf{t}_1 + \mathrm{n}_{\mathrm{i},} \tag{2.5}$$

Therefore,

$$[\hat{x},\ \hat{y}] \quad = \arg\min \sum_{i=1}^{N} \left[c(\widetilde{t_\iota} - t_s) - \sqrt{(x_i - x)^2 + (y_i - y)^2} \right]^2 \tag{2.6}$$

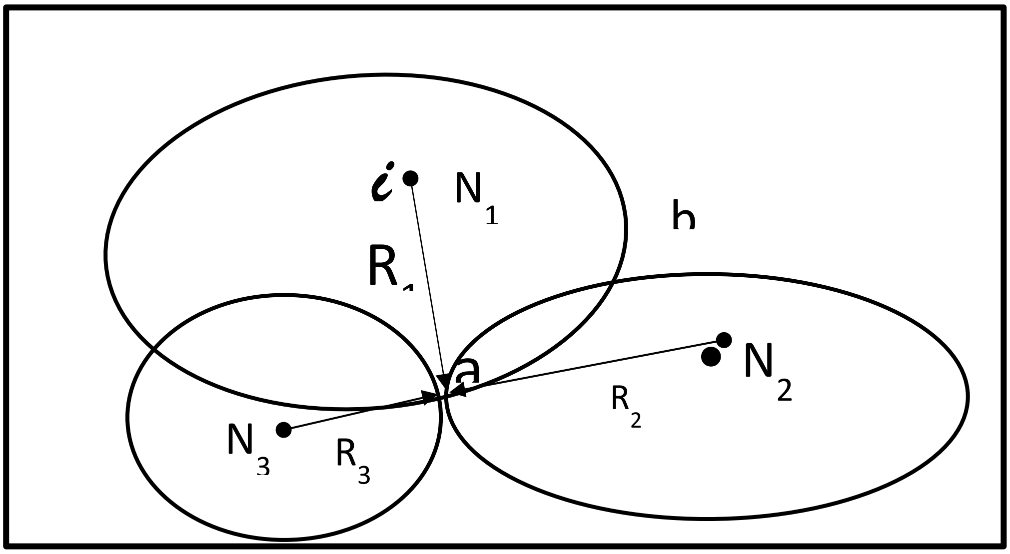

Figure 2.6 - Final TOA Target Location in Coplanar Scenario.

Equation 2.6 could be linearized by assuming $\widehat{\theta}$ is the estimate of θ. Then, the vector of observed distances using TOA measurement r can be modelled as:

$$r = f(\theta) + n \tag{2.7}$$

Therefore, where f(θ) is a function $\mathbb{R}^2 \rightarrow \mathbb{R}^N$ which maps the two-dimensional position vector θ

to an N-dimensional vector of distances to each of the N base nodes expressed as Equation 2.8. Using the notation in Equation 2.8, the LSS estimate can be modelled for simulation estimation as shown in Equation 2.9:

$$f(\theta) = \begin{bmatrix} \sqrt{(x_1 - x)^2 + (y_1 - y)^2} \\ \sqrt{(x_2 - x)^2 + (y_2 - y)^2} \\ \vdots \\ \vdots \\ \vdots \\ \sqrt{(x_N - x)^2 + (y_N - y)^2} \end{bmatrix} \quad (2.8)$$

$$\widehat{\theta} = \arg\min[r - f(\theta)]^T\,[r - f(\theta)] \quad (2.9)$$

Drawbacks of TOA. Despite the wide acceptance and utilization of TOA in many positioning systems, it has a few drawbacks as highlighted in 2.3.2.1.1, 2.3.2.1.2 and 2.3.2.1.3.

2.3.2.1.1. TOA estimation technique requires that the system clocks in all base nodes and the target node be precisely synchronized. This is to avoid errors in the calculation of distances as this will in-turn affect the accuracy of location estimation [13].

2.3.2.1.2. The transmitted signals in TOA estimation must be labelled with a time-stamp to enable the base node to determine the exact time at which the signal was transmitted at the target node. Consequently, the addition of a time stamp to the signal will in effect increase the complexity of the signal with its the likelihood of introducing error into the estimation process [13].

2.3.2.1.3 TOA estimation requires that the positions of the base nodes be known. Thus, for dynamic nodes to be used, they will have to be given GPS capability [14].

2.3.2.2. Time-Difference-of-Arrival (TDOA) Estimation.

TDOA estimation involves the measurement of time-difference between the signals arriving at two base nodes. It bears similarity with TOA estimation on the count that its method also assumes that the positions of base nodes are known. However, unlike TOA estimation where node positions are located on spherical planes, the TDOA estimation utilizes the geometrical properties of a hyperbola [31]. To estimate TDOA, the base station that first receives the signal from the target node is considered as the reference base station. As shown in the figure 2.7, the reference base station is $\mathbf{N_1}$. While the other two base nodes $\mathbf{N_2}$ and $\mathbf{N_3}$ are used for TDOA measurement, in coplanar scenario. Consequently, two TDOA measurements are made with respect to the reference base station $\mathbf{N_1}$. If a non-coplanar case is in consideration, then positions of four base nodes would be needed while three TDOA measurements are required [16]. As a first step to estimation, the potential target location will be on a hyperbola that is formed using the TDOA measurement (1–2) with respect to the reference base station. Similarly, the final target location will be the point of intersection of the two hyperbolae that are formed using two TDOA measurements (1–2) and (1–3) with respect to the reference base station $\mathbf{N_1}$; Hence, TDOA is called hyperbola locationing. The TDOA estimation can be expressed mathematically as Equation 2.10. If we assume that TDOA($\mathbf{t}_1$) is the time the signal is received; (TOA) at the i^{th} base node and $\mathbf{t}_s$ is the time the signal was sent while τ_1 is the time it takes the signal to travel to the reference node; the i^{th} base node $(x_i \;\; y_i)$ at distance R_1:

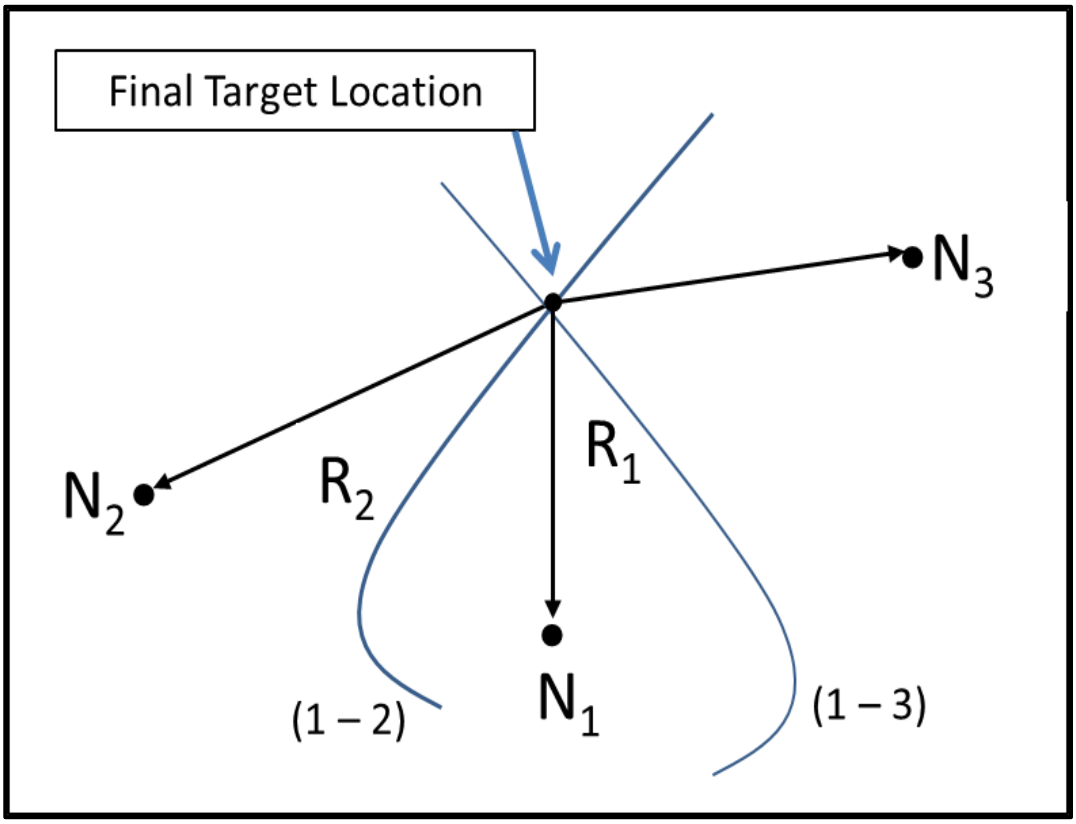

Figure 2.7 Final TDOA Target Locations in Coplanar Scenario.

$$\mathrm{TDOA}(t_i) = \tau_i + t_s = \frac{R_1}{C} + t_s \tag{2.10}$$

thus Equation 2.10 could be expressed geometrically as Equation 2.11:

$$\mathrm{TDOA}(t_i) = \frac{\sqrt{(x_i - x)^2 + (y_i - y)^2}}{\mathrm{c}} + t_s \tag{2.11}$$

The importance of TDOA becomes apparent since we have three unknowns (x, y and t_s). However, we can eliminate one of the variables; t_s by taking just the time-difference between i^{th} position and a hypothetic position j (where i ≠ j) such that we get Equation 2.12.

$$t_i - t_j = \tau_i + t_s - (\tau_j + t_s) = \tau_i - \tau_j$$

$$= \frac{R_i}{C} - \frac{R_j}{C} \tag{2.12}$$

This essentially gives Equation 2.13 when expanded and the coordinate values are inserted.

$$t_i - t_j = \frac{\sqrt{(x_i - x)^2 + (y_i - y)^2} - \sqrt{(x_j - x)^2 + (y_j - y)^2}}{\mathrm{c}} \tag{2.13}$$

Since we have infinite number of (x,y) pairs, that would make Equation 2.13 to be true, therefore it is desirable to create a second non-linear equation such as $t_j - t_k$ so that we can have two unknowns that would be solved using two equations (Equations 2.13 and 2.14).

$$t_j - t_k = \frac{\sqrt{(x_j - x)^2 + (y_j - y)^2} - \sqrt{(x_k - x)^2 + (y_k - y)^2}}{\mathrm{c}} \tag{2.14}$$

Geometrically, Equation 2.14 can be expressed as Equation 2.15 if $\Delta\tau$ is the measured TDOA

$$\Delta\tau c = \sqrt{(x - \delta)^2 + y^2} - \sqrt{(x + \delta)^2 + y^2} \tag{2.15}$$

If $\Delta\tau c$ in equation 2.15 is defined as m giving $\Delta\tau c = m$ then we get:

$$\mathrm{m} + \sqrt{(x - \delta)^2 + y^2} = \sqrt{(x + \delta)^2 + y^2} \tag{2.16}$$

When we square both sides of the equation and rearrange, we get a hyperbola equation as expressed in Equation 2.17: and the least square solution (LSS) is as indicated in Equation 2.18.

$$1 = \frac{x^2}{(\delta^2 - \frac{m^2}{4})/(\frac{4\delta^2}{m^2} - 1)} - \frac{y^2}{(\delta^2 - \frac{m^2}{4})} \tag{2.17}$$

$$[\hat{x}, \hat{y}] = \arg\min \sum_{j=1}^{N} \sum_{i \neq 1}^{n} \left\{ c\left(\tilde{t}_i - t_j\right) - \sqrt{(x_i - x)^2 + (y_i - y)^2} + \sqrt{(x_j - x)^2 + (y_j - y)^2} \right\}^2 \tag{2.18}$$

Just like TOA, TDOA estimation also assumes known positions of base nodes. However, its coplanar scenario requires 2 base nodes while its non-coplanar scenario requires 3 base nodes. Additionally, TDOA addresses the first drawback of TOA by removing the requirement of synchronizing the target node clock with base node clocks. Moreover, TDOA also takes care of the second drawback of TOA since the transmitted signal from the target node in TDOA need not contain a time stamp, as TDOA measures time difference in the arrival time at the respective base nodes. This simplifies the structuring of transmitted signals and removes potential sources of error. In TDOA, all base nodes receive the same signal transmitted by the target node. Therefore, as long as base nodes' clocks are synchronized, the error in the arrival time at each base node due to unsynchronized clocks with the target node will be the same [16].

2.3.2.3. DOA Estimation

In DOA estimation technique, the base nodes determine the angle of the arriving signal instead of its timings. To allow base stations to estimate DOA, they should be equipped with antenna arrays, and each antenna array should be equipped with radio frequency (RF) front-end components. However, this incurs higher cost, complexity and power requirements compared to TOA and TDOA systems of the same rating [31]. Figure 2.8 illustrates how to determine the DOA. The main lobe of an antenna array is steered in the direction of the peak incoming energy of the arriving signal while the potential target location will lie on a straight line whose direction; ϕ_1, is determined by peak incoming energy signal using antenna array. In the same vein, the final target will be a point that passes through the intersection of two lines whose directions ϕ_1 and ϕ_2 are determined by peak incoming energy signals using antenna arrays at the two base nodes $\mathbf{N_1}$ and $\mathbf{N_2}$. DOA estimation bears some similarities with TOA and TDOA techniques. For instance, just like in TOA and TDOA, DOA also requires that positions of the base nodes must be known. Moreover, just like TDOA, it only requires two DOA measurements in coplanar scenario while three measurements are required in non-coplanar scenario. Since DOA is the arrival angle of the emitted source signal observed at the receiver then the DOA at the ith receiver could be expressed as equation 2.19:

$$\tan(\phi_1) = \frac{y-y_1}{x-x_1}, \quad i = 1, 2,3 \ldots \ldots \ldots, L \tag{2.19}$$

With $L \geq 2$ the measurement in the presence of errors denoted ($r_{DOA,i}$) is given by

$$\mathrm{r}_{DOA,i} = \phi_i + \mathrm{n}_{DOA,i}$$

$$= \tan^{-1}\left(\frac{y-y_1}{x-x_1}\right) + \mathrm{n}_{DOA,i}, \quad i = 1, 2,3 \ldots \ldots \ldots, L \tag{2.20}$$

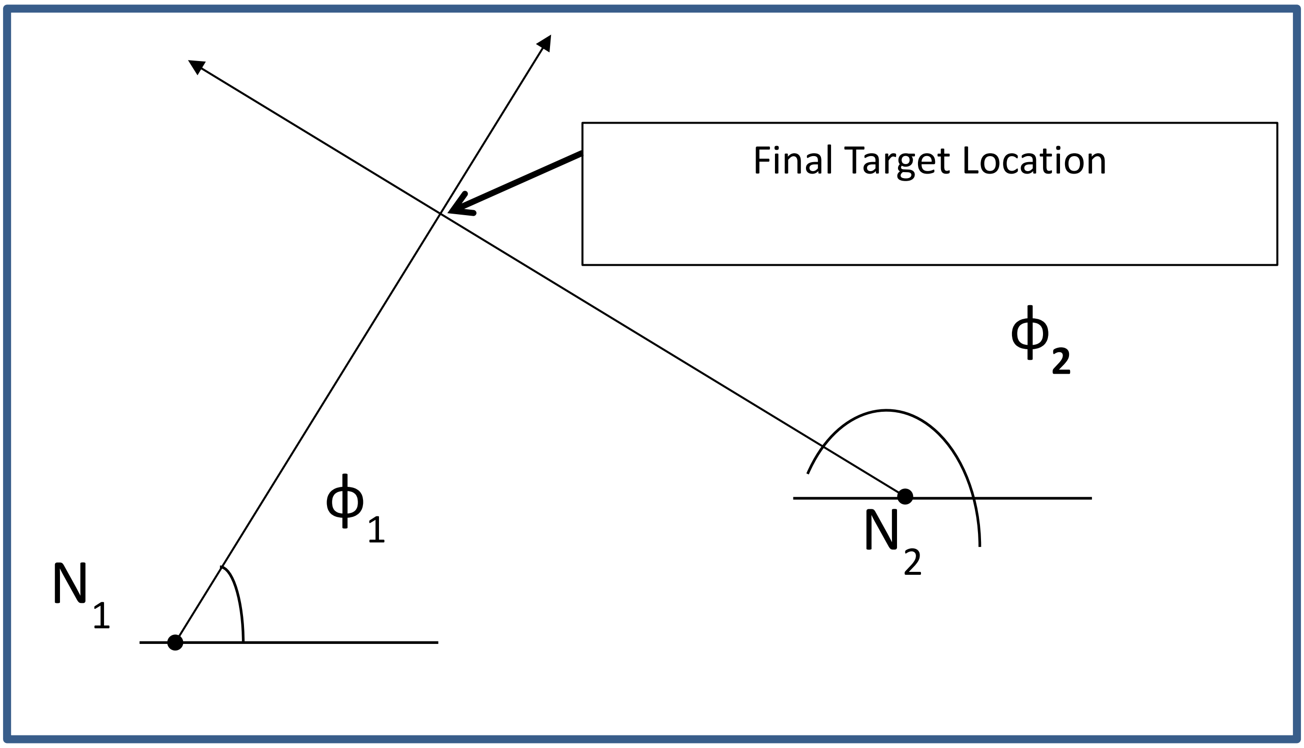

Figure 2.8. Final DOA Target Location in Coplanar Scenario.

2.3.2.4. RSS Estimation.

RRS is similar to the TOA as multiple base nodes collaborate to localize a target node via triangulation (see Figure 2.6). However, instead of measuring the TOA at base nodes, the estimation is carried out using the received signal strength (RSS) [16]. In this method, the strength of the received signal indicates the distance traveled by the signal. However, it is assumed that the transmission strength and channel characteristics (or environment in which the signal is traveling) are known. For RSS technique, a coplanar case requires three base nodes and three RSS measurements. Assuming that the source transmitted power in the absence of a disturbance is P_i , then the average power received at the i^{th} base node denoted $P_{r,i}$ is given as equation 2.21:

$$P_{r,i} = K_i P_i d_i^{-\alpha} = K_i P_i \|x - x_1\|_2^{-\alpha}, \text{ I} = 1,2\ldots,\text{L} \tag{2.21}$$

2.4. Cognitive Cooperative Wireless Localization

Network-based localization techniques constitute an improvement on traditional geo-position-based methods. Here it is expected that the un-localized but cognitive nodes will estimate their positions through collaboration with one another to conduct position estimation. This requires schemes to be developed that could be used to propagate the location information throughout the network. Techniques for accomplishing this type of location estimation are known interchangeably as collaborative position location, network localization and cooperative localization [32]. Consequently, the afore-listed terms would be used interchangeably in this Thesis. More specifically, the term collaborative position location would be used sparingly except for mentioning purposes to avoid confusion with traditional position location techniques.

2.4.1. Location-aware Communication Applications

In conventional infrastructure-based position location systems, wireless devices measure signals from GPS satellites or cellular base stations referred to as anchor nodes to obtain their location estimates. However, the need to provide location estimates for multiple target nodes in the light of explosion in the number of deployed mobile devices and sensors has increased the need for self-aware nodes. Self-localization capability is a highly desirable characteristic for wireless networks and it is envisioned to play prominent role in the 5G wireless environment. A location-aware wireless device enables utilization of diverse services such as location determination for emergencies, location-sensitive billing, fraud detection, resource management, intelligent transportation systems as well as security and defence applications amongst many others. The difficulty of achieving highly precise location estimates in many indoor and outdoor wireless environments has led to a number of investigations into hybrid utilization of techniques and parameters together with accompanying positional algorithms [33]. This thesis therefore focuses on UWB approaches that could improve location accuracy and coverage in the 5G setting.

2.4.2. Cooperative Localization.

The goal of cooperative localization is for network nodes to have capability to self-localize such that every node would know its own state by way of a two or three dimensional positional details and other observables such as velocity and orientation. Cooperative localization typically consists of two phases. The first phase is the measurement phase during which nodes measure state information while the second phase is the location-update phase. However, the measurement phase is affected by uncertainties due to sources of noise, multipath, blockages, interference, clock drift and environmental effects [34]. It must be noted however that the underlying transmission technology and algorithm used are critical factors in how these sources of error affect measurement and indeed the performance of a cooperative wireless localization system. Therefore, more emphasis is now placed on software based localization systems since they can be implemented using the existing infrastructure [35]. Figure 2.9, illustrates a potential two target nodes T_a and T_b that wish to determine their respective locations. However, the nodes will not be able to localize due to insufficient number of connections represented by solid lines to base nodes (BN): BN_1, BN_2, and BN_3, BN_4 respectively. But this could be mitigated if the nodes connect using the dashed-lines for a node to node (N2N) connection. It could therefore be deduced that collaboration between nodes potentially improves positioning and coverage. This thesis furthers this view with UWB technology.

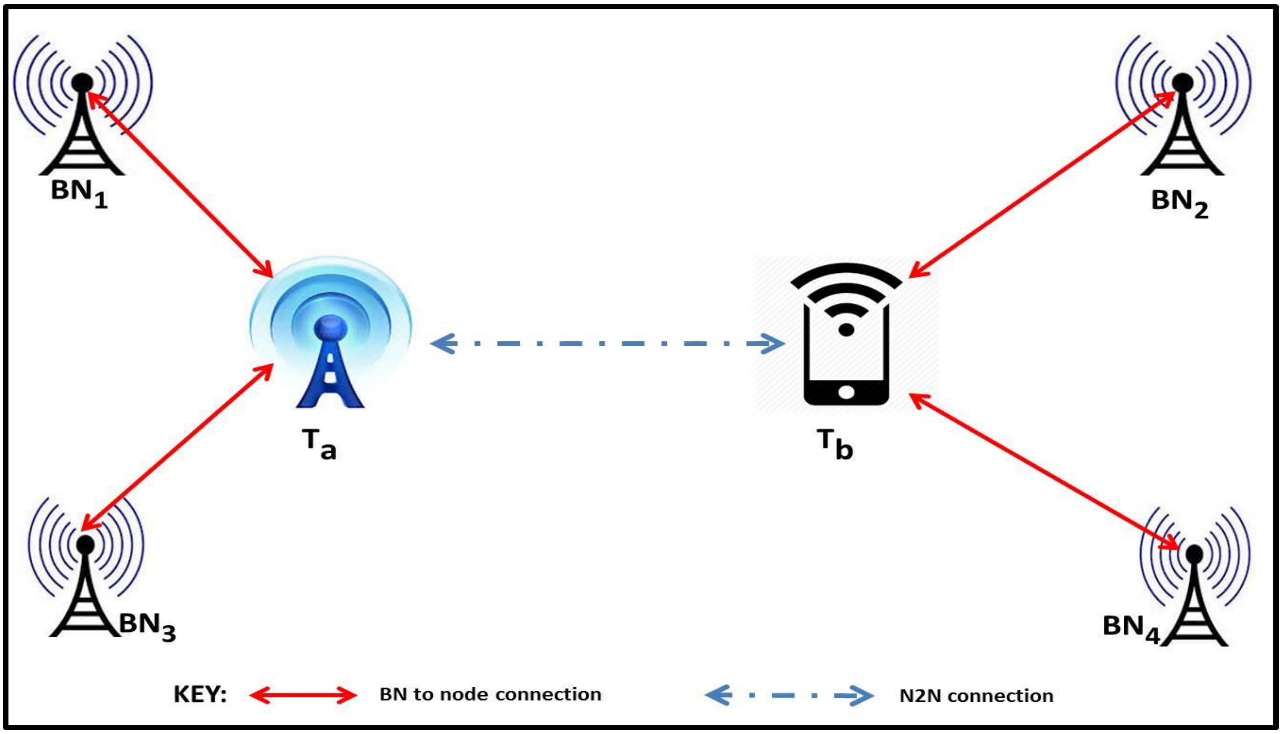

Figure 2.9 - Illustration of a Potential Cooperative Localization Scenario.

2.5. Overview of UWB Cooperative Localization.

2.5.1. Features of UWB Technology.

Until recently, only niche applications like radar or military communications deserved to be called UWB. However, numerous applications now utilize UWB radio frequency bands that covers from 3.1 GHz to 10.6 GHz standardized through the Federal Communications Commission (FCC). The most promising aspects of UWB radios are their potential for high-precision localization and the added advantages like wall penetration capability, low transmission power, simple receiver structure and high spatial resolutions. Moreover, UWB receivers can resolve individual multi-path components (MPC). Therefore; they are capable of accurately estimating the arrival time of the first signal path [36]. UWB systems can be classified into three different types namely carrier-less impulse radio (IR) - (IR-UWB), single carrier (SC) - (SC-UWB) and multi-carrier (MC) – (MC-UWB) [37]. It is believed that among these variants, IR-UWB is the most promising for ubiquitous communication and positioning since it has the advantage of a simple transceiver with fewer components and low-power transmissions, especially at the receiver end where it is not needed to locally generate the carrier, provide several stage mixing (multiplier) circuits amongst other requirements. This Thesis therefore adopts the IR-UWB as the core of its proposal for utilization of UWB in the 5G wireless network implementation.

2.5.2. Highlights of UWB localization standards.

The UWB IEEE802.15.4a WPAN standard supports a physical layer (PHY) for short-range low data rate communications and precise localization [38][39]. UWB has localization capacity for sub-meter accuracies at distances smaller than 300 meters while it utilizes third, fourth, and fifth-order modified Hermite polynomials (MHPs) as illustrated in Figure 2.10 [40]. For UWB systems operating under regulatory constraints, it is important to employ optimal pulse shapes in order to utilize available bandwidth and power while UWB channels are characterized by dense multipath that comes in clusters [41]. This thesis therefore explores UWB pulses with key spectral properties to determine optimal UWB channels. At present, in order to avoid harmful interference from UWB devices to existing systems, the emission limit mask for highest power spectral density emission level for indoor UWB devices is set at -41.3dBm/MHz with potential extension. According to IEEE, the IEEE802.15.4a UWB spectrum is subdivided into 14 bands each with a bandwidth of 528MHz as detailed in Table 2.1 [41].

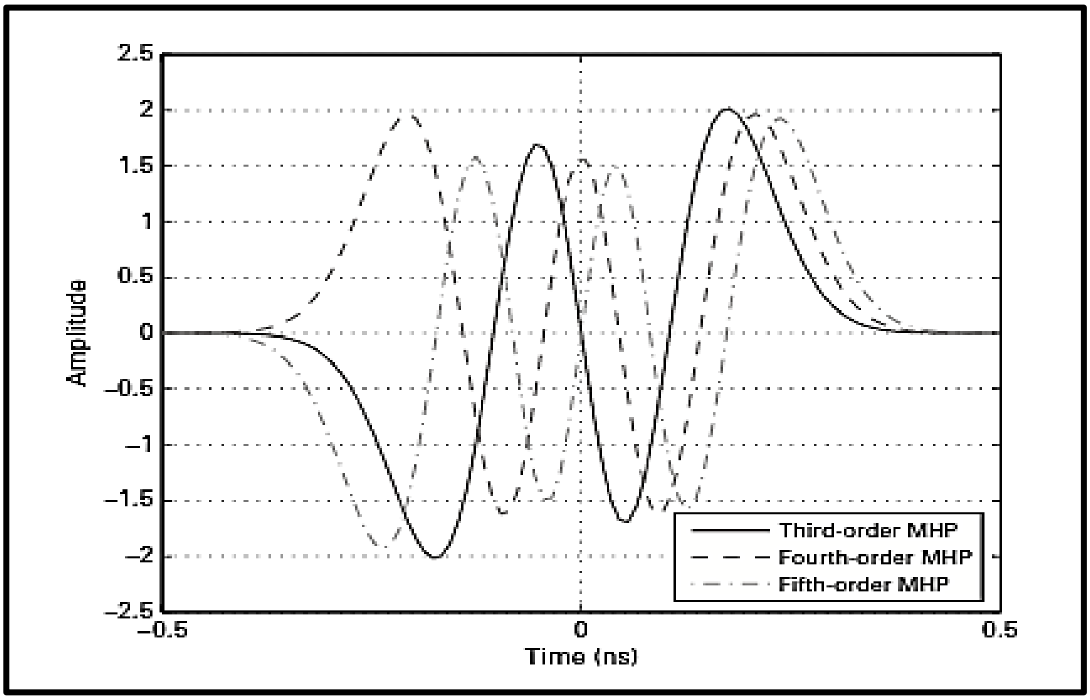

Figure 2.10. UWB pulses based on modified Hermite polynomials [41].

Table 2.1 - UWB channels for the IEEE 802.15.4a standard [41].

Channel No.	Center freq. (MHz)	Bandwidth (MHz)	UWB band	Mandatory
0	499.2	499.2	Sub-GHz	Yes
1	3494.4	499.2	Low band	No
2	3993.6	499.2	Low band	No
3	4492.8	499.2	Low band	Yes
4	3993.6	1331.2	Low band	No
5	6489.6	499.2	High band	No
6	6988.8	499.2	High band	No
7	6489.6	1081.6	High band	No
8	7488.0	499.2	High band	No
9	7987.2	499.2	High band	Yes
10	8486.4	499.2	High band	No
11	7987.2	1331.2	High band	No
12	8985.6	499.2	High band	No
13	9484.8	499.2	High band	No
14	9984.0	499.2	High band	No
15	9484.8	1354.97	High band	No

2.5.3. Overview of UWB propagation modelling.

Since deterministic channel model cannot be utilized to satisfactorily describe the wireless propagation environment, the UWB channel is usually expressed by propagation model in Equation 2.22 [42].

$$h(t) = \sum_{i=0}^{\infty} h_i \delta(t - \tau_i) \tag{2.22}$$

Where h_i is the amplitude of the ith channel path.

and τ_i is the delay of the ith channel path.

In UWB channels, each of the multipath components that come in clusters is otherwise resolved as a single path by narrowband signals. This can then be modelled with impulse response in Equation 2.23 where $\alpha_{m,n}$ and $\theta_{m,n}$ are multipath gain and phase respectively; and T_m is the arrival time of the first path of the mth cluster and $\tau_{m,n}$ is the delay of the nth ray inside the mth cluster relative to T_m.

$$h(t) = \sum_{m=0}^{\infty} \sum_{n=0}^{\infty} \alpha_{m,n} exp(j\theta_{m,n})\, \delta(t - T_m - \tau_{m,n}) \tag{2.23}$$

Although, theoretically, each channel realization can contain an infinite number of multipath components, but in practice, the number of multipath is usually considered to be finite by ignoring the very weak trailing paths. Therefore, when the multipath component $\theta_{m,n}$ is modelled as independent uniform random variables in $[0\ 2\pi]$ and the amplitude $\alpha_{m,n}$ as independent random variable, the power delay profile (PDP) can be modelled as equation 2.24 [42].

$$E\{\alpha_{m,n}^2\} = E\{\alpha_{m,n}^2\}e^{-T_m/\rho}e^{-T_{m,n}/\gamma} \tag{2.24}$$

Where ρ is the constant decay rate for clusters; and
And γ is the constant decay rate for the rays

Hence the cluster and ray arrival times are represented by the probability density functions (PDF) in Equations 2.25 and 2.26 respectively. Figure 2.11 is a representation of the Power delay profile of UWB Sale-Valenzuela (SV) channel for the UWB channel model [42].

$$p(T_m|T_{m-1}) = \mu exp[-\mu(T_m - T_{m-1})], m > 0 \tag{2.25}$$

$$p(\tau_{m,n}|\tau_{m,(n-1)}) = \lambda exp[-\lambda(\tau_{m,n} - \tau_{m,(n-1)})], n > 0 \tag{2.26}$$

It is believed that UWB will play significant role for cooperative localization in the 5G environment. Furthermore, software-based location algorithms would allow for ease of localization system implementation since existing hardware could still be used in the upcoming 5G environments [43] [44]. The possibility that nodes could extract information about their relative positions from signals already used for communication without any additional overhead is indeed a probable added advantage for UWB IEEE 802.15.4a WPAN standard.

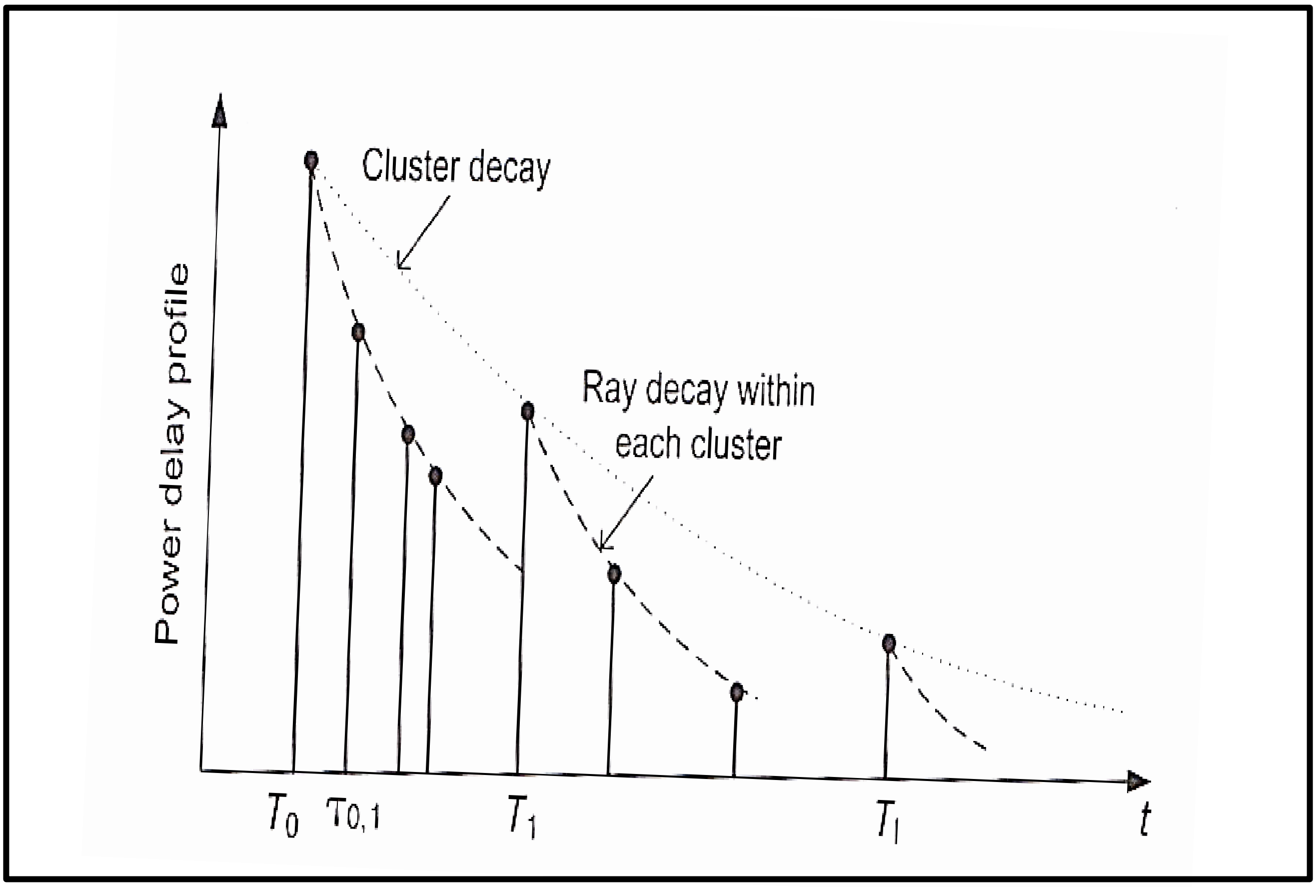

Figure 2.11. Power delay profile of the UWB Sale-Valenzuela Channel Model[42]

Review of Related Works

2.6. Related Works on UWB Optimal Localization Channel

2.6.1. Overview of UWB IEEE802.15.4a WPAN Standard.

2.6.1.1. UWB IEEE802.15.4a Standardization.

Figure 2.12 highlights the IEEE802.15 work group (WG) that handles the UWB standardization. The task groups (TG) IEEE 802.15.3a (TG3a) and IEEE 802.15.4a (TG4a) are the two TGs within 802.15 WG that develop their standards based on UWB technology [45]. While TG3a supports high-rate WPANs at short ranges of less than 1.0 metre, the TG4a supports low-rate WPANs. The IEEE 802.15.4a standard is an improved version of IEEE 802.15.4 and it provides data communications and high-accuracy positioning for low data rate networking with ultra-low complexity, ultra-low power consumption and scalable data rate of 110 - 851 kbps and 6.81 - 27.24 Mbps [46]. This standard can operate on three different bands.

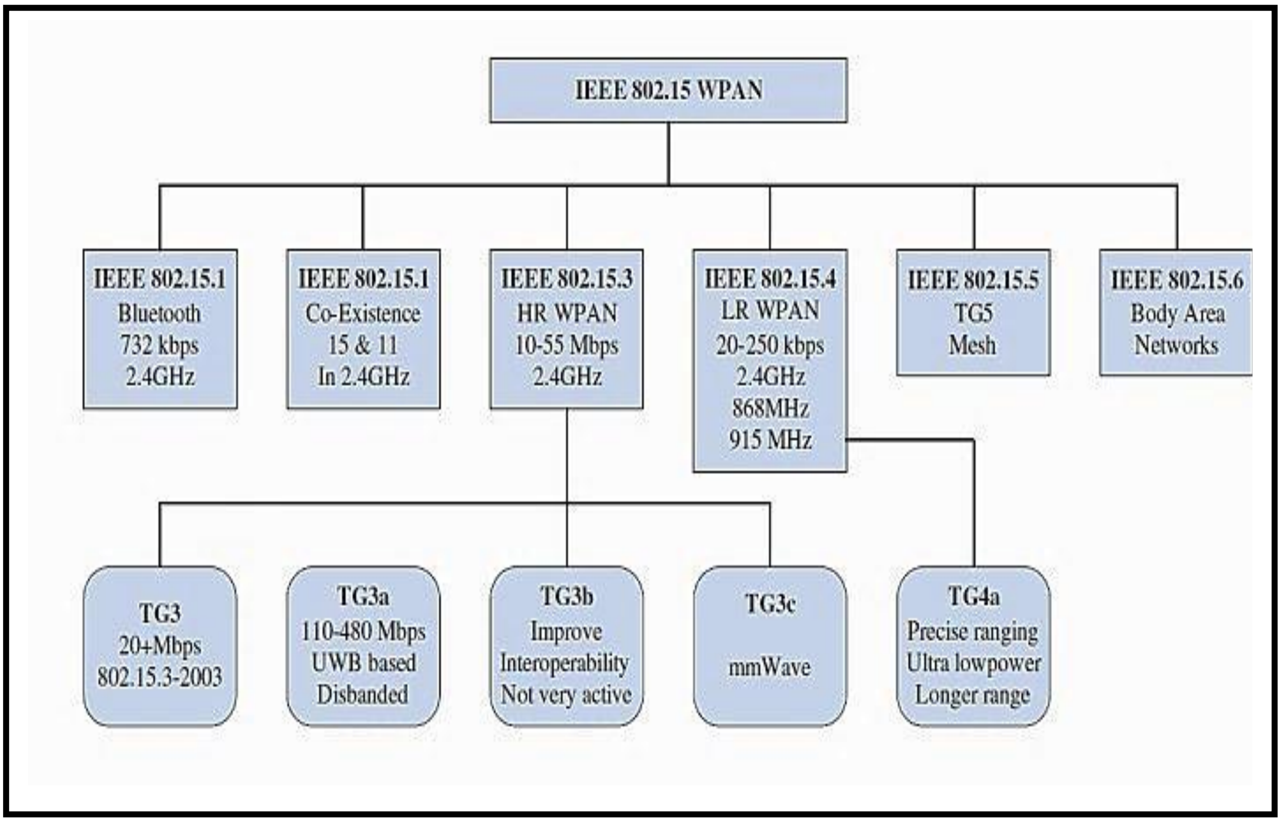

Figure 2.12. Highlights of the IEEE802.15 WPAN work groups [65]

The operating bands of the IEEE 802.15.4a are sub-gigahertz L band (250-750 MHz), the low band (3.1-5.0 GHz) and the high band (6.0-10.6 GHz). The objective of TG3a is a higher speed physical layer (PHY) enhancement for IEEE802.15 while TG4a provides an amendment to IEEE 802.15.4 for an alternative PHY aimed at both communications and high precision ranging capability. The specification is based on two optional PHYs for UWB impulse radio (IR) and chirp spread spectrum (CSS). ISO/IEC 26907-2007 standard outlines the specification for high rate UWB PHY and medium access control (MAC) layers for a decentralized complex system. Due to the importance of location-awareness in wireless networks, the TG4a developed UWB-based physical layer standard for short-range networks with precision ranging capability [46]. It could be shown with simulations that it is possible to measure the arrival time of UWB pulses with an accuracy that is comparable to or even better than that of current state-of-the-art technology [47]. The key requirement is an optimal UWB localization channel that could be adapted to comply with the FCC regulations for UWB emissions. This should be such as can also cope with signal interference of narrow-band communication services in the 3.1-10.6GHz band like WLAN standard IEEE802.1la. Therefore, most of the scenarios and test cases of this research utilizes radio access technology (RAT) covering UWB frequencies with its synonymous large bandwidths. Figure 2.12 highlights UWB bands labelled with corresponding centre frequencies.

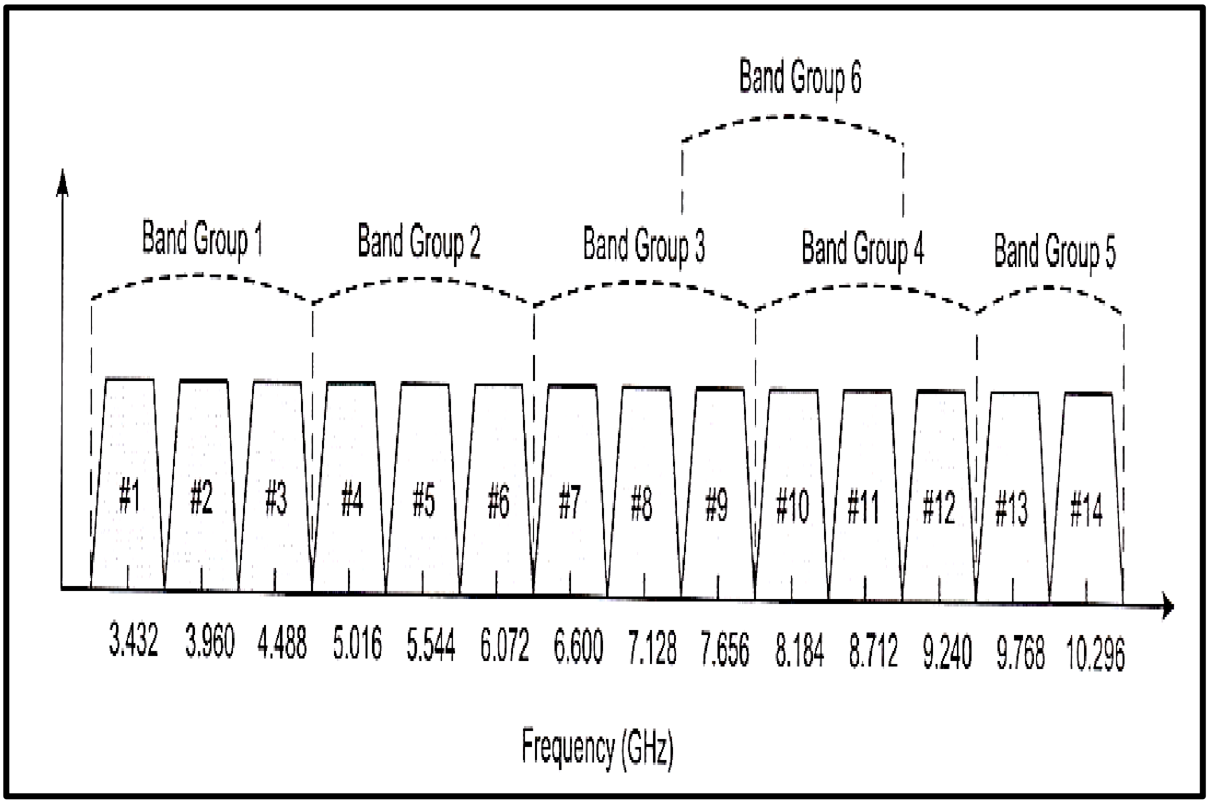

Figure 2.13. UWB bands labelled with corresponding centre frequencies [68].

2.6.1.2. UWB IEEE802.15.4a Regularization.

The unlicensed use of UWB technology is limited by FCC to applications such as imaging systems and vehicular radar as well as indoor and handheld UWB systems. In order to avoid harmful interference from UWB devices to existing systems, FCC has set the emission limit for each type of UWB implementation known as the emission mask. For example, the highest power spectral density (PSD) emission level for indoor UWB devices is -41.3dBm/MHz in the range of 3.1 - 10.6GHz as shown Figure 2.14 [48]. A UWB spectrum can be accessed either by generating a series of extremely short duration pulses or the aggregation of a number of narrowband subcarriers having bandwidth over 500MHz. This leads to two transmission approaches for UWB technology which are: IR and multiband orthogonal frequency division multiplexing (MB-OFDM). The IEEE802.15.4a specifies two optional signalling formats based on IR-UWB and CSS. The IR-UWB system can use 250-750MHz, 3.244-4.742GHz, or 5.944-10.234GHz bands; whereas the CSS uses the 2.4 - 2.4835GHz band. For the IR-UWB option, there is also a ranging capability, whereas the CSS signals can only be used for data communication [48]. It could be observed that much of current researches are gear towards MB-OFDM approaches, However, it is believed that the data communication and ranging capability of IR-UWB suggests a better opportunity for its application in the 5G setting.

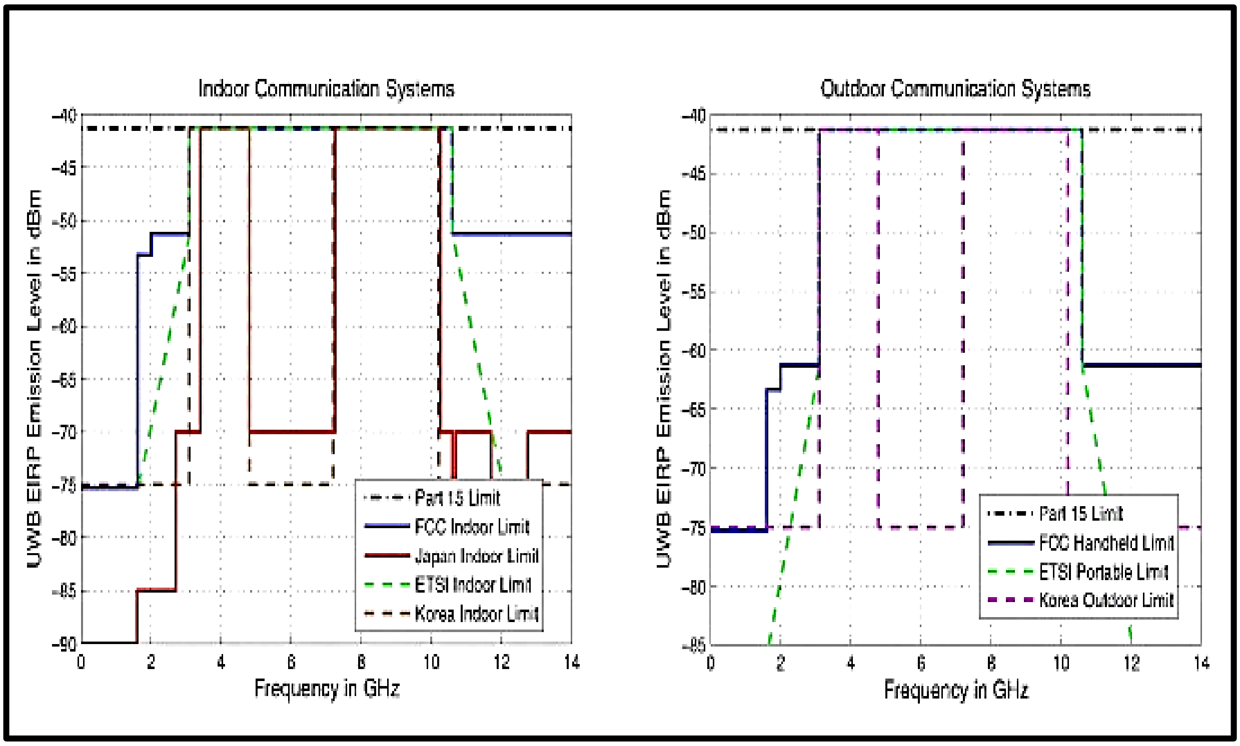

Figure 2.14. FCC Emission limits for UWB communication [48].

2.6.2. Highlights of UWB localization transmission approaches.

As highlighted in Section 2.6.1.2, the two main UWB localization transmission approaches are MB-OFDM and IR. In MB-OFDM, the UWB spectrum is exploited by transmitting OFDM symbols on several sub-bands using frequency hopping technique with large bandwidths synonymous with UWB. MB-OFDM accesses the entire UWB spectrum by altering the carrier frequency according to some time-frequency (TF) hopping pattern. However, the IR approach transmits pulses that occupy the entire allowable frequency band. IR transmits information by altering the amplitude, polarity or shape of the UWB pulse which corresponds to pulse position modulation (PPM), pulse amplitude modulation (PAM), on-off keying (OOK), or pulse shape modulation (PSM) [49]. The continuous transmission of uniformly spaced pulses gives rise to strong spectrum spikes occurring at integer multiples of the pulse repetition frequency. Therefore, time hopping (TH) and direct sequence (DS) techniques are adopted to mitigate the frequency spikes by randomizing the pulse train. TH and DS can also enable multi-access in UWB systems. Specifically, TH is often applied to low data rate UWBs with low pulse duty cycles while DS is suitable for medium to high data rate transmissions with high duty cycles.

2.6.3. UWB Optimal Localization Channel.

Optimal UWB localization channel is essentially a ranging accuracy endeavour. There are numerous recent research studies that aim at improving UWB ranging/localization accuracy. One research direction is joint estimation of range and location. In [50-52], it is shown that a two-step approach that uses independent decisions in ranging and localization steps is asymptotically optimal at high SNRs. However, it requires perfect estimates of delays, attenuations, and pulse shapes related to the received multipath components (MPCs), in order to construct an optimum correlation template at the receiver, which is very difficult to achieve in practice. Without perfect information of the channel parameters, such a two-step method returns unreliable TOA estimates during the ranging step. Since the measurements are separately performed at each reference node, without a constraint that all the measurements correspond to the location of the same mobile terminal, such approaches are suboptimal [53]. A better approach could be to make least commitment, where intermediate information is preserved and propagated till the end [54]. In other words, the received channel responses should not be discarded until a final decision regarding the target node location is made. In [55], the ranging thresholds are set so that the residual error is minimized. However, for [56] the ranging algorithm yields several range estimates with associated likelihood values; these 'soft' range estimates are then utilized in the positioning algorithm which employs the projections onto convex sets (POCS) technique. It real world, localization accuracy may often be much worse than that predicted by simulations. A major factor in the prediction gap is assumed to be due to the differences between theoretical noise models; which is commonly assumed to be Gaussian distributed and empirical noise characteristics. While [57] focuses on multi-hop localization, the prediction gap applies to localization systems in general if improper noise models are used. Similarly, the ranging noise in a UWB system may have a significantly different probability distribution than a Gaussian noise depending on the employed ranging algorithm [58] [59]. If not properly accounted for, this may yield inferior localization accuracy in practice. Further research is therefore needed to close the gap between theoretical and practical results in order to obtain an optimal UWB channel. This is discussed in Chapter 3 of this Thesis along with experimental outcomes.

2.7. Related Works on UWB Localization Techniques

2.7.1. UWB localization measurements.

The major task in wireless geolocation is to estimate the mobile positions; hence, the performance metrics can be the same as those for the evaluation of an estimation algorithm, including statistical error performance [60, 61]. Examples of this include bias and root mean square error (RMSE) as well as algorithmic computational complexity. Reference [62] held that UWB LOS/NLOS measurement metrics can also be adopted such that on a two-dimensional plane, the LOS distances between a mobile and at least three participating BSs can be used to locate a mobile terminal. However, one of the most important problems in wireless geolocation is the manipulation of the sources of errors such as multipath propagation, NLOS propagation, and multiple access interference. For localization in mixed LOS/NLOS environments, one may also have to consider the performance metrics in view of the error behaviour of the detection between the LOS and the NLOS components [62].

2.7.2. UWB detection Techniques.

The initial step toward estimating the mobile position in wireless geolocation is the characterization of LOS or NLOS paths. It is in fact sufficient to consider either the NLOS detection or the LOS detection. After identifying the LOS or the NLOS components, a further step usually is the NLOS mitigation after which the mobile position can be determined from those appropriate portions after the classification [63-66]. Based on statistical theory, the discrimination between the LOS and the NLOS components can be cast into a hypothesis-testing problem. This problem is an inquiry to determine to which of the two classes: (LOS or NLOS) that a given observation belongs. Various ideas have been proposed to decide whether the incoming path is LOS or NLOS and these works were based on range measurements. In Reference [67], the range is modelled as a linear combination of history times and if the NLOS is present, then measured range will be larger than the modelled range. Under certain conditions however, the rejection of LOS/NLOS hypothesis can be confirmed by analysing a residual rank test. For instance in [68-72], a set of four hypothesis-testing criteria were derived for the Gaussian NLOS probability model, where the prior probability density function (PDF) can be either known or unknown. Both the unknown mean and the unknown standard deviation of the NLOS are either deterministic or random. In [73] however, the NLOS range error is modelled as a non-Gaussian random variable. If the probability of NLOS corruption is small and the NLOS involves a large traveling TOA, the range measurements were then averaged for the test of outliers. If there is no NLOS component, the test variable is likely to be a normal-distributed random variable. Results showed however, that the test of normality performed accurately. Similarly, in [74], the PDF of the range measurement was approximated using some window functions around the samples to fit the estimated PDF to a known measurement PDF in order to determine whether a given BS signal belongs to the LOS or the NLOS of the MS.

In addition to the foregoing, Pearson's test statistic was used in [74] to compare the estimated PDF of the first arriving path with certain reference PDFs, such as Rayleigh, Rician, normal, and lognormal distributions. However in [75], four algorithms were proposed to identify the NLOS where the first method considers the cumulative distribution of the received signal envelopes, computes the test ratio, and then compares the computed test ratio with a bound. The second and the third approaches observe the level crossing rate and the average fade duration, respectively. The fourth algorithm takes into account the power of the received signal and then sees whether the computed signal power is close to an NLOS/LOS or not. Interestingly, in [76], the amplitude of signal components is used to observe a sudden decrease of the signal-to-noise ratio (SNR) from the LOS to the NLOS condition. While most techniques rely heavily on traditional estimation and detection methods, it is also possible to explore techniques based on estimation theory. Reference [77] is devoted to novel approaches that estimate detection and ranging parameters as realization of random variables. This research therefore explores this view further for a more accurate detection and ranging using UWB signals while it focuses on LOS sufficient enhancements.

2.7.3. UWB NLOS propagation

NLOS propagation is a prominent phenomenon in position location applications. Indeed, the presence of NLOS propagation can significantly degrade the localization accuracy of any collaborative position location method. Therefore, it is a necessity to develop methods to mitigate NLOS propagation. There exist many approaches and algorithms for mitigating the adverse effect of

NLOS propagation but mainly in the context of infrastructure-based or non-collaborative position location as in cellular systems. For example, in [78], the authors proposed two NLOS mitigation algorithms for time difference of arrival (TDOA) and TDOA/AOA position location schemes while in [79], the authors proposed a technique that utilized the statistics about mean excess delay, first detected path power to subtract the statistical value of NLOS error from the measurement range. In [80], the authors proposed a weighted LS scheme based on NLOS identification using multipath channel statistics. Also techniques based on Kalman filters [81] have been developed for NLOS mitigation. It is observed that the major difficulty of directly applying state-of-the-art NLOS mitigation techniques is the high computational complexity along with other additional requirements. It must be noted however, that UWB mitigation will neither increase the computational complexity nor put additional constraints on the minimum number of LOS range estimates. In view of these, a simple and effective NLOS mitigation method based on prior knowledge of NLOS condition is presented using the range estimate model. The range estimate model assumed as follows:

$$r_{ij} = d_{ij} + n_{ij} \qquad \text{if it is LOS} \tag{2.31}$$

$$r_{ij} = d_{ij} + n_{ij} + b_{ij} \qquad \text{if it is NLOS} \tag{2.32}$$

The very last term b_{ij} represents an unknown NLOS bias, which is positive and much larger than the noise standard deviation. Although exponentially distributed NLOS bias and Rayleigh distributed NLOS bias have been utilized but are hampered by errors and unduly large error margins. It must be noted however, that the most common way to statistically describe the NLOS bias is to model b_{ij} as being uniformly distributed. Despite the additional complexity associated with the corresponding signal processing, NLOS identification is a practically useful step to mitigate the effect of NLOS propagation. This research investigated NLOS mitigation which incorporated NLOS identification and knowledge about mean or minimum NLOS bias. Focus was specifically on incorporating NLOS mitigation method into the IPPM technique without significantly increasing computational complexity.

2.8. Related Works on UWB Mitigation Methods

2.8.1. UWB detection and ranging mitigation.

In many practical scenarios for UWB, detection and ranging activities involve NLOS paths between the target node and a reference node, which could degrade the positioning accuracy. A simple way to mitigate the NLOS effects is to identify the NLOS reference nodes and discard them during localization [82]. However, there is always the probability of wrong identification that could result in detection of a LOS reference node as NLOS, or vice versa. Moreover, if an NLOS reference node is not used for localization, the remaining number of available reference nodes and their geometry may not be suitable for obtaining an accurate estimate of the target node's location. Indeed, an NLOS reference node may carry useful information about the location of the target node, which can be utilized to improve the localization accuracy. Since the NLOS bias in a TOA estimate is always positive and is usually relatively lower than the error due to background noise, the location of the target node is bounded by a circle centred at the NLOS reference node. This circle has a radius equal to the range estimate of the NLOS reference node, and can be used as a constraint while calculating the location of the target node. However, Quadratic and linear programming techniques for NLOS localization are introduced in [83] [84] where the constraints in the algorithms are obtained from the NLOS reference nodes.

Another way to mitigate the effects of the NLOS bias is to use a weighted least squares algorithm as [85] canvases. It was argued that the contribution of the NLOS measurements may be weighted appropriately and suppressed in the localization algorithm. The weights may be obtained from the variances of the range estimates, or from different statistics of the multipath components of the received signal [86]. Another mitigation methods that utilized a database technique was explored in [87] based on the Kriging algorithm to address the effects of NLOS bias. First, during off-line stage, the NLOS bias errors are recorded at a number of target node locations. Then the universal Kriging technique is used to interpolate the NLOS errors at untrained locations. Thereafter, during the online stage, the NLOS error correction matrix obtained by kriging is used for improving the accuracy of the location estimate. An illustration of basic operation of the algorithm is depicted in Figure 2.15. It is believed that despite the numerous NLOS identification and mitigation algorithms in the literature, there is still room for improvement thus signposting research space for designing efficient UWB ranging localization techniques in practical NLOS scenarios. A major gap in literature is that much of the ubiquitous communication mitigation methods have been focused on MB-OFDM UWB systems. It is believed that multipath channel statistics based on IR-UWB could be a much more promising prospect as proposed in Chapter 4.

2.8.2. UWB multiple access interference mitigation.

UWB is an attractive radio technique for sharing the same frequency band by using very short pulses to spread the spectrum of the signal, enabling coexistence with other narrow band signals. However, UWB systems have the potential to interfere with each other and with other wireless systems. The influence of UWB interference to other wireless systems is of interest to this research. On the other hand, the interference that a UWB system suffers from other wireless systems, is also an important topic for study. In order to accommodate multiple users in the same channel, it is essential to use efficient multiple access mechanisms for localization. Orthogonal channels are mostly used since they can be assigned in time, frequency, code, or space domains. A commonly used multiple access technique in ad-hoc and sensor network systems is the carrier sense multiple access (CSMA) where only a single user is allowed to access the channel within a certain time period. However, due to the high bandwidth to data-rate ratio of UWB systems, such a single-channel approach for UWB multiple access may be wasteful as pointed out in [88] [89]. Instead, [90] introduced a time hopping (TH) TH-CDMA-MAC protocol for improved scalability and faster convergence time of the location estimates.

It must be noted however, that despite proper multiple access designs, there may still be interference from other users especially from a simultaneously operating piconet (SOP) and this may degrade the ranging accuracy. Hence, efficient interference mitigation algorithms may be required to achieve accurate localization. A generalized successive interference cancellation matching pursuits (GSIC/MP) algorithm is proposed in [91] for mitigating the effects of multiple access interference in CDMA systems. It provides reliable channel estimates for sparse multipath channels with weak direct paths. Since it can combat near and far effects, it can be used in scenarios where no power control is available. A method for mitigation of the multi-user interference in time-hopping and direct-sequence non-coherent UWB systems is introduced in [92][93]. A block diagram summarizing the basic principle of the algorithm is illustrated in Figure 2.16. To summarize the concept, first, a 2-D image of the signal is obtained by de-spreading it with the desired user's spreading code and observing the samples over multiple ranging symbols. When the rows of the 2-D image are observed, the desired signal repeats itself at each row, while the experienced interference has a random pattern since it has a different spreading waveform. Hence, interference can be suppressed by applying a non-linear filter on the columns of the 2-D image. Then, 2-D to 1-D conversion is performed followed by an appropriate TOA estimation algorithm.

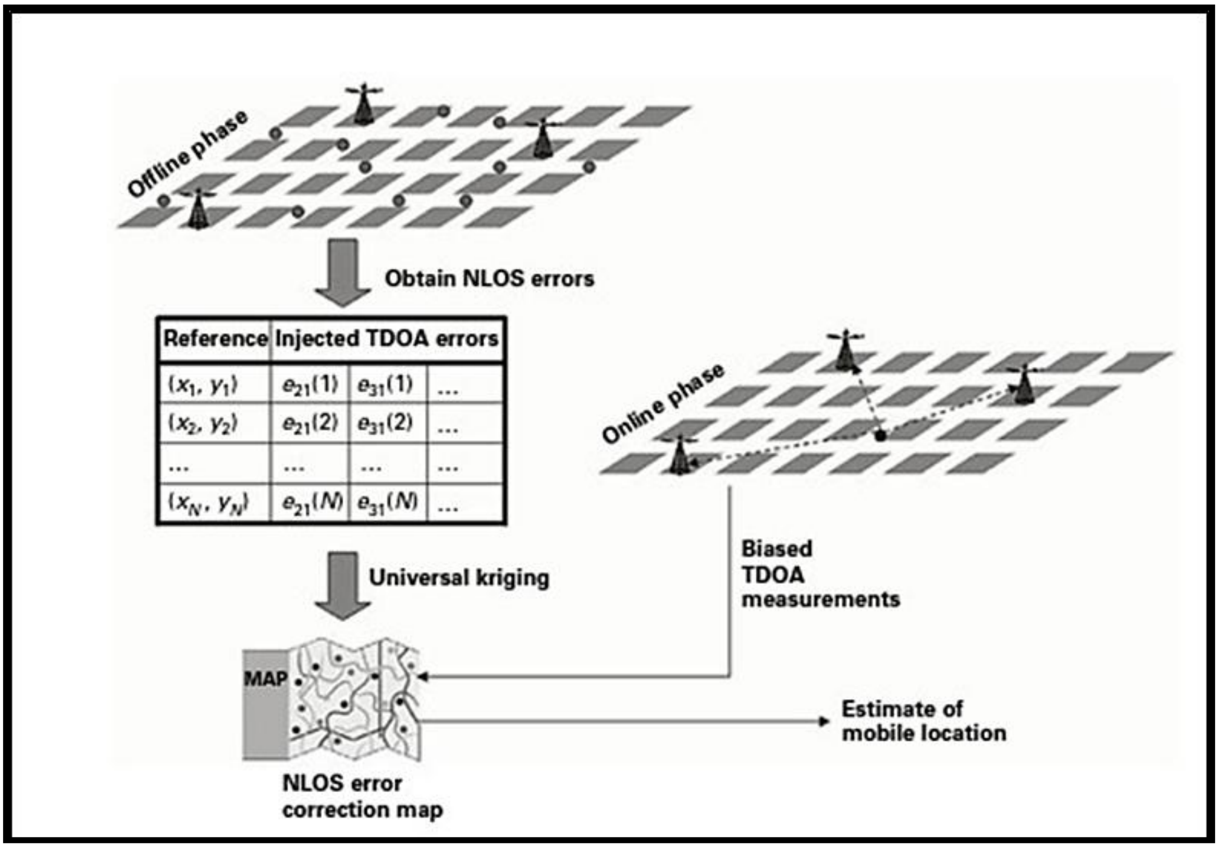

Figure 2.15 - An illustration of the Kriging Technique for NLOS Mitigation [87].

It is interesting to point out that while interference to the ranging system may be from other UWB transmitters, accuracy of UWB localization systems is also affected from narrowband interference. The impact of narrowband and wideband interference on the accuracy of practical UWB ranging systems is evaluated in realistic multipath environments [94]. Further analysis of the issue and development of efficient narrowband interference cancelation algorithms may be an interesting research direction. Another way of limiting the interference to other users in a network is to implement power control. In [95], it is shown that localization accuracy fluctuates or "fades" as a target node moves through the network of reference nodes. If power control is used, fluctuations in the localization error can be reduced and localization accuracy can be improved [96]. Intelligent power control techniques may also be used to minimize the interference to other users while simultaneously maintaining satisfactory localization accuracy. This research observes that most of the desirable features of UWB mitigation in literature utilize various forms of MD-OFDM UWB techniques while IR-UWB mitigation approaches appear to embody most of the features at low complexity of design. The research therefore proposes a IR-UWB multi-carrier type transmission pulse and template waveforms as the basis of its mitigation method in Chapter 4

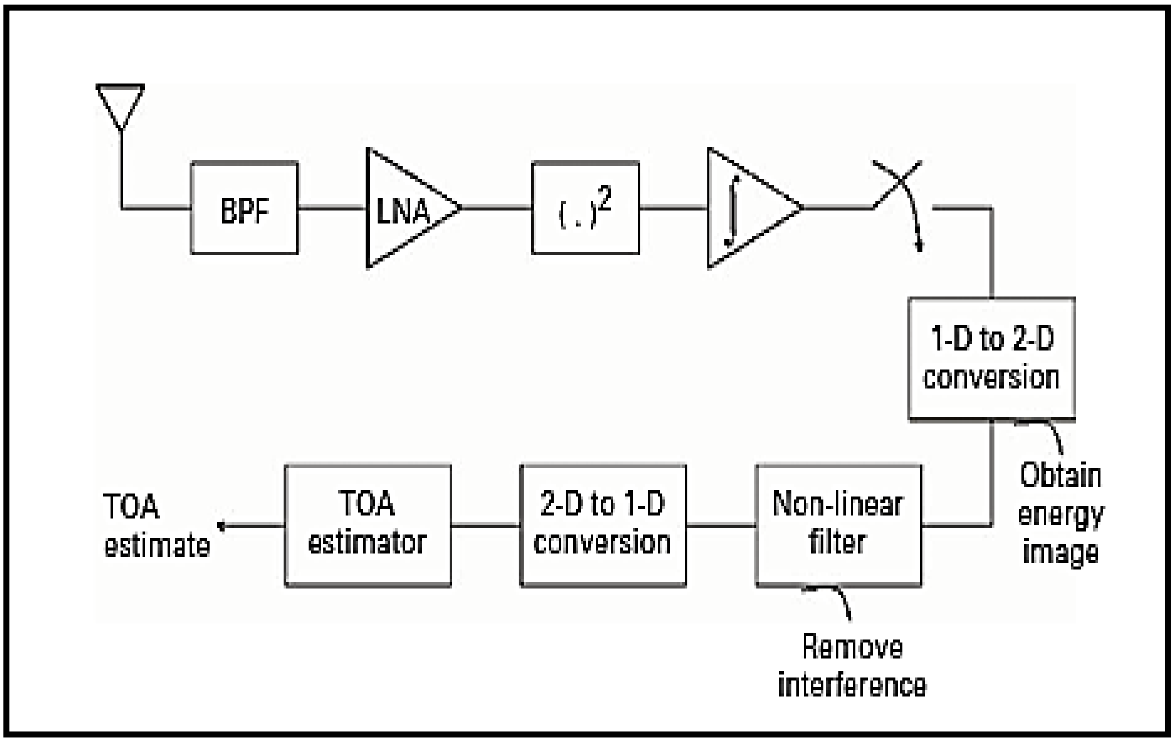

Figure 2.16 - Summary block diagram of UWB multiuser interference cancellation using non-linear filter. [119]

2.9. Related Works on 5G Wireless Architecture

2.9.1. Overview of wireless access technologies: 1G – 5G

Generations of wireless access technologies have played key roles that revolutionized the field of wireless mobile communications from 1G to 4G while 5G could be said to be around the corner. Figure 2.17 highlights trends in wireless communication systems from 1G to 5G.

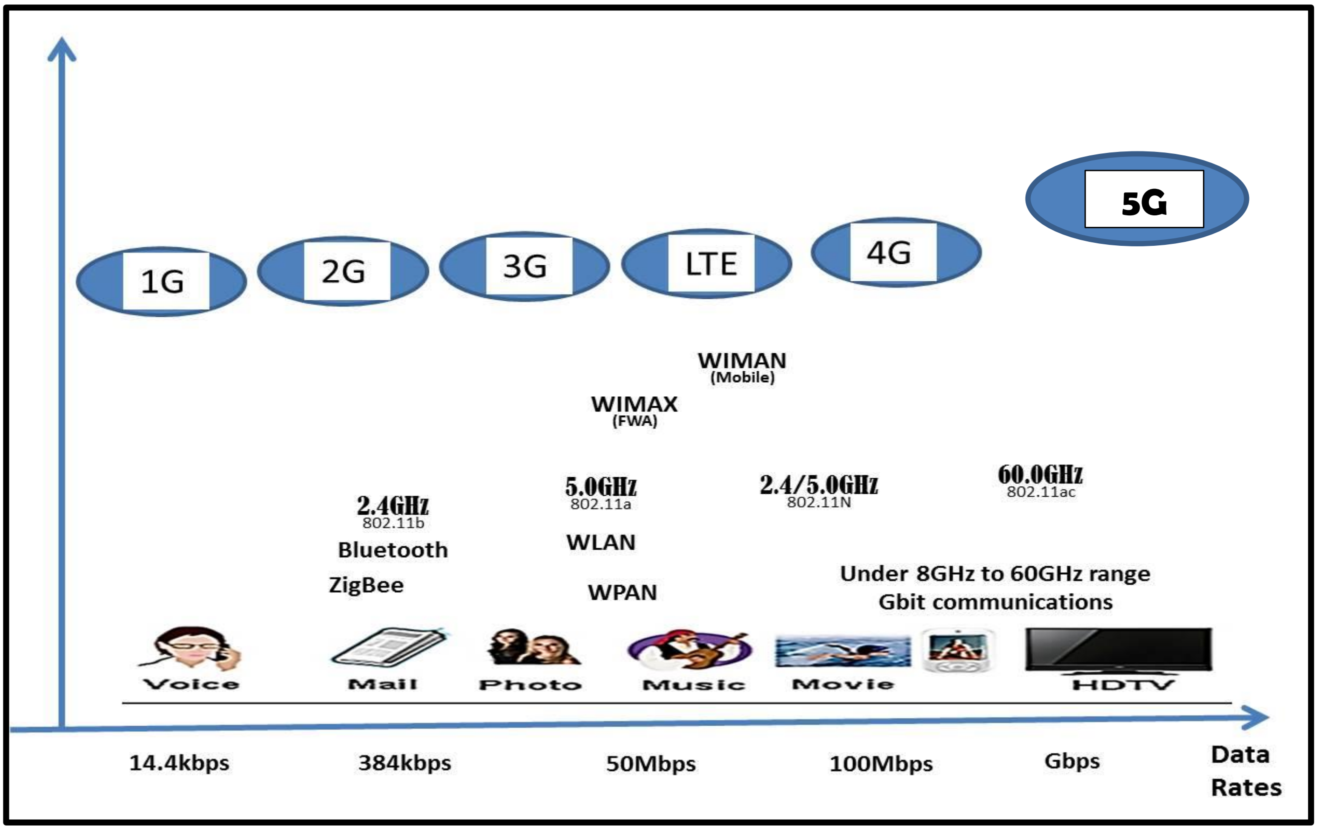

Figure 2.17. Adapted Trends in Wireless Communication Systems – 1G to 5G [97]

2.9.1.1. First Generation (1G) Wireless Access.

The 1G wireless access emerged in the early 1980s and it was analog. It featured mobile radio telephones and such technologies as mobile telephone system (MTS), advanced mobile telephone system (AMTS), improved mobile telephone service (IMTS), Nordic mobile telephone (NMT), total access communications system (TACS) and push to talk (PTT). The 1G period is based on the radio signal technology and voice was the main traffic at maximum data rate of 19.3Kb/s. Through 1G, a voice call gets modulated to a higher frequency of about 150MHz and up as it is transmitted between radio towers using a technique called Frequency-Division Multiple Access (FDMA). But 1G failed in some field such as overall connection quality, low capacity, unreliable handoff, poor voice links, and no security at all since voice calls were played-back in radio towers, making these calls susceptible to unwanted eavesdropping by third parties [97].

2.9.1.2. Second Generation (2G) Wireless Access.

The 2G system, fielded in the late 1980s and finished in the late 1990s, was planned mainly for voice transmission with digital signal at 64Kbps. 2G wireless cellular mobile services was a step ahead of 1G services with facility of short message service (SMS) unlike 1G that had its prime focus on verbal communication. Its vital eminent technologies were global system for mobile (GSM) and code division multiple access (CDMA). The 2G bandwidth was 30-200 KHz [97].

2.9.1.3. Enhanced digital GSM Evolution (EDGE) (2.5G)Wireless Access.

An intermediate generation of access technology is the 2.5G. This describes 2G-systems that have implemented a packet switched domain in addition to the circuit switched domain. It featured switched circuit and packet switched technologies like the general packet radio service (GPRS) and it provided higher data rate of 144Kbps. GPRS, EDGE and CDMA 2000 were the most prominent 2.5G technologies. The 2.5G system uses the GSM infrastructure on the basis of code division multiple access (CDMA) [97].

2.9.1.4. Third Generation (3G) Wireless Access.

In 3G, data and voice services were provided at speeds of 64Kbps – 2Mbpss. In addition to verbal communication, it includes data services, access to television/video, categorizing it into triple play service. 3G operates at a range of 2100MHz and has a bandwidth of 15-20MHz. High speed internet service, video chatting are the assets of 3G. With the help of 3G, we can access many new services too; one of such service is the global roaming [98].

2.9.1.5. LTE and WIMAX - 3.75G Wireless Access.

Long term evolution (LTE) and Fixed Worldwide Interoperability for Microwave Access (WIMAX) are the key technologies of 3.75G. They are aimed at improved mobile data services to supplement network capacity and provide a substantial number of users the facility to access a broad range of high speed services like on demand video, peer to peer sharing and composite Web services along with supplementary spectrum accessible for operators to manage their networks [98].

2.9.1.6. Fourth Generation (4G) Wireless Access.

The 4G wireless access is a successor of the 2G and 3G variants. 4G promises data rates of 100Mbps at the lower end and above 1000Mbps at the upper end. Its standards include the third generation partnership project (3GPP) which laid down the foundations of the long term evolution (LTE) advanced standards. 4G has its target values of peak spectrum efficiency for LTE Advanced systems set to 30bps/Hz and 15 Bps/Hz in downlink and uplink transmission respectively. Apart from the multiple access schemes, 4G also features enhanced multiple-input multiple-output (MIMO) channel transmission techniques and extensive coordination among multiple cell sites called coordinated multipoint (CoMP) transmission/reception techniques. Other 4G innovations are multimedia message service (MMS), digital video broadcasting (DVB), video chat, high definition TV content and mobile TV[98]

2.9.1.7. Fifth Generation (5G) Wireless Access.

It is believed that the exponential increase in the demand of the users would usher-in 5G to replace 4G with 5G using a technique which is explained by considering the case of the base station communicating with the mobile stations [99]. It is generally considered that 5G would cater for six key expectations that were not effectively addressed by 4G. These are higher capacity, higher data rate, lower End to End latency, massive device connectivity, reduced cost and consistent Quality of Experience provisioning [100]. Table 2.2 outlines a summary comparison of wireless access generations from 1G to 5G featuring deployment year, data bandwidth, technologies, and other network details.

Table 2.2. Comparison of generations of wireless access systems: 1G - 5G [101].

Features	1G	2G	3G	4G	5G
Start/deployment	1970-1980	1990-2004	2004-2010	Now	Probably 2020
Data bandwidth	2kbps	64kbps	2Mbps	1Gbps	Higher than 1 Gbps
Technologies	Analog cellular	Digital cellular	CDMA, UMTS EDGE	Wi-max LTE wi-fi	WWWW (coming soon
Service	Mobile telephony	Digital voice, SMS, packetized data	Integrated audio, video and data	Dynamic information access	Dynamic information access with AI capability
Multiplexing	FDMA	TDMA/CDMA	CDMA	CDMA, TDD/FDD	CDMA
Switching	Circuit	Circuit, packet	Packet	All packet	All packet
Core network	PSTN	PSTN	Packet	Internet	Internet

2.9.2. Categorization of wireless access by functionality

Wireless access technologies can also be categorized based on functionality as: the cellular networks, the broadband radio access (BRAN), WLAN, the digital voice & video broadcasting (DVB), the satellite communication networks, and the ad-hoc & sensor networks. The cellular access solutions include 2G network; the GSM, the 2.5G as well as the GPRS. All these are based on the TDMA applications. Also included amongst the cellular network access is the 3G network known as the universal mobile telecommunication system (UMTS) based on CDMA. The cellular based access solutions are proposed to offer 100Mb/s bandwidth in the future 4G/5G wireless. Additionally, the BRAN is based on frequency division multiple access (FDMA) and space time coding with proposal to offer 1Gb/s data rate in the 4G/5G environment. Finally, the DVB and satellite operate on orthogonal frequency division multiplexing (OFDM) as well as the ad-hoc sensor networks in a class of mobile and worldwide multimedia communications. This research accepts the view that proliferation of access systems necessitates integration of all legacy access technologies in the future 5G/Future wireless environment.[102]

2.9.3. The Concept of 5G Wireless.

A major conceptual thrust of 5G is the prospect of the world wide wireless web (WWWW). This is hypothesized as a real wireless world of communication without limitation that is expected to eradicate limitations regarding access and zone issues [103]. Other concepts include wearable devices with artificial intelligence (AI) capabilities and internet protocol (IP) version 6 (IPv6), where a visiting IP address is assigned according to location and connected network [104]. This is envisaged as one unified global standard for pervasive networks expected to provide ubiquitous communications. Users could simultaneously connect to several wireless access technologies and seamlessly move between heterogeneous wireless networks using the concept of "always best connected. Other concepts include dynamic radio resource management and distributed SDN [104].. Furthermore, the concept of high altitude stratospheric platform station (HAPS) systems is also expected to be implemented. 5G might also solve the problem of frequency licensing and spectrum management issues since the 5G terminals might have SDN with different modulation and error-control schemes [105]. It could therefore be inferred that 5G promises very exciting future for wireless access across the globe. However, issue of appropriate architecture still persists.

2.9.4. Challenges to 5G Architecture.

The major challenge of 5G architecture centres on integration of various standards in the long line of wireless access evolution. Additionally, integration of various standards requires systematic and time consuming approach as well as resolution of interconnectivity issues and knowledge sharing [106]. The challenge in the design of terminals is connected to the management of trade-offs between the flexibility of how to use the spectrum and needed space and power to a given platform. New methods offer design dimensions that allow the system to adapt to the opportunities and requirements of the terminals in a manner that could maximize the spectral efficiency and also maximize the battery power [107]. As a result of growing level of acceptance of wireless technologies in different fields, challenges and types of wireless systems associated with them are changing. However, for 5G, key challenges include avalanche of traffic, explosion of number of devices and diversity of requirements such as latency, reliability, low cost and energy consumption. This multiplicity of requirements is in turn stretching the limits of available technologies [108]. Additionally, vision of super core is based on IP platform that allows all network operators (GSM, CDMA, Wi-Max, Wire line) be connected to one super core with massive capacity single network infrastructure. It is however believed that implementation of the super core concept is also a challenge despite its promising expectation [109].

2.9.5. Visions for 5G Architecture.

One of the most perplexing problems facing deployment of 5G technology is how to make future devices to seamlessly access several different legacy mobile and wireless networks. Moreover, notwithstanding the widely agreed notion that 5G wireless should have seamless integration with an all-IP core, issues regarding approach and the best architecture still persist. Nevertheless, three views have become most prominent [110]. The first of these three views proposes a multi-nodal device that lets the user, device, or network initiate handoff between networks without the need for network modification or interworking devices. The second proposal foresees an overlay network consisting of several universal access points (UAP) supporting multiple protocols that store user, network, and device information and also performs handoff as the user moves from one UAP to another. The third view outlines a single protocol device capable of automatically switching between networks such that will make it possible for wireless networks to support a common protocol to access satellite-based and terrestrial networks. This is referred to as the concurrent future wireless vision and has seamless terminal mobility in network layer 2 (L2) as its key enabling factor [110][111]. It could however be observed that the proposal for achieving L2 terminal mobility is not entirely novel. Pure L2 mobility solutions have been widely discussed especially in [112][113]. These research directions are especially geared towards the scalability issue such that standard Ethernet is solved with the transparent interconnection of lots of links (TRILL) protocol. The difference between earlier methods and the proposal of this research is two-fold. On the one hand, earlier solutions rely only on L2 mobility. This research however proposes to achieve terminal mobility between RSs aggregated at the same router at L2 using UWB, whereas terminal mobility across aggregated routers is supported at L3. On the other hand, the control procedures in [113] rely on target area update (TAU) messages exchanged between base stations, customer edge switches and serving gateways. However, in this research, IP media access control (IP-MAC) bindings are stored in a distributed hash table (DHT), distributed over the nodes. In line with the split between the data plane and the control plane, and the logically centralised control plane promoted by SDN, this research envisions a 5G setup where mobility is handled through IPv6 stateless address auto-configuration (SLAAC) [114]. A similar approach to the problem, only based on L2 mobility, is described in [115] where the authors promoted a hierarchical Ethernet transport network architecture (HETNA) compliant with the IEEE802.3 Ethernet standard, but operating differently, to solve the scalability issue of broadcast Ethernet.

It could be observed that with location-based MAC addressing schemes and forwarding mechanisms within HETNA domains, the authors promoted the adoption of Ethernet in the backhaul of cellular networks where the mapping between IP and MAC addresses is centrally stored in an address resolution system (ARS) [116]. To address the IP and MAC mapping issue, ARS proposes adoption of a distributed implementation that utilizes either DNS-like fashion or DHT concepts. However, this approach is considered to be limiting and constraints users. Authors in [117] thereafter explored cloud networking (CLOUDNET) concepts that are considered suitable for mobility and cellular network integration in 5G. Although the cellular networks have evolved into multi-radio access technology (multi-RAT) and multi-layer heterogeneous network, but they are gradually becoming incapable in the face of emerging mobile internet applications and increasing digital data. Moreover, traditional single-RAT base station deployments are becoming unbearable to operators due to operating and maintenance burden [118]. Therefore, some state-of the art techniques, such as cloud and SDN are gradually introduced to cellular networks by way of network architecture that are based on cloud RAN (C-RAN). It should be noted that whereas [110-111] only focused on L2 mobility, while [112-115] projects CLOUDNET concepts, much has not been said about a multi-layered core that integrates all these possibilities with UWB as overlay in an heterogeneous ecosystem envisaged for 5G setting. This research however, proposes interworking of L2 and L3 mobility that incorporates the CLOUDNET concepts with UWB as the core of a multilayers network for 5G environment. Meanwhile an internetworking at L2 that caters for L3 mobility with cloud applications at large is believed to be relevant for the design of the solution proposed by this research as a viable architecture for 5G using UWB considering the gaps identified in literature including [113], [114] and [115].

2.9.6. 5G Design Approaches.

The goals are to increase coverage; offload backhaul; provide fall-back connectivity; increase spectrum utilization and capacity per area. This form of architecture is expected to provide a consistent framework that integrates different centralized and decentralized approaches. For instance, this novel architectural concept can take advantage of the developed technology components in a scalable way. Some good examples are radio links, multi-node/multi-antenna technologies, multi-layer and multi-RAT networks, and spectrum usage. It must be stated that to efficiently support the vast range of identified approaches, an air interface providing a “one-size-fits-all” solution no longer seems to be the favourable choice. Instead, the air interface for the future mobile radio system should become more flexible, providing different solutions for particular cases and applications under a common umbrella framework [116]. For this purpose, waveforms, coding and modulation schemes, and suitable transceiver structures require investigation. Additionally, faster than Nyquist (FTN) transmission technique for increasing the data rate at the cost of higher complexity of the receiver design is most desirable. This research approaches 5G architecture based on the concept to ensure consistent integration of currently available and other newly developed technology components. D2D communication using UWB is explored so that user-plane traffic does not pass-through any network infrastructure in order to free-up the licensed spectrum.

Unlike the traditional communications where traffic has to go through the BS even if the users are within short range of each other, D2D techniques allow nodes to transfer data directly to each other without traversing the BS or a core network. D2D communication in cellular network can be categorized into both In-Band and Out-Band based on the spectrum in which D2D communication occurs. The motivation for choosing In-Band communication is usually the high control over licensed spectrum. In-Band communication can be further divided into both underlay and overlay modes. In underlay D2D communication, cellular and D2D communications share the same licensed spectrum. In contrast, D2D links in overlay communication are given dedicated cellular resources. The motivation behind using Out-Band (such as ISM 2.4G) D2D communication is to eliminate the interference between D2D and cellular link. The majority of D2D communication literatures focus on the In-Band pattern, and the main research aspects are the interference issues between D2D and cellular communications and resource allocation. Nevertheless, some other researchers propose utilizing the Out-Band pattern so that the cellular spectrum is not affected by the D2D. Moreover, the network controls the radio resource usage of the direct links to minimize the resulting multi-user interference [116].

It is believed that filtered and filter-bank-based multi-carrier schemes are considered potential new waveform candidates for the future mobile radio system because they allow for efficient use of fragmented spectrum, and facilitate spectrum sharing with other services and applications. In the context of advanced transceiver design, full duplex transmission seems to be a promising technology, allowing a node to simultaneously transmit and receive a signal, thus increasing the spectral efficiency of the link. The new scenarios will also yield the introduction of new classes of devices and services, which should be efficiently supported by appropriate multiple access (MA), medium access control (MAC), and radio resource management (RRM) techniques. Improvements on multi-node/multi-antenna (MIMO) technologies are addressed to achieve the performance and capability targets of 5G wireless systems [117] [118]. Moreover, MIMO is considered most suitable in order to deliver very high data rates and spectral efficiency, as well as enhanced link reliability, coverage, and energy efficiency with advanced inter-node coordination. Consequently, this Thesis proposes the 5G-COMUSA which that utilizes an IR-UWB network overlay and chapter 5 espouses the various levels of the proposed 5G-COMUSA architecture designs along with D2D connectivity schemes. The chapter contributes to the on-going discourse on future 5G architecture with 5G-COMUSA as a probable architecture that utilizes UWB for localization as well as device-to-device and device-to-relay station signal links in 5G setting.

Research Overview

2.10. Research Hypothesis Scenario and Methodology

2.10.1. Hypothesis:

UWB cooperative wireless identification is essentially a hypothesis testing problem and the model adopted for this research is depicted Figure 2.18; where the source block generates one of the possible outputs which could either be NLOS or LOS hypothesis. The random observations are generated based on the condition in the decision rule block of probability density function (PDF) $f(\{\cdot\,|H_0\})$ or $f(\{\cdot\,|H_1\})$ while the likelihood ratio $\wedge(\mathrm{r})$ is compared with a threshold, and then a decision is made on whether LOS or NLOS is available. One of the methods used for LOS/NLOS hypothesis is the Rician K-factor generally used as a power ratio LOS and NLOS component to form a hypothesis testing to identify NLOS situations [119]. For instance, given a conditional power delay profile (PDF) of K under LOS and NLOS situations, to determine the K_{th} threshold, the probability of false alarm K is as stated in Equation 2.33; expressed on the decibel scale and defined where K_{dB} under LOS and NLOS is Gaussian. Additionally, the mean and standard deviation (STD) of $f(\{K_{dB}|LOS\}$ and $f(\{K_{dB}|NLOS\}$ are given as (μ_1 σ_1) and (μ_0 σ_0) respectively while the K_{th} threshold is the interception expressed mathematically in Equation 2.34. Furthermore, the detection probability P_D of NLOS condition indicating that the NLOS hypothesis is true computed by expression in Equation 2.35 while that of NLOS false alarm probability
condition is Equation 2.36.

$$K_{dB} = 10log_K \quad (2.33)$$

$$K_{th} = \frac{(\sigma_0^2\mu_1 - \sigma_1^2\mu_0) - \sqrt{(\sigma_0^2\mu_1 - \sigma_1^2\mu_0)^2 \; -(\sigma_0^2 - \sigma_1^2)\left(\sigma_0^2\mu_1^2 - \sigma_1^2\mu_0^2 - \sigma_1^2\sigma_0^2 In\,\frac{\sigma_0 P(H_1)}{\sigma_0 P(H_0)}\right)}}{(\sigma_0^2 - \sigma_1^2)} \quad (2.34)$$

$$P_D = \int_{-\infty}^{K_{th}} f(K_{dB}^{NLOS} = k)\,dk = 1 - Q\big((K_{th} - \mu_0)/\sigma_0\big) \quad (2.35)$$

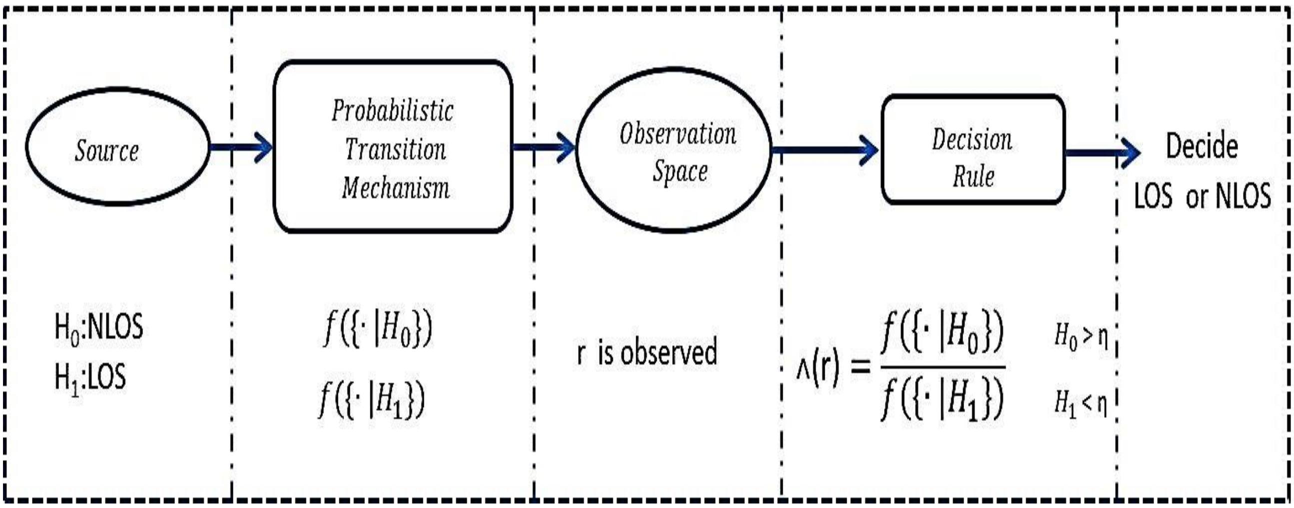

Figure 2.18:- Research Hypothesis Model for ULOSTECH LOS Sufficient Identification.

$$P_F = \int_{-\infty}^{K_{th}} f(K_{dB}^{NLOS} = k)\, dk = 1 - Q\big((K_{th} - \mu_1)/\sigma_1\big) \qquad (2.36)$$

It is believed that single node IR-UWB identification techniques could enable precise ranging and localization by incorporating extremely short duration pulses. In this case, the multipath component of the received signal can be well resolved which makes it very promising for localization. Consequently, channel models of UWB have been extensively characterized for LOS and NLOS conditions. However, these techniques have the disadvantage that they may mistakenly detect non-dominant direct path channel condition as NLOS because the direct path (LOS) in this case is not the strongest signal but still detectable by appropriate receiver architecture. This then demands other techniques to address the short comings as investigated in this research.

2.10.2. Scenario

The research investigated a scenario that foresees a 5G/Future wireless cell with a moderately high density of highly cognitive relay stations (RS) than base stations (BS) while there will always be enough mobile stations (MS) to collaborate within ubiquitous spatial distances of 50m between devices as envisages for the 5G setting. It is thus proposed that this scenario could also potentially allow for RS-MS link and MS-MS link to be implemented with unlicensed IR-UWB links. Therefore, given this scenario, the algorithm developed was used to compute positioning parameters in a cooperative format for specific MS requests for location positioning determination. Figure 2.19 is the pictorial representation of the research scenario. The underlying principle is that nodes would help one another to determine their location. This would be done in spite of their inability to independently determine their individual positions. With the potential of a cooperative localization algorithm, nodes are expected to work together in a peer-to-peer manner to make measurements which would then be relayed to the MS for computation using a highly scalable algorithm. This scenario is believed to potentially free-up the licensed spectrums in node to node and node to RS communications.

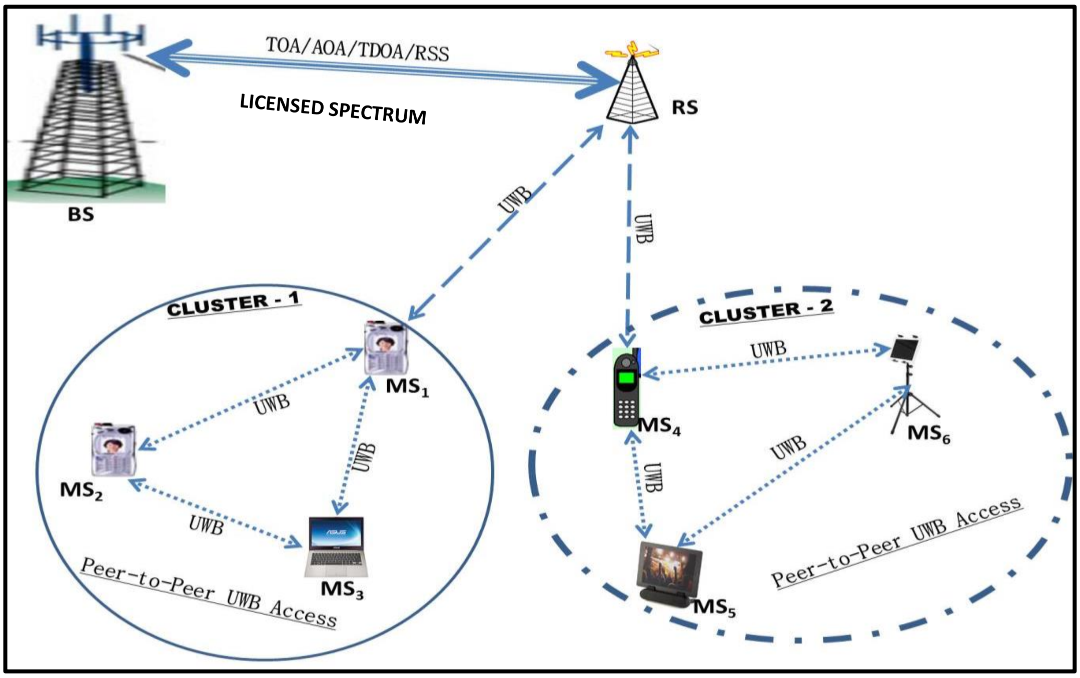

Figure 2.19. Schematic Scenario for 5G/Future Wireless Cooperative Localization using UWB.

2.10.3. Methodology

The problem is formulated as determining the position of a node on a general two-dimensional plane with a number of participating BS receivers. Each participating BS receiver is assumed to receive either a LOS or an NLOS component of the transmitted UWB signal. The 2 step *ULOSTECH* technique is then used to transform a number of the TOAs into mobile position and the coordinates which are then reviewed. After the TOAs are estimated and reviewed, the effective TOA will be passed onto the estimator to determine the position of the node. It is however assumed that for any given estimation process, the instantaneous TOA and the position of the node are constant. It is further assumed that the estimator is unbiased such that equation 2.37 is true and its estimation error variance can be expressed as equation 2.38.

$$\widehat{\tau_b} = \arg min \ a_b^2(\tau)E_s - 2a_b\ (\tau) \int_0^{T_0} \Re\left(r_b^*(t)s(t-\tau)\right)dt \qquad (2.37)$$

T_0 is Where $a_b\ (\tau) = \sqrt{K\ (d_0/c\tau)\frac{1}{2}\gamma b}$ is the path gain as a function of the TOA τ,

$\Re(\cdot)$ is the real part of the transmitted signal,

the observation period in which the TOA and the node position are constant.

Assuming unbiased estimator, the estimation error variance is given by equation 2.38:

$$E_{nb(t)}\{\widehat{\tau_b} - \tau_b\} = 0 \qquad (2.38)$$

In the second stage of the node position estimation process of the *ULOSTECH*, the TOAs from either NLOS or LOS are computed and the variance of the TOA perturbation is determined to enable assignment of LOS TOA vector. The initial value of the node position is then optimized using the least square (LS), weighted least square (WLS) and maximum likelihood (ML) criteria respectively and the root mean square error variance is also determined. The algorithm modelling and simulation for *ULOSTECH* is detailed in Chapters 4 while the proposed mitigation methods are outlined in chapter 5.

2.11. Summary

This chapter has reviewed the background information necessary to understand the rest of this thesis regarding UWB IEEE802.15.4a cooperative localization in 5G setting. The chapter also provides a review of related works by other researchers in the field which helped to inform the author's decision to provide solutions that supersede the current state of the art. It could be observed that very little literature considered the possibilities of IR-UWB overlay concurrent super-core network to cater for in-band ubiquitous simultaneous communications and localization in the 5G setting.

CHAPTER THREE

IR-UWB LOS Sufficient Localization for 5G

3.0. Chapter overview.

3.1. Prospect of ULOSTECH – The IR-UWB LOS sufficient localization for the 5G setting.

3.2. ULOSTECH modelling.

3.3. SIMULATION EXPERIMENT 3.1 – Assessment of ULOSTECH IEEE.802.15.4a optimal channel model realization

3.4. SIMULATION EXPERIMENT 3.2 – Assessment of mis-timing probability for ULOSTECH channel sensing.

3.5. SIMULATION EXPERIMENT 3.3 - Determination of shadowing variance for ULOSTECH propagation in LOS and NLOS conditions

3.6. SIMULATION EXPERIMENT 3.4 - Determination of ULOSTECH root mean square errors for position estimates in LOS and NLOS conditions

3.7. ULOSTECH positioning mitigation

3.8. SIMULATION EXPERIMENT 3.5 - Assessment of ULOSTECH NLOS mitigation technique

3.9. Summary.

IR-UWB LOS Sufficient Localization for 5G

3.0. Chapter Overview

This Chapter focuses on the *ULOSTECH* algorithm for LOS sufficient IR-UWB localization. It presents the derivation and modelling of ULOSTECH along with key results of simulation experiments in MATLAB environment. These experiments include ULOSTECH sampling variance, RMSE as well as cluster decay. Other experiments include UWB IEEE.802.15.4a optimal channel mis-timing probability for IR-UWB-based estimation and multiple channel LOS/NLOS conditions in three scenarios covering least square (LS), weighted LS (WLS) and maximum likelihood (ML) estimates methods. The chapter concludes with ULOSTECH positioning mitigation technique for optimal UWB localization channel in a 5G setting.

3.1. Prospects of ULOSTECH – IR-UWB LOS Sufficient Localization for the 5G Setting

In sections 2.5, 2.6 and 2.7 of Chapter 2, in this thesis, UWB technology along with a review of related UWB localization works were highlighted. Simulation experiments of the various facets of the ULOSTECH model in MATLAB environment suggests of a new peer-to-peer WLAN that satisfies the vision for the 5G setting. On the one hand, ULOSTECH does not require access at a peak data rate that could consume the full bandwidth of the transmission medium and neither does it require a conventional access protocol. This is because the UWB bandwidth is typically much greater than the peak bandwidth required by any ad-hoc radio node in operation as of the present. More specifically therefore, ULOSTECH utilizes IR-UWB capability to enable an overlay network that supports combined D2D communication and localization. In a traditional cellular communication system network layout as shown in figure 3.1, mobile terminals (MT) require localization signals from at least 3 different BSs in order to calculate their position in two dimensions (2D). Moreover, the MTs operate independent from one another without any cooperation during positioning services and this puts strains on network resources [120]. ULOSTECH however, leverages cooperative positioning based on signal propagation delay estimation for a wireless communications system. Experimental investigations reveal that the ULOSTECH overlay method could enable large scale signal propagation models while numerical analysis provides lower bounds on the achievable positioning accuracy that spans parameters like cell size and user density. Additionally, pairs of nodes as well as clusters of devices could be interconnected within the same band for combined communication and positioning data exchange by one or more dedicated links. These are non-shared and unlicensed radio spectrum channels created by a time, frequency, or code division multiplexing scheme. It is suggested that the potential of ULOSTECH to address key network challenges will play significant roles towards the realization of envisaged scenarios in the 5G setting.

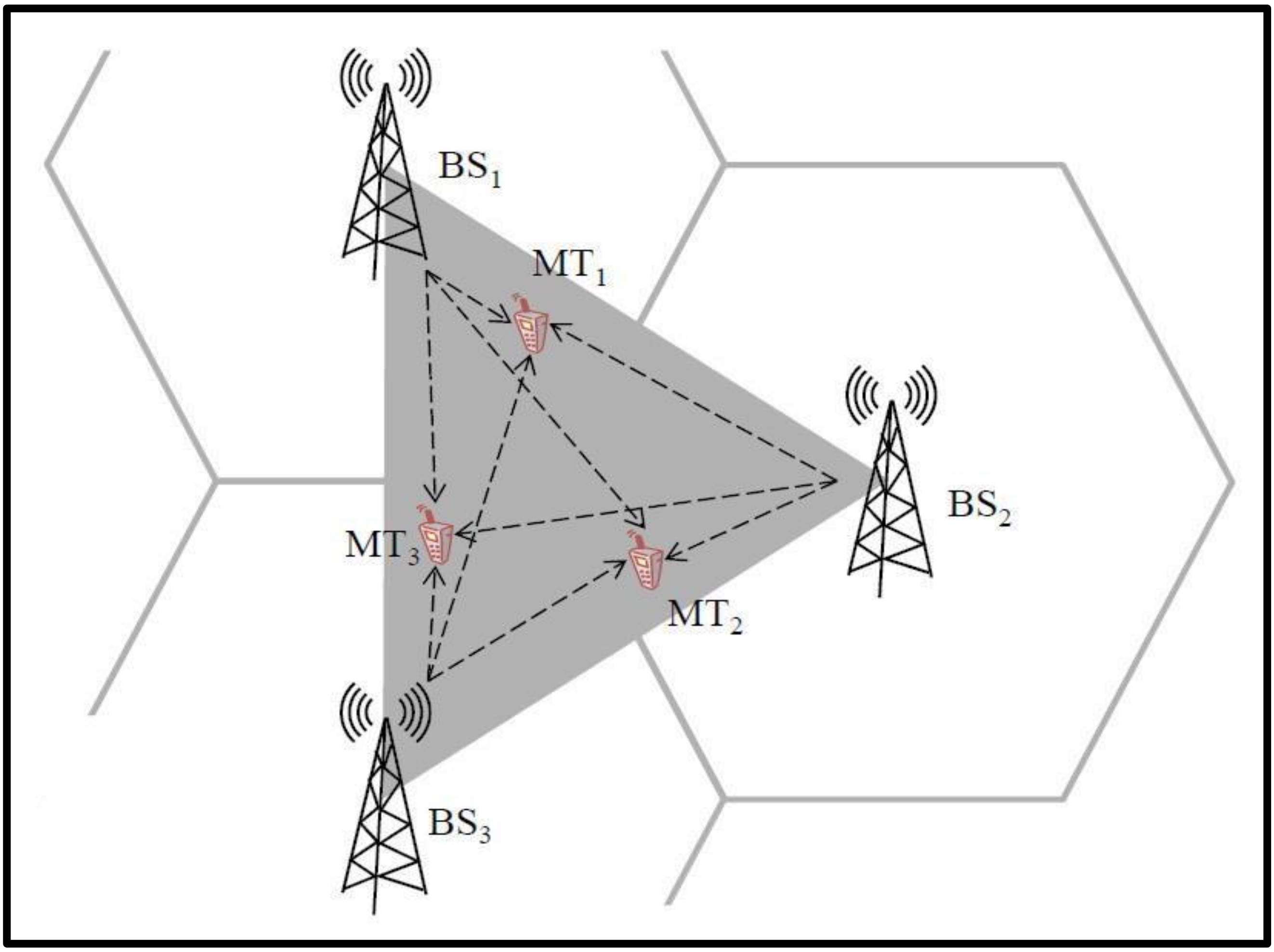

Figure 3.1. Current cellular positioning layout requiring devices to link 3 base stations for localization [120].

It could be observed that ULOSTECH simulation experiments indicate sampling variance and the RMSE that are within tolerable limits with improvement ratio of about 0.36 above traditional cellular standards. ULOSTECH also addresses the dominant challenges of NLOS in positioning propagations by modelling an algorithm that is able to accurately localize target devices irrespective of LOS or NLOS condition through a scheme that makes the presence of NLOS irrelevant to accuracy of the positioning service. Further ULOSTECH simulation experiments demonstrate a novel P2P WLAN scheme that heuristically establishes the optimum route for traffic flow. With no medium access protocol needed for ULOSTERCH D2D information exchange, collisions cannot occur and retransmissions is unnecessary. Moreover, the available capacity grows with the number of non-interfering channels created due to sufficient spatial separation. ULOSTECH therefore, presents characteristics that are comparable to a multi-hop wavelength-division multiplexed (WDM) network albeit with different dynamics and constraints. Results of simulation experiments suggest that application of these techniques provide a distinct WLAN advantage achievable only via IR-UWB radio technology, and therefore explores several opportunities based on this novel approach.

ULOSTECH further harnesses the capability of combined communication and localization to model an N2N–dissemination-based combined communication and localization scheme that has been successfully modelled in simulation experiments for large network scenario with higher density of devices. This utilizes a refined low system-load technique where each device adaptively chooses neighbouring nodes, updates its position estimate by minimizing a local cost-function, and then passes this updated position within the cluster database. This update process uses an N2N–dissemination-based scheme with about 1,000 comparable device density per unit area as large-scale networks that are expected in 5G setting. Neighbour nodes are selected from the range in which the strength of received signals is greater than an experimentally based threshold. More specifically, results of simulation experiments on the ULOSTECH large network N2N-dissemination-based combined communication and localization indicates that the sub-algorithm presents more accurate location estimation better than trilateration method and less complex than multidimensional scaling while its mean distance error is 1.024 – 4.64 less than that of distributed weighted multi-dimensional scaling (DWMDS) method. This suggests the capability for concurrent support of ultra-dense D2D localization along with communication links. The ULOSTECH ultra-dense large network D2D-propagation-based combined communication and localization scheme is presented in Chapter 4. The rest of this chapter details the mathematical modelling of ULOSTECH as well as simulation of its sampling variance and root mean square errors and NLOS mitigation technique.

3.2. ULOSTECH Modelling

This Section details the derivation and modelling of *ULOSTECH.* It entails an IR-UWB D2D overlay network in a 5G setting. We consider an IR-UWB overlay network containing clusters of N devices and 2N partitions of independent IR-UWB radio channels (RC) denoted RC_a, RC_b, RC_c.......RC_n and expandable to (RC_n + 1) with high density of RS in spatial proximity of less than 50m to clusters of devices denoted D_a, D_b D_c.......D_n and expandable to (D_n + 1). Furthermore, the BS is linked to RS by licensed spectrum signals while the RS to devices as well as D2D links is achieved via IR-UWB for combined communications and localization services as outlined in figure 3.2. However, the scheme for cluster formation and cluster head selection techniques are discussed in section 4.2. For the ULOSTECH modelling, this thesis envisions that accurate localization could be achieved irrespective of the presence of NLOS bias or not as LOS IR-UWB propagation would be enough for effective localization estimation. This is modelled as follows:

We consider

(A) A power matrix denoted N x N, where element $P_{a...n}$ represents the power needed for a successful transmission from device D_a to device D_n including the effects of path loss and fading.

(B) A second M x M, traffic matrix where element $T_{a...n}$ represents the traffic originating from D_a to D_n

It is assumed as follows: (Chapter 1, section 1.4 refers)

(A) The instantaneous TOA and the position of the nodes are constant

(B) The estimator is unbiased.

(C) True estimation will be based on maximum likelihood criteria given by (1.1); and here denoted equation 3.1.

$$\widehat{\tau_b} = \arg min \ \{a_b^2(\tau)E_s - 2a_b \ (\tau) \int_0^{T_0} \Re \left(r_b^*(t)s(t-\tau)\right)dt\} \tag{3.1}$$

Where $a_b \ (\tau) = \sqrt{K \ (d_0/c\tau)^{\frac{1}{2}}\gamma b}$ is the path gain as a function of the TOA τ,

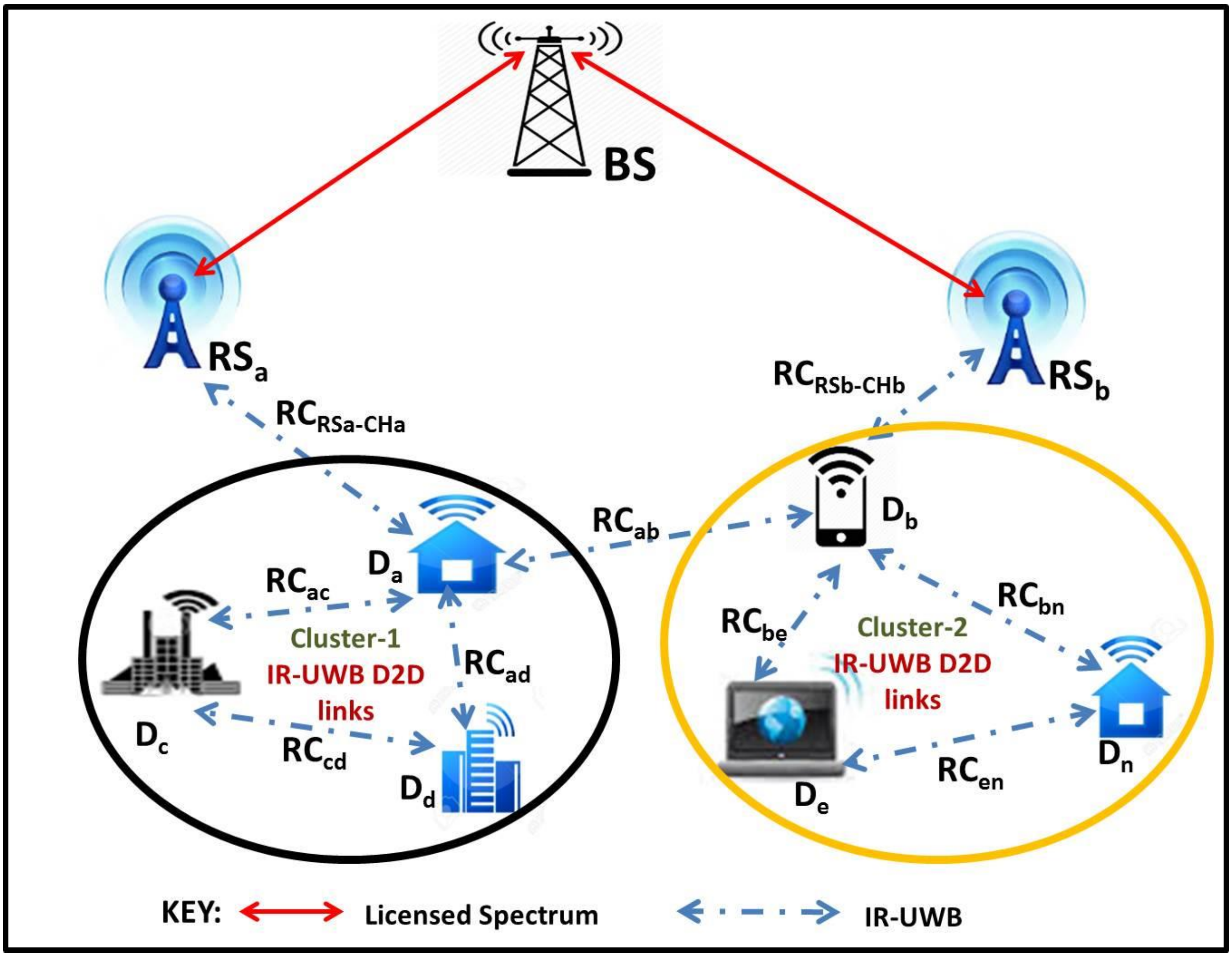

Figure 3.2. Proposed ULOSTECH combined D2D communication and positioning network layout

$\Re(\cdot)$ is the real part of the transmitted signal,

and T_0 is the observation period in which the TOA and the node position are considered constant.

Assuming unbiased estimator, the estimation error variance is given by equation 3.2:

$$E_{nb(t)}\{\widehat{\tau_b} - \tau_b\} = 0 \qquad (3.2)$$

If we consider likelihood expectation with respect to effective root mean square (RMS) bandwidth, then Equation 3.2 could be expressed as Equation 3.3:

$$E_{nb(t)}\left\{\left(\widehat{\tau_b} - \tau_b\right)^2\right\} = \frac{1}{\frac{E_s}{\sigma_n^2} 8\pi^2 \overline{\beta^2} a_b^2 \left(1 + \frac{1}{16\pi^2 \overline{\beta^2} \tau_b^2} \gamma_b^2\right)} \qquad (3.3)$$

Where $E_{nb(t)}\{\cdot\}$ is the expectation with respect to $nb(t)$

Therefore $\bar{\beta}$; the effective RMS bandwidth of the IR-UWB signal could be expressed as equation 3.4

$$\bar{\beta} = \sqrt{\frac{\int_{-\infty}^{\infty} f^2 |S(f)|^2 df}{\int_{-\infty}^{\infty} |S(f)|^2 \, df}} \tag{3.4}$$

wherein S(f) is the Fourier transform of the transmitted IR-UWB signal s(t); then we can consider the LOS TOA vector in Equation 3.5 by expressing the LOS distance as Equation 3.6;

$$\bar{\tau} = [\tau_{M+1} \quad \tau_{M+2} \quad \ldots \ldots \; \tau_B]^2 \tag{3.5}$$

$$\overline{\emptyset} = \frac{\partial}{\partial \boldsymbol{p}} \overline{\boldsymbol{d}}^T \; (\boldsymbol{p}) \; \in \; \mathbb{R}^{2x(B-M)^2} \tag{3.6}$$

Where $\overline{\boldsymbol{d}} = c\bar{\tau}$ is the LOS distance; $\emptyset$ can be expressed as Equation 3.7

$$\overline{\emptyset} = \begin{bmatrix} \cos(\emptyset_{M+1}) & \cos(\emptyset_{M+2}) & \cdots\cdots & \cos(\emptyset_B) \\ \sin(\emptyset_{M+1}) & \sin(\emptyset_{M+1}) & \cdots\cdots & \sin(\emptyset_B) \end{bmatrix} \tag{3.7}$$

Therefore $\emptyset_b$ can be defined as Equation 3.8

$$\emptyset_b = \arctan\left(\frac{y_b - y}{x_b - x}\right) \tag{3.8}$$

Where (x, y) is the node position and (x_b, y_b) is the position of the b^{th} RS.

Therefore, the possible likelihood expectation (PLE) vector and the LOS TOA variance vector are expressed as Equations 3.9 and 3.10 respectively.

$$\gamma = [\gamma_1 \quad \gamma_2 \cdots\cdots \quad \gamma_B]^T \tag{3.9}$$

$$\bar{\sigma}^2 = [\sigma_{M+1}^2 \quad \sigma_{M+2}^2 \cdots\cdots \quad \sigma_B^2]^T \tag{3.10}$$

In line with Equation 3.6, it could be deduced that:

$$\sigma_B^2 = E_{nb(t)}\left\{(\widehat{\tau_b} - \tau_b)^2\right\} \tag{3.11}$$

Therefore, if we take the first-order Taylor series around the true value of $\bar{\boldsymbol{\tau}}$ we have equation 3.12

$$\boldsymbol{\tau} = \hat{\boldsymbol{\tau}}\,(\boldsymbol{p}) + \left(\frac{\partial}{\partial \boldsymbol{p}}\bar{\boldsymbol{\tau}}^T\ (\boldsymbol{p})\right)^T \widehat{\left(\widehat{\boldsymbol{P}} - \boldsymbol{P}\right)} + \vartheta(\left\|\widehat{\boldsymbol{P}} - \boldsymbol{P}\right\|_E) \tag{3.12}$$

This can also be expressed as equation 3.12b

$$= \boldsymbol{\tau}(\boldsymbol{p}) + \frac{1}{C}\bar{\emptyset}^T(\widehat{\boldsymbol{P}} - \boldsymbol{P}) \tag{3.12b}$$

The pseudo-inverse of Equation 3.12 therefore results in equation 3.13

$$(\widehat{\boldsymbol{P}} - \boldsymbol{P}) = \mathrm{c}(\bar{\emptyset}\,\bar{\emptyset}^T)^{-1}\bar{\emptyset}\left(\bar{\bar{\boldsymbol{\tau}}} - \bar{\boldsymbol{\tau}}\,(\boldsymbol{p})\right) \tag{3.13}$$

When we take expectation of error square matrix $(\widehat{\boldsymbol{P}} - \boldsymbol{P})(\widehat{\boldsymbol{P}} - \boldsymbol{P})^T$ from Equation 3.13 with respect to $\bar{\bar{\boldsymbol{\tau}}}$ we have equation 3.14

$$E_{\bar{\bar{\tau}}}\left\{\left(\widehat{\boldsymbol{P}}-\boldsymbol{P}\right)\left(\widehat{\boldsymbol{P}}-\boldsymbol{P}\right)^{T}\right\}=$$
$$\mathrm{c}^{2}(\overline{\emptyset}\,\overline{\emptyset}^{T})^{-1}\,\overline{\emptyset}E_{\bar{\bar{\tau}}}\left\{\left(\bar{\bar{\boldsymbol{\tau}}}-\ \bar{\boldsymbol{\tau}}\,(\boldsymbol{p})\right)\left(\bar{\bar{\boldsymbol{\tau}}}-\ \bar{\boldsymbol{\tau}}\,(\boldsymbol{p})\right)^{T}\right\}\overline{\emptyset}^{T}(\overline{\emptyset}\,\overline{\emptyset}^{T})^{-1} \qquad (3.14)$$

$$=\ \mathrm{c}^{2}(\overline{\emptyset}\,\overline{\emptyset}^{T})^{-1}\,\overline{\emptyset}D\ \ \overline{\emptyset}^{T}(\overline{\emptyset}\,\overline{\emptyset}^{T})^{-1}$$

If we assume that both LOS and NLOS are present, we then introduce the error variance:
$\boldsymbol{\eta}\in\ \mathbb{R}^{(M+2)xl}$ as:

$$\boldsymbol{\eta}=\ [\boldsymbol{p}^{T}\quad \boldsymbol{l}^{T}]^{T} \qquad (3.15)$$

Therefore the analysis of $\boldsymbol{\tau}\,(\boldsymbol{\eta})$ results in equation 3.16

$$\hat{\boldsymbol{\tau}}\ =\boldsymbol{\tau}\,(\boldsymbol{\eta})+\ \left(\frac{\partial}{\partial\boldsymbol{\eta}}\overline{\boldsymbol{\tau}}^{T}(\boldsymbol{\eta})\right)^{T}\widehat{(\widehat{\boldsymbol{\eta}}-\boldsymbol{\eta})}+\ \vartheta(\|\widehat{\boldsymbol{\eta}}-\boldsymbol{\eta}\|_{E}) \qquad (3.16)$$

$$=\boldsymbol{\tau}(\boldsymbol{\eta})+\ \nabla_{\eta\tau}^{T}(\widehat{\boldsymbol{\eta}}-\boldsymbol{\eta})$$

But the Jacobian matrix $\nabla_{\boldsymbol{\eta}\boldsymbol{\tau}}$ is given by

$$\nabla_{\eta\tau}=\ \frac{1}{c}\begin{bmatrix}\widetilde{\emptyset} & \overline{\emptyset}\\ \boldsymbol{I} & \boldsymbol{O}\end{bmatrix} \qquad (3.17)$$

And $\widetilde{\emptyset}\in\ \mathbb{R}^{2\mathrm{xM}}$ is given by:

$$\widetilde{\emptyset}=\begin{bmatrix}\cos(\emptyset_{1}) & \cos(\emptyset_{2}) & \cdots\cdots & \cos(\emptyset_{M})\\ \sin(\emptyset_{1}\,) & \sin(\emptyset_{1}\,) & \cdots\cdots & \sin(\emptyset_{M})\end{bmatrix} \qquad (3.18)$$

Using first order-order Taylor series expansion of equation 3.16, we get

$$\widehat{\boldsymbol{\eta}}-\boldsymbol{\eta}\ \ =\ \left(\nabla_{\eta\tau}\nabla_{\eta\tau}^{T}\right)^{-1}\nabla_{\eta\tau}^{T}(\hat{\boldsymbol{\tau}}-\boldsymbol{\tau})$$

$$=\frac{1}{C^{2}}\begin{bmatrix}\widetilde{\emptyset}\widetilde{\emptyset}\ \ +\overline{\emptyset}\overline{\emptyset}^{T} & \overline{\emptyset}\\ \overline{\emptyset}^{T} & \boldsymbol{I}\end{bmatrix}\frac{1}{C}\begin{bmatrix}\widetilde{\emptyset} & \overline{\emptyset}\\ \boldsymbol{I} & \boldsymbol{O}\end{bmatrix}(\hat{\boldsymbol{\tau}}-\boldsymbol{\tau}) \qquad (3.19)$$

If we square both side of equation 3.19 we get

$$(\hat{\boldsymbol{\eta}}-\boldsymbol{\eta}\quad)(\hat{\boldsymbol{\eta}}-\boldsymbol{\eta}\quad)=c\begin{bmatrix}\left(\overline{\emptyset}\,\overline{\emptyset}^{T}\right)^{-1} & -\left(\overline{\emptyset}\,\overline{\emptyset}^{T}\right)^{-1}\widetilde{\emptyset}\\ -\widetilde{\emptyset}^{\boldsymbol{T}}\left(\overline{\emptyset}\,\overline{\emptyset}^{T}\right)^{-1} & 1+\ \widetilde{\emptyset}^{\boldsymbol{T}}\left(\overline{\emptyset}\,\overline{\emptyset}^{T}\right)^{-1}\widetilde{\emptyset}\end{bmatrix}\begin{bmatrix}\widetilde{\emptyset} & \overline{\emptyset}\\ \boldsymbol{I} & \boldsymbol{O}\end{bmatrix}(\hat{\boldsymbol{\tau}}-\boldsymbol{\tau})\quad(3.20)$$

And further rearrangement of equation 3.20 gives equation 3.21

$$(\hat{\boldsymbol{\eta}}-\boldsymbol{\eta}\quad)(\hat{\boldsymbol{\eta}}-\boldsymbol{\eta}\quad)=c\begin{bmatrix}\boldsymbol{O} & \left(\overline{\emptyset}\,\overline{\emptyset}^{T}\right)^{-1}\widetilde{\emptyset}\\ \boldsymbol{I} & -\widetilde{\emptyset}^{\boldsymbol{T}}\left(\overline{\emptyset}\,\overline{\emptyset}^{T}\right)^{-1}\overline{\emptyset}\end{bmatrix}(\hat{\boldsymbol{\tau}}-\boldsymbol{\tau})\qquad(3.21)$$

Therefore the error variance of $\hat{\boldsymbol{\eta}}$ can be expressed as equation 3.22:

$$E_{\tau}|(\hat{\boldsymbol{\eta}}-\boldsymbol{\eta}\quad)(\hat{\boldsymbol{\eta}}-\boldsymbol{\eta}\quad)^{T}|=$$

$$c^{2}\begin{bmatrix}\boldsymbol{O} & \left(\overline{\emptyset}\,\overline{\emptyset}^{T}\right)^{-1}\widetilde{\emptyset}\\ \boldsymbol{I} & -\widetilde{\emptyset}^{\boldsymbol{T}}\left(\overline{\emptyset}\,\overline{\emptyset}^{T}\right)^{-1}\overline{\emptyset}\end{bmatrix}\begin{bmatrix}\mathbf{D}(\widetilde{\boldsymbol{\sigma}}^{2}) & \boldsymbol{O}\\ \boldsymbol{O} & \boldsymbol{D}(\overline{\boldsymbol{\sigma}}^{2})\end{bmatrix}\begin{bmatrix}\boldsymbol{O} & \boldsymbol{I}\\ \widetilde{\emptyset}^{\boldsymbol{T}}\left(\overline{\emptyset}\,\overline{\emptyset}^{T}\right)^{-1} & -\widetilde{\emptyset}^{\boldsymbol{T}}\left(\overline{\emptyset}\,\overline{\emptyset}^{T}\right)^{-1}\overline{\emptyset}^{T}\end{bmatrix}\quad(3.22)$$

Further expansion of equation 3.22 and substitution of values gives equations 3.23, 3.24 and 3.25 respectively:

$$=c^{2}\begin{bmatrix}\boldsymbol{O} & \left(\overline{\emptyset}\,\overline{\emptyset}^{T}\right)^{-1}\widetilde{\emptyset}\\ \boldsymbol{I} & -\widetilde{\emptyset}^{\boldsymbol{T}}\left(\overline{\emptyset}\,\overline{\emptyset}^{T}\right)^{-1}\overline{\emptyset}\end{bmatrix}\begin{bmatrix}\boldsymbol{O} & \mathbf{D}(\widetilde{\boldsymbol{\sigma}}^{2})\\ \boldsymbol{D}(\overline{\boldsymbol{\sigma}}^{2})\widetilde{\emptyset}^{\boldsymbol{T}}\left(\overline{\emptyset}\,\overline{\emptyset}^{T}\right)^{-1} & -\boldsymbol{D}(\overline{\boldsymbol{\sigma}}^{2})\widetilde{\emptyset}^{\boldsymbol{T}}\left(\overline{\emptyset}\,\overline{\emptyset}^{T}\right)^{-1}\overline{\emptyset}^{T}\end{bmatrix}\quad(3.23)$$

$$=c^{2}\begin{bmatrix}\boldsymbol{O} & \left(\overline{\emptyset}\,\overline{\emptyset}^{T}\right)^{-1}\widetilde{\emptyset}\\ \boldsymbol{I} & -\widetilde{\emptyset}^{\boldsymbol{T}}\left(\overline{\emptyset}\,\overline{\emptyset}^{T}\right)^{-1}\overline{\emptyset}\end{bmatrix}\begin{bmatrix}\boldsymbol{O} & \mathbf{D}(\widetilde{\boldsymbol{\sigma}}^{2})\\ \boldsymbol{D}(\overline{\boldsymbol{\sigma}}^{2})\widetilde{\emptyset}^{\boldsymbol{T}}\left(\overline{\emptyset}\,\overline{\emptyset}^{T}\right)^{-1} & -\boldsymbol{D}(\overline{\boldsymbol{\sigma}}^{2})\widetilde{\emptyset}^{\boldsymbol{T}}\left(\overline{\emptyset}\,\overline{\emptyset}^{T}\right)^{-1}\overline{\emptyset}^{T}\end{bmatrix}\quad(3.24)$$

$$
= c^2 \begin{bmatrix} \left(\bar{\emptyset}\,\bar{\emptyset}^T\right)^{-1}\bar{\emptyset}\boldsymbol{D}(\bar{\boldsymbol{\sigma}}^2)\,\bar{\emptyset}^T\left(\bar{\emptyset}\,\bar{\emptyset}^T\right)^{-1} & -\left(\bar{\emptyset}\,\bar{\emptyset}^T\right)^{-1}\bar{\emptyset}\boldsymbol{D}(\bar{\boldsymbol{\sigma}}^2)\,\bar{\emptyset}^T\left(\bar{\emptyset}\,\bar{\emptyset}^T\right)^{-1} \\ -\bar{\emptyset}\left(\bar{\emptyset}\,\bar{\emptyset}^T\right)^{-1}\bar{\emptyset}\boldsymbol{D}(\bar{\boldsymbol{\sigma}}^2)\,\bar{\emptyset}^T\left(\bar{\emptyset}\,\bar{\emptyset}^T\right)^{-1}\boldsymbol{D}(\bar{\boldsymbol{\sigma}}^2) & +\ \bar{\emptyset}\left(\bar{\emptyset}\,\bar{\emptyset}^T\right)^{-1}\bar{\emptyset}\boldsymbol{D}(\bar{\boldsymbol{\sigma}}^2)\,\bar{\emptyset}^T\boldsymbol{D}(\bar{\boldsymbol{\sigma}}^2)\,\bar{\emptyset}^T\left(\bar{\emptyset}\,\bar{\emptyset}^T\right)^{-1}\bar{\emptyset}^T \end{bmatrix} \tag{3.25}
$$

From equation 3.25, it could be observed that it is similar to equation 3.14 which signifies that localization the same level of accuracy could be achieved irrespective of the presence of NLOS or not. It is therefore possible to deduce equation 3.26

$$
E_\tau|(\hat{\boldsymbol{p}} - \boldsymbol{p}\ \ )(\widehat{\boldsymbol{p}_\tau} - \boldsymbol{p}\ \ )^T| \ = \ c^2\ \left(\bar{\emptyset}\,\bar{\emptyset}^T\right)^{-1}\bar{\emptyset}\boldsymbol{D}(\bar{\boldsymbol{\sigma}}^2)\,\bar{\emptyset}^T\left(\bar{\emptyset}\,\bar{\emptyset}^T\right)^{-1} \tag{3.26}
$$

The implication of Equation 3.26 is that, for ULOSTECH implementation, LOS component of the received propagation is sufficient for accurate localization irrespective of the presence of NLOS bias as this could be effectively mitigated by the ULOSTECH scheme since the error variance remains the same under both conditions. It is therefore desirable to observe the propagation performance of ULOSTECH under experimental conditions covering sampling variance and root mean square errors conditions as well as the optimal channel and mitigation effects. Consequently the remaining of this chapter presents results of experimental investigations on ULOSTECH techniques. As earlier discussed in section 2.6.3, optimal UWB channel determination is basically a ranging accuracy endeavour. It suffices to mention that typical approaches for UWB ranging in the literature are based on matched filtering (MF) of the received signal. The technique also form the basis of proposals in [121[122] and [123]. This is mostly because the time index of MF maximization is amongst the simplest TOA estimate techniques.

The MF approaches have limited TOA precision, as the strongest path may not necessarily be the first arriving path. Lee and Scholtz therefore proposed generalized maximum-likelihood (GML) approach to search the paths prior to the strongest path in order to determine the leading edge of a received signal [124]. It could be observed that the information included in the paths after the strongest path were neglected and this can be used to enhance strongest path detection. Due to above practical concerns and limitations, energy detection based ranging offered becomes more feasible since it does not require accurate timing or pulse shapes [125]. It is suggested that the foregoing limitation could be addressed with a threshold based energy sensing technique like ULOSTECH that also caters for the square law errors. Although threshold-based techniques are mentioned in literature, a detailed analysis of threshold selection is not available to the best knowledge of the author of this thesis. Based on the derived ULOSTECH model, energy detection cluster decay and mistiming probability based thresholds are simulated and analysed to ascertain the performance with respect to SNR. Three different estimation bounds are employed which are LS, WLS and ML respectively. Additionally, the mitigation techniques were also investigated through simulation experiments. Results of the simulation experiments show the performance trade-offs of the algorithms for different scenarios.

3.3. SIMULATION EXPERIMENT 3.1 - Assessment of ULOSTECH IEEE.802.15.4a Optimal Channel Model Realization

3.3.1. Overview of the ULOSTECH Channel Cluster decay Experiment

These simulation experiments were conducted to enable determination of ULOSTECH IEEE.802.15.4a optimal channel model realization. PDF realizations for the S-V channel model has been discussed in chapter 2 section 2.5.3 of this thesis. Therefore, the PDP expression in equation 2.24 form the basis of the simulation experiments while the multipath components were modelled as independent uniform random variables that were generated in MATLAB environment. This on the one hand determines the number of clusters contained in each PDF realizations as well as to enable realization of an optimal IR-UWB-based IEEE.802.15.4a localization channel using standard parameters comparable to narrow band signals. Moreover, the comparative evaluations were based on the constant decay rate for a cluster in equation 2.25 and the constant decay rate for rays in Equation 2.26. Table 3.1 details the parameters used in the PDP simulation of the ULOSTECH channel model realization.

3.3.2. Experimental Procedure

The MATLAB codes developed for this experiment is at Appendix-1 while the algorithm simulation steps are as follows. In the first WHILE LOOP of the algorithm, clusters are generated with their arrival times determined by PDF Equation 2.24 and the loop terminates if the newly generated cluster arrival time is larger than the maximum channel delay; in which case this cluster arrival time is discarded. In the FOR LOOP, rays are generated for each cluster with their arrival times determined by PDF Equation 2.26. Then, the power of each ray is calculated according to Equation 2.24. For each cluster, the WHILE LOOP terminates if the newly generated ray arrival time is larger than the maximum channel delay.

Table 3.1:- Simulation parameters for ULOSTECH PDP channel model realization

S/N	Parameter	Symbol	Value
1	Distributed cluster arrival random variable	Λ	1/200ns^{-1}
2	Distributed ray arrival random variable	ʎ	1/20ns^{-1}
3	Constant decay rate for cluster	Γ	60ns
4	Constant decay rate for rays	γ	20ns

3.3.3. Simulation Results

A graphical representation of the results obtained from the simulation experiments conducted is as shown in Figure 3.3.

3.3.4. Analysis of Results

The simulation result depicted in Figure 3.3 indicates that the simulated channels possesses characteristics that are comparable to modified version of the S-V model in the light of earlier works in this area as outlined in chapter 2 section 2.5.3. It could be observed that the ULOSTECH channels incorporates the path loss and the lognormal distributed shadowing. Moreover, the phase $\alpha_{m,n}$ is constrained to 0 or π with equal probability according the standards of IEEE 802.15.4a channel model. This enables it to output a channel that is characterized in a baseband channel model. It should be noted however, that the linear dependence of the cluster decay rate was catered for with the utilization of variable ray decay rates through the simulation process. Furthermore, when log scale is used for the y-axis, it became apparent that both clusters and rays decay exponentially which confirms that ULOSTECH propagation agrees with a baseband characteristic of IR-UWB signals. It is believed that the ULOSTECH codes employed for realization of optimal localization channel agrees with the IEEE 802.15.4a UWB standards. This thus suggests that the developed algorithm merits the baseband signal characteristics that transverses a wide IR-UWB spectrum in clusters and thus will be suitable for employment as signal overlay for node-to-node communication in the 5G environment.

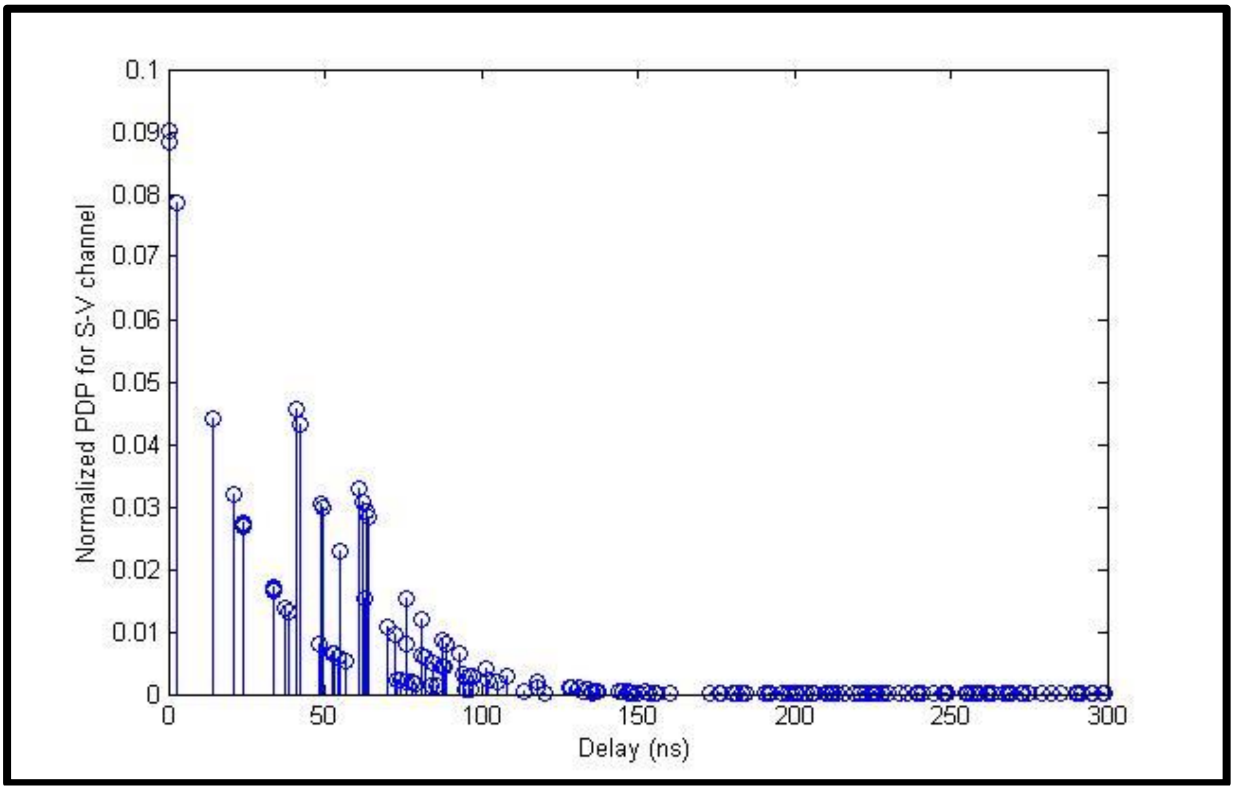

Figure 3.3:- Simulated Optimal ULOSTECH IEEE 802.15.4a Channel Realization for the LOS environment.

3.4. <u>SIMULATION EXPERIMENT 3.2</u> – Assessment of mistiming probability for ULOSTECH channel sensing.

3.4.1. Overview of the ULOSTECH Channel Sensing Experiment

This simulation experiment was conducted with the objective to determine mistiming probability of ULOSTECH signal for IEEE.802.15.4a channel sensing. This was conducted using the ULOSTECH energy detection-based estimation profile. The methodology adopted is an energy detection-based estimation procedure that assumes that the channel has independent distributed samples through-out the simulation process. This enabled simulation with different values of the parameters to achieve resulting characteristic of a base-band signal with sub-bands. This is very significant in that simulation could be conducted with different values of the parameters concurrently with a number of signal sub-bands. This suggest a large bandwidth capability.

3.4.2. Experimental Procedure

The MATLAB codes developed for this experiment is presented in Appendix-2. Since time synchronization is very critical for localization estimation accuracy, an algorithm for accurate and effective timing is therefore most imperative and can be achieved with a robust probability of mistiming algorithm. This experiment therefore assesses the low-complexity estimation capability of ULOSTECH with emphasis on its mistiming probability. Consequently, parameters were set and simulated for ULOSTECH as an energy detection-based TOA estimator while sampling was established at equally spaced sequence. It was assumed that the estimator $r_{b,n}$ denote the baseband signal from b[th] sub-band and $\{S_{b,n}\}_{n=0}^{N-1}$ is the transmitted synchronization sequence. The sampled channel was then obtained by the matched filtering equation given by Equation 3.27 [126]. Moreover, the fine timing is achieved by finding the first segment of K samples with energy exceeding the defined threshold where K and the threshold depend on LOS or NLOS channel environment. It was further assumed that the signal has been sampled into discrete taps for all B sub-bands such that the B[th] sub-band can be expressed as Equation 3.28 where all the $h_{b,n}$. are considered to be noise-free samples of the signal and L_1 and L_2 represent the ambiguity of coarse timing. In particular, with the availability of multiple sub-bands, ULOSTECH estimation simply combines the energy from all sub-bands via non-coherent combining expressed as Equation 3.29

$$\mathrm{h}_{b,d} = \sum_{n=0}^{n-1} \mathrm{r}_{b,d+n} s^{b,n} \tag{3.27}$$

$$\bar{\mathrm{h}}_{b,n} = \begin{cases} \mathrm{h}_{b,n-L_1} + \eta_{b,n,} & n\epsilon[L_{1,}\ L_1 + L - 1] \\ \eta_{b,n,} & n\epsilon[0,\ L_1 - 1]\ and\ n\epsilon[L_1 + L,\ L_1 + L + L_2] \end{cases} \quad b\epsilon[1, B] \tag{3.28}$$

$$k = \arg\max \sum_{b=1}^{B} \sum_{n=p}^{p+L-1} \left|\bar{\mathrm{h}}_{b,n}\right|^2 \qquad (3.29)$$

3.4.3. Simulation results

The simulation results as depicted in Figures 3.4 and 3.5 show the probability of mistiming curves as functions of SNR for energy detection-based estimator algorithm.

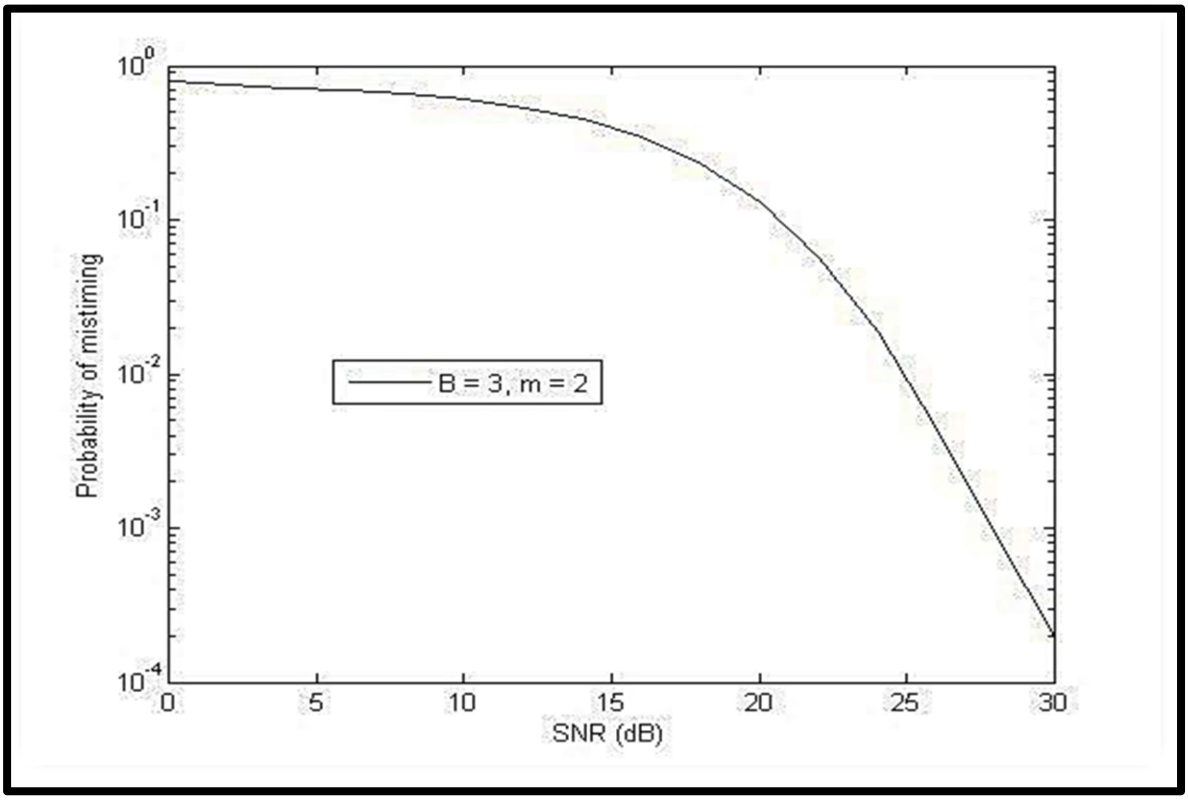

Figure 3.4:- Simulated probability of mistiming as a function of SNR for ULOSTECH

3.4.4. Analysis of Results

The ULOSTECH simulation results depicted in Figures 3.4 and 3.5 show the probability of mistiming curves as functions of SNR for energy detection-based estimation. In the simulation, the sampled channel had L=12 independently distributed channel taps and L_1=L_2=5 pure noise terms. It was observed that the channel has an exponentially decaying PDP with the last tap being about 20dB weaker than the first tap which shows that the estimator can achieve a higher diversity gain in comparison with narrow band signals. The implication is that by the non-coherent use of combining, ULOSTECH can achieve diversity gain which is proportional to the number of sub-bands and the channel diversity. This is very significant since it is a low complexity estimation scheme which makes it applicable in the 5G environment with ease of data transfer. It is also novel in that simulation could be conducted with different values of the parameters concurrently with a number of signal sub-bands. Here, an energy detection-based TOA estimation process was used to observe the reaction of developed codes to various mistiming scenarios in a 5G setting. It is believed that the concurrent use of signal sub-bands ensures the efficient use of complete bandwidth as channels for data exchange with no in-band interference due to separation by frequency.

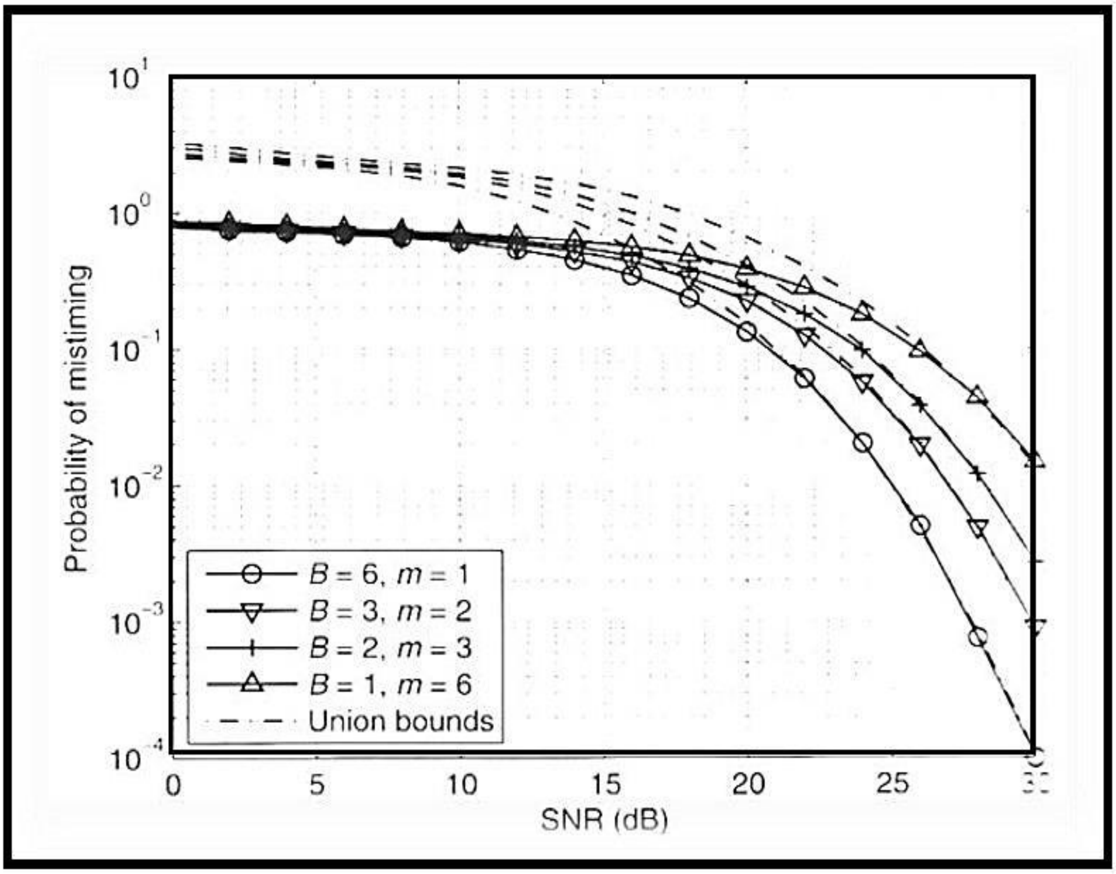

Figure 3.5:- Simulated comparative probability of mistiming as a function of SNR for optimal UWB channel.

3.5. SIMULATION EXPERIMENT 3.3 Determination of Shadowing Variance for ULOSTECH Propagation in LOS and NLOS Conditions

3.5.1. Overview of the ULOSTECH Shadowing Variance Experiment

The simulation experiments were conducted to determine the resulting sampling shadowing variance of the transmitted IR-UWB signal for ULOSTECH position estimates in varying scenarios. This was investigated in both LOS and NLOS conditions. Random variables were generated in MATLAB environment for the simulations. The simulations where repeated for LS WLS and ML estimation conditions respectively. This is to explore the resulting variance for ULOSTECH under varying estimation conditions. The resulting variances for each method are then plotted.

3.5.2. Experimental Procedure

The procedure for the simulation experiment consists of the following steps in the 3 phases of LS, WLS and ML respectively while the MATLAB codes are detailed in Appendix 1.

PHASE -1 - LS

Step 1. Find the LS likelihood position of the target node using combination of ray decay rate and cumulative TOA estimates.

Step 2. Calculate TOA residual which is the absolute difference of the actual timings and the obtained the TOA via estimated target position.

Step 3. Select the NLOS propagation whose TOA residual denotes the root mean square of the base node TOA residual

Step 4. Exclusion of NLOS propagation on Step 3 followed by final estimation of the LS position for overall positioning accuracy.

Step 5. Plot the resulting shadowing variance against SNR.

PHASE - 2 - WLS

Step 1. Find the WLS likelihood position of the target node using combination of ray decay rate and cumulative TOA estimates.

Step 2. Calculate TOA residual which is the absolute difference of the actual timings and the obtained the TOA via estimated target position.

Step 3. Select the NLOS propagation whose TOA residual denotes the root mean square of the base node TOA residual

Step 4. Exclusion of NLOS propagation on Step 3 followed by final estimation of the WLS position for overall positioning accuracy.

Step 5. Plot the resulting shadowing variance against SNR.

PHASE -3 - ML

Step 1. Find the ML likelihood position of the target node using combination of ray decay rate and cumulative TOA estimates.

Step 2. Calculate TOA residual which is the absolute difference of the actual timings and the obtained the TOA via estimated target position.

Step 3. Select the NLOS propagation whose TOA residual denotes the root mean square of the base node TOA residual

Step 4. Exclusion of NLOS propagation on Step 3 followed by final estimation of the ML position for overall positioning accuracy.

Step 5. Plot the resulting shadowing variance against SNR.

3.5.3. Simulation Results

A graphical representation of the results obtained from the simulation experiments conducted is as shown in Figure 3.6. This details a combined representation of results under LOS and NLOS propagation conditions.

3.5.4. Analysis of Results

This simulation experiment was conducted to determine the resulting shadowing variance from sampling of the transmitted IR-UWB signal in both LOS and NLOS scenarios. The result of the simulation shows that the UWB channel has envelopes of evenly distributed phases despite random variables generated by MATLAB functions used. This confirms that the same shadowing variance is experienced throughout the sampling period for any given range of SNR either in LOS or NLOS condition. It was however observed that the performance in NLOS condition varies from 0.05 variance for ML, to 0.07 for WLS and 0.1 for LS simulations. This could be detrimental if the NLOS component is not effectively mitigated. It is of particular note that under LOS condition, the shadowing variance remains relatively the same for LS, WLS and ML simulations. The significance of this is that the ULOSTECH performs within acceptable parameters under many scenarios and gives optimal performance irrespective of the bounds parameters in those given scenarios as the accuracy of its localization would not be degraded.at a peak variance of 0.03. It could thus be deduced that ULOSTECH is a promising proposition for the 5G setting.

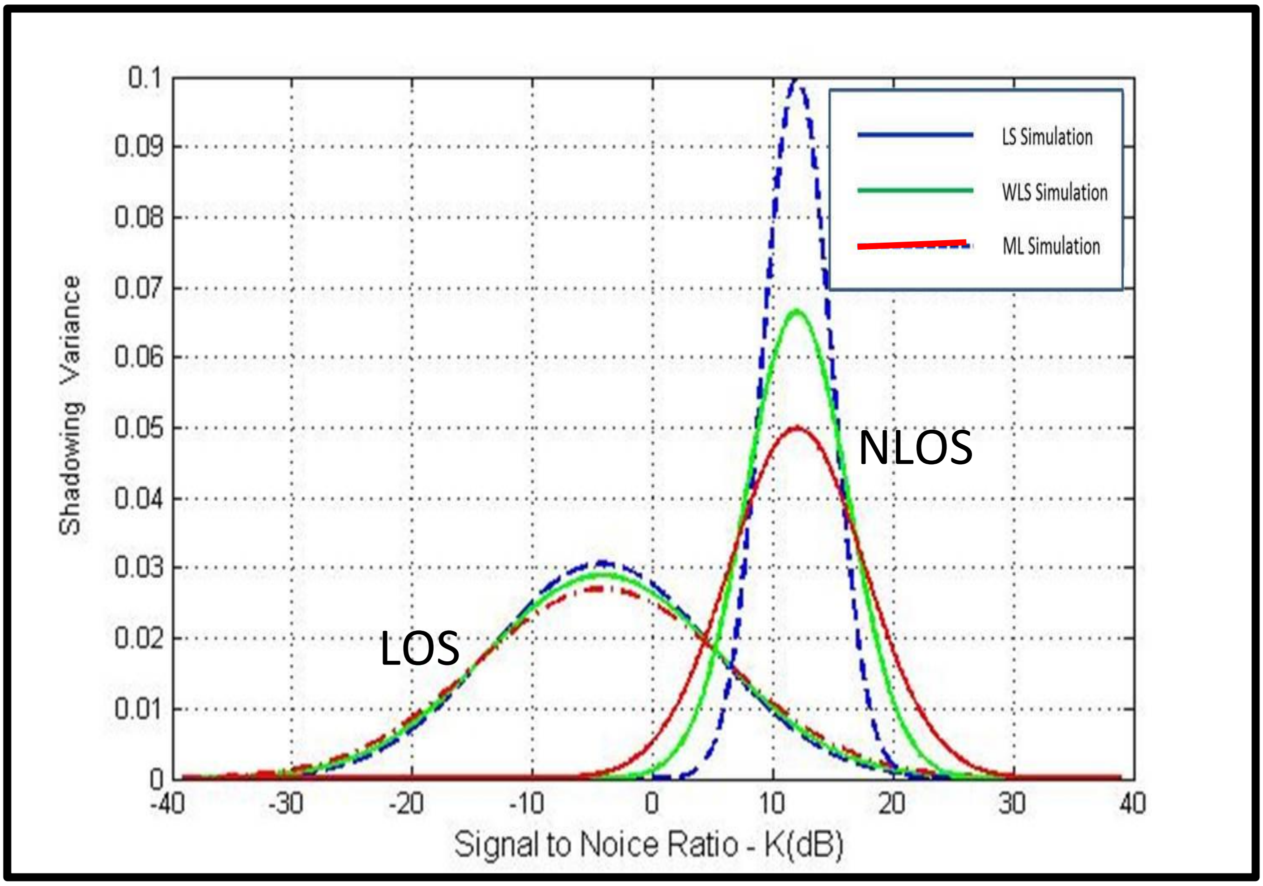

Figure 3.6:- ULOSTECH Shadowing Variance as a function of SNR for LOS & NLOS

3.6. SIMULATION EXPERIMENT: 3.4 - Determination of ULOSTECH Root Mean Square Errors for Position Estimates in LOS and NLOS Conditions

3.6.1. Overview of the ULOSTECH Root Mean Square Errors' Experiment

The simulation experiments in this section were conducted to determine the resulting RMSE of ULOSTECH position estimates in varying scenarios. Random variables were generated in

MATLAB environment for the simulations. For a complete experiment cycle with a set of parameters, the simulations were 3 different estimation bounds for comparison. These estimation bounds are LS WLS and ML estimations The simulation experiments were conducted for both LOS and NLOS conditions while the resulting variances for each method are then plotted.

3.6.2. Experimental Procedure

The procedure of the simulation experiment consists of the following steps in the 3 phases of LS, WLS and ML respectively while the MATLAB codes are detailed in Appendix 2.:

PHASE -1 - LS

Step 1. Find the LS likelihood position of the target node using combination of ray decay rate and cumulative TOA estimates.

Step 2. Calculate TOA residual which is the absolute difference of the actual timings and the obtained the TOA via estimated target position.

Step 3. Select the NLOS propagation whose TOA residual denotes the root mean square of the base node TOA residual

Step 4. Exclusion of NLOS propagation on Step 3 followed by final estimation of the LS position for overall positioning accuracy.

Step 5. Plot the resulting RMSE against transmitted SNR.

PHASE - 2 - WLS

Step 1. Find the WLS likelihood position of the target node using combination of ray decay rate and cumulative TOA estimates.

Step 2. Calculate TOA residual which is the absolute difference of the actual timings and the obtained the TOA via estimated target position.

Step 3. Select the NLOS propagation whose TOA residual denotes the root mean square of the base node TOA residual

Step 4. Exclusion of NLOS propagation on Step 3 followed by final estimation of the WLS position for overall positioning accuracy.

Step 5. Plot the resulting RMSE against transmitted SNR.

PHASE -3 - ML

Step 1. Find the ML likelihood position of the target node using combination of ray decay rate and cumulative TOA estimates.

Step 2. Calculate TOA residual which is the absolute difference of the actual timings and the obtained the TOA via estimated target position.

Step 3. Select the NLOS propagation whose TOA residual denotes the root mean square of the base node TOA residual

Step 4. Exclusion of NLOS propagation on Step 3 followed by final estimation of the ML position for overall positioning accuracy.

Step 5. Plot the resulting RMSE against transmitted SNR.

3.6.3. Simulation Results

A graphical representation of results of the simulation experiments conducted is shown in Figure 3.7. It details a combined representation of results obtain under LS, WLS and ML scenarios.

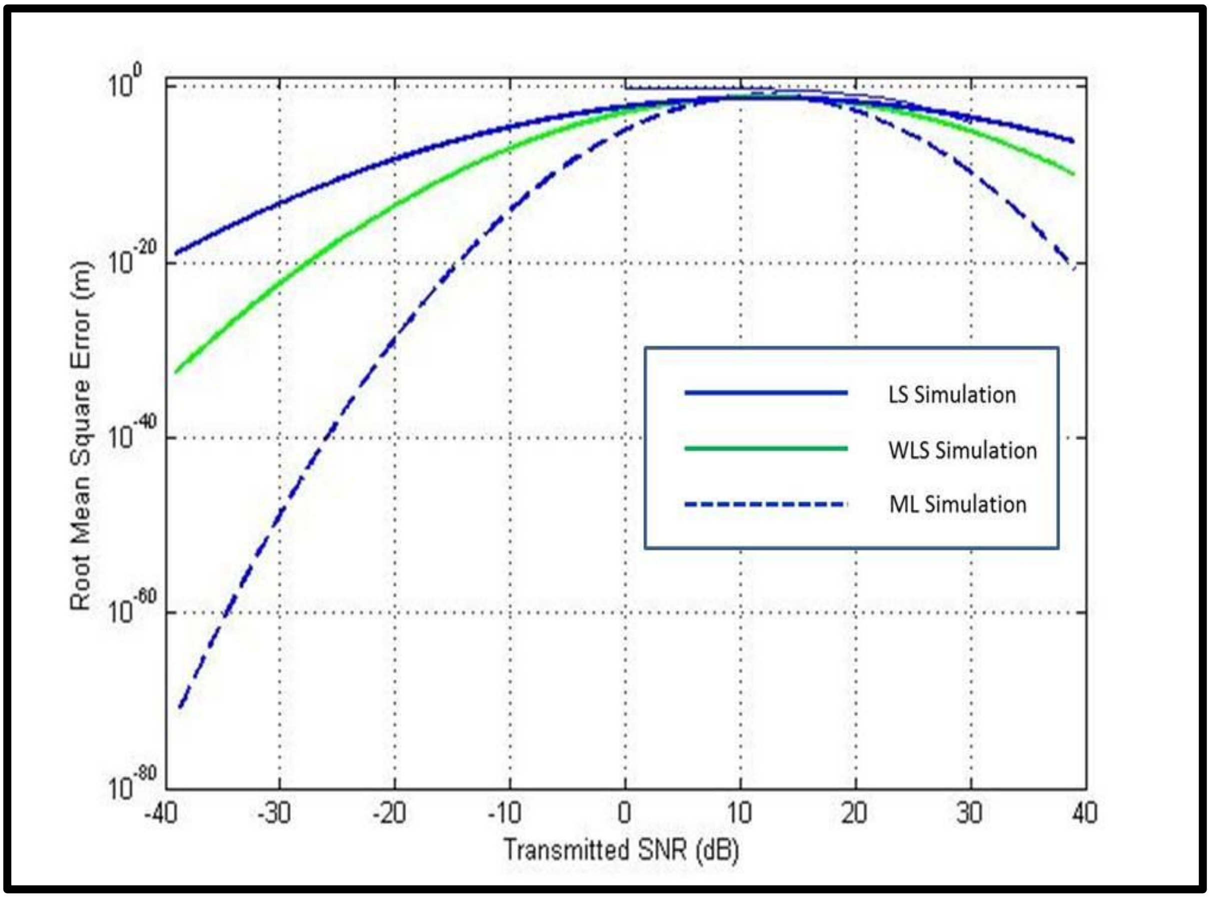

Figure 3.7:- RMSE UWB Position Estimate as a Function of transmitted SNR.

3.6.4. Analysis of Results

Results of the simulation show that the error performance of the ULOSTECH location estimate increases with increasing SNR values as in Fig 3.7. This suggests that the transmitted SNR should be reasonably high in order to maintain an acceptable received SNR. Furthermore, it could be deduced that, for ULOSTECH node position estimation based on time delay, the use of LOS TOAs is sufficient to achieve the same performance as that obtained by use of a combination of both the LOS and the NLOS TOAs. This thus suggests that ULOSTECH reduces estimation computation time and complexity while also addressing the inadequacies of NLOS UWB propagation which makes it a promising proposition for localization in 5G setting. Furthermore, the possibility that nodes could extract information about their relative positions from signals already used for communication without any additional overhead is indeed a probable added advantage for UWB IEEE 802.15.4a WPAN standard.

3.7. ULOSTECH Positioning Mitigation

The overall framework of this method includes an initialization step and an iterative update step where only local UWB communications between nodes in spatially close proximity are necessary in both steps. In the initialization step, each unlocalized node obtains an initial solution for its location. The approach adopted is termed the closest-peer anchor initialization. Specifically, if an unlocalized node has connecting anchor(s), it will use the location of its closest anchor, determined from range estimates, as its initial solution. However, if an unlocalized node does not have a connection to any anchor, it will then use the average location of its surrounding nodes' initial solution. In particular, if the i^{th} and the j^{th} nodes are neighbours, the projection of θ_i onto the feasibility set given by the range estimate r_{ij} is as represented in Equation 3.30.

$$\mathrm{P}_{ij}^{col}\left(\widehat{\theta_\iota}\right) = \widehat{\theta_J} + r_{ij} \frac{\widehat{\theta_\iota} - \widehat{\theta_J}}{\left\|\widehat{\theta_\iota} - \widehat{\theta_J}\right\|} \qquad (3.30)$$

Since only local information exchange is needed, the iterative update process can be distributed and the computational complexity scales linearly with network size. Therefore, each unlocalized node examines weather or not its residual changes over the previous iteration. The **i**th unlocalized node's residual based on its neighbours' current estimated locations is defined as in Equation 6.4 where $\aleph(i)$ is the set of the ith node's neighbouring nodes and $|.|$ denotes cardinality. If its residual has not changed more than the precision parameter δ for k consecutive iterations, the ith node will quit the iterative update step and mark itself as localized. The overall update process terminates after all of the unlocalized nodes have been marked as localized. The developed algorithm to implement this process is explained in the following paragraphs. The propagation function is modelled as a linear function in equation 3.31

$$\Phi^{col}(\widehat{\theta_\iota}) = \frac{1}{|\aleph(i)|} \sum_{j\epsilon\aleph(i)} \left(r_{ij} - \left\|\widehat{\theta_\iota} - \widehat{\theta_J}\right\|\right)^2 \tag{3.31}$$

It should be noted that the set of ith node's neighbours with LOS range estimates will participate only if $\left\|\widehat{\theta_\iota} - \widehat{\theta_J}\right\| \geq r_{ij}$ is satisfied. Hence the projection on to a ranging cicle will utilize the knowledge about the minimum NLOS bias expressed as follows:

$$\mathrm{P}_{ij}^{col,NLOS-B}(\widehat{\theta_\iota}) =$$

$$\begin{cases} \widehat{\theta_J} + r_{ij} \dfrac{\widehat{\theta_\iota} - \widehat{\theta_J}}{\left\|\widehat{\theta_\iota} - \widehat{\theta_J}\right\|} & j\epsilon\aleph_L(i) \\ \widehat{\theta_J} + (r_{ij\_}b_l) \dfrac{\widehat{\theta_\iota} - \widehat{\theta_J}}{\left\|\widehat{\theta_\iota} - \widehat{\theta_J}\right\|} & j\epsilon\{k \backslash k\epsilon\aleph_N(i), \left\|\widehat{\theta_\iota} - \widehat{\theta_J}\right\| \geq r_{ik\_}b_L \end{cases} \tag{3.32}$$

It can be observed that Equation 3.32 is a modified projection method that enhances and corrects the NLOS range estimates by subtracting the estimated minimum NLOS bias from each NLOS range estimate. It was discovered that this has the effect of mitigating NLOS bias, depending on the accuracy of the estimated minimum NLOS bias. However, considering that the actual NLOS bias may be larger or smaller than the mean NLOS bias, the approach may actually overestimate or under estimate the NLOS bias contained in each individual NLOS range estimate. Therefore, it is safe to say that the performance may depend on the actual statistics of the NLOS bias which ULOSTECH predicts with 0.98 accuracy ratio.

3.8. SIMULATION EXPERIMENT: 3.5 – Assessment of ULOSTECH NLOS mitigation technique

3.8.1. Overview of the ULOSTECH NLOS Mitigation Experiment

3.8.2. Procedure

SETUP FOR SIMULATION EXPERIMENT – 3.5-A

In the first NLOS mitigation simulation experiment, the considered network had two unlocalized nodes θ_1 and $\theta_{2,}$ as well as four other nodes $\theta_{3,}$ $\theta_{4,}$ $\theta_{5,}$ $\theta_{6,}$ of known locations. The anchors were located at $\theta_3 = [0{,}0]$, $\theta_4 = [0{,}10]$, $\theta_5 = [10{,}10]$ and $\theta_{6,} = [10{,}0]$. Here node 1 is able to measure its range to anchors θ_3 and $\theta_{4,}$ as well as its range to node 2. Additionally, node 2 is able to measure its range to anchors θ_5 and θ_6 as well as its range to to node 1.

SETUP FOR SIMULATION EXPERIMENT - 3.5-B

In the second NLOS mitigation simulation experiment, the examined network has 200 unlocalized nodes in spatial proximity and 20 devices uniformly distributed over at 100 x l00 m^2 square area, forming a random network. For NLOS scenarios, different percentages of NLOS range estimates of 20%, 40%, 60%. and 80% were considered and which corresponds to various degrees of NLOS conditions. The range estimate noise and NLOS bias models as considered to zero-mean independent Gausssian distributed range estimate noise and uniformly distributed NLOS bias between $[B_{min}, B_{max}]$. In-addition, to ensure range model noise is accurately modelled, the path loss exponents for LOS and NLOS range estimates were set differently. Thus the following four estimate parameters were set for notational simplicity.

(1) IPPM:- IPPM approach without mitigation.

(2) IPPM-NM-ID:- The IPPM approach with NLOS mitigation based on NLOS identification only

(3) IPPM-NM –(ID,Min):- IPPM approach with NLOS mitigation based on NLOS identification plus an estimate of the minimum NLOS bias.

(4) IPPM-NM-(ID, mean):- IPPM approach with NLOS mitigation based on NLOS identification plus an estimate of the mean NLOS bias.

3.8.3. Abridged Algorithm

.Initialization:

(1) Obtain initial process guess $\varphi = [\widehat{\theta_1}, \widehat{\theta_2}, \widehat{\theta_3}, \widehat{\theta_4} \ldots\ldots\ldots\ldots \widehat{\theta_N}]$ using the closest peer anchor initialization.

(2) Set $[\widehat{\theta_{N+1}}, \widehat{\theta_{N+2}}, \widehat{\theta_{N+3}}, \ldots\ldots\ldots\ldots \widehat{\theta_{N+M}}] = A =$ $[\theta_{N+1,}\ \theta_{N+2,}\ \theta_{N+3,\ldots\ldots\ldots\ldots\ldots}\theta_{N+M,}\ ]$ which remains unchanged during the main loop.

(3) Set l_1= 0, δ as a positive number and k as a positive integer;

(4) Let F_1=0 and W_1=0 for i=1,2,3,4……., N;

(5) $\Phi = \Phi^{col}(\widehat{\theta_\iota})$, for i=1,2,3,4………..,N;

Main Loop:

(6) While (any of F_1 is equal to 0) {

(7) For i=1,2,3,4,……………….,N; if F_1 = 0

(8) $\widehat{\theta_\iota} \leftarrow (\frac{1}{|\aleph(i)|}) \sum_{j\epsilon\aleph(i)} \mathrm{P}_{ij}^{col}(\widehat{\theta_\iota})$, and $\Phi_{i,l+1} = \Phi^{col}(\widehat{\theta_\iota})$;

(9) If $\left| \Phi_{i,l} - \Phi_{i,l+1} \right| < \delta$

(10) Let W_1= W_1+ 1; if $W_1 \geq$ k, Let F_1=1;

(11) Otherwise Let $W_1 = 0$;

(12) l = l + 1;

]

In the above algorithm, F_1 indicates wether the ith node has been localized and W_1 records the number of consecutive iterations that the ith node's residual has not decreased more than δ. Once $W_1 \geq$ k, we set F_1=1 and consider the ith unlocalized node as localized. From the foregoing, it could be observed that anchor locations, that is, $\theta_{j,}$ for j=n+1, n+2,…………., n+m, will remain unchanged during the whole process. Furthermore, it iis observed that collaborative iteration provides W_1 as a means of accumulating observations over multiple iterations regarding whether an unlocalized node is indeed localized. Another advantage is that the computational load is low, mainly because of the simple operation involved in updating node locations which scalels linearly with n.

3.8.4. Simulation Results

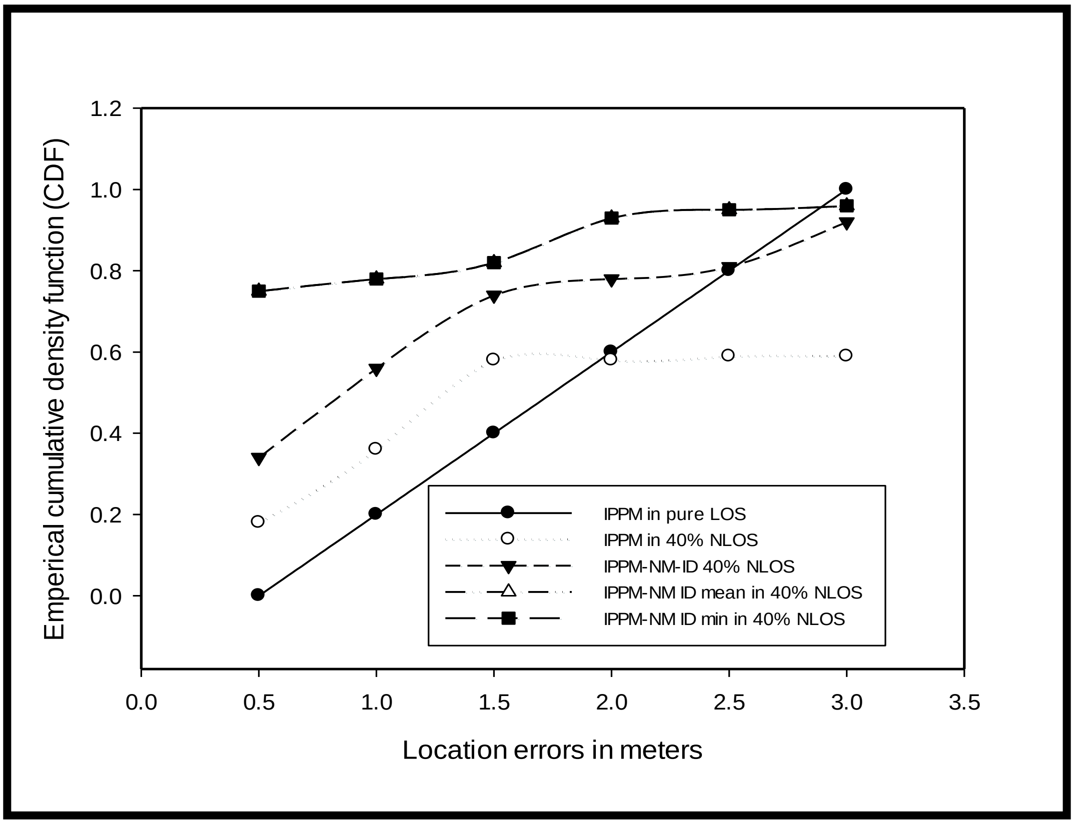

Figure 3.8:- Simulated empirical Cumulative Density Function (CDF) as a Function of Localization Error.

As shown in Figure 3.9, CDF of the localization errors presented were plotted. It demonstrates that the IPPM-NM-(ID, min) has the best performance while the ordinary IPPM had the worse performance since it does not mitigate NLOS bias. It is also observed that compared to IPPM-NM-ID, IPPM-NM-ID-mean has the advantage of reducing large localization errors, as a result of the observed smaller values of mean localization error.

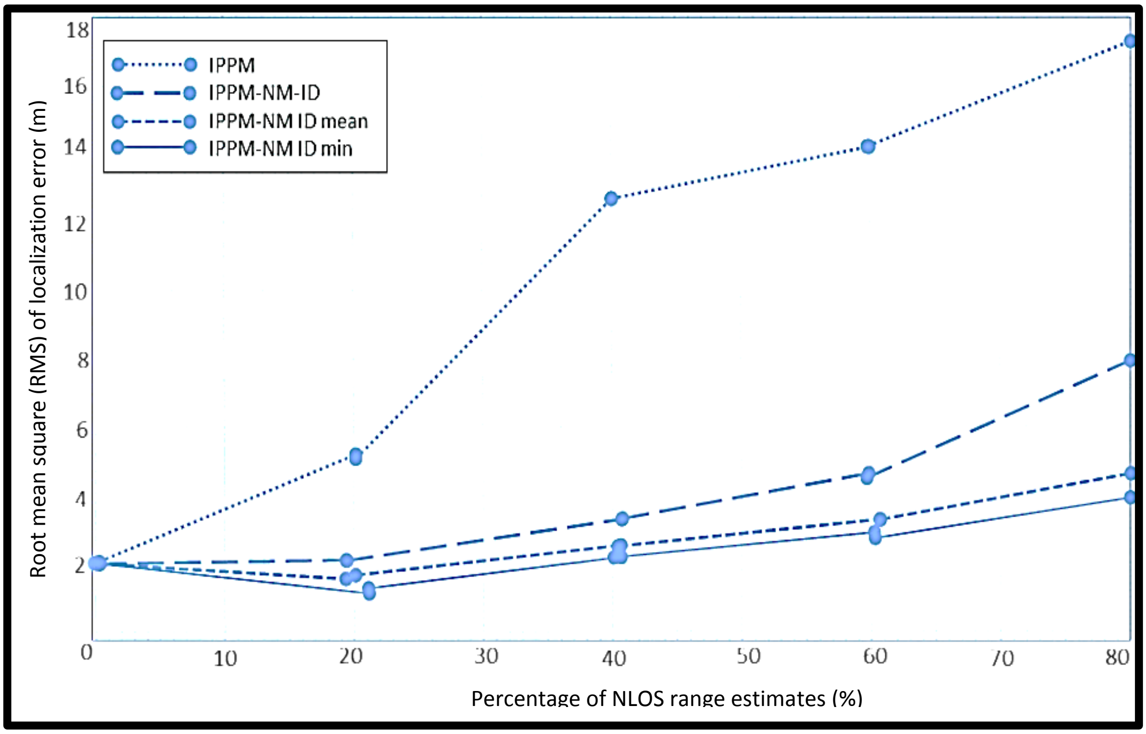

Figure 3.9:- Simulated mean localization Error (averaged over 100 noise and NLOS realizations) versus the percentage of NLOS range estimates.

3.8.5. Analysis of Results

In Figure 3.9 the mean localization error is plotted using the NLOS mitigation methods versus the percentage of NLOS range estimates for the network averaged over 100 range estimation noise and NLOS bias realizations. For each tested percentage of NLOS estimates, the corresponding number of NLOS range estimates are randomly selected from all the available range estimates in the network and they are kept unchanged over different noise and NLOS bias realizations. From the Figure 3.9, it is demonstrated that without NLOS mitigation, IPPM suffers significant performance degradation as the percentage of NLOS range estimates increases with increasing percentage RMSE. In particular, in pure LOS scenario, that is, the percentage of NLOS range estimates equals to zero, the IPPM has a mean localization error of 2.3 m, which increases to 12.8 m in the presence of 40% NLOS range estimates and on to 17.3 m in the presence of 80% NLOS range estimates. Conversely, all three NLOS mitigation methods are capable of reducing the mean localization error in varying degrees. It can also be deduced that subtracting the minimum NLOS bias from NLOS estimate is more trustworthy than subtracting the mean NLOS bias since the actual NLOS bias may be smaller or larger than the mean NLOS bias. It must be noted however that the simulation results are based on the perfect knowledge about NLOS identification, the minimum NLOS bias, and the mean NLOS bias. It could thus be reasonably concluded that the amount of information available about NLOS links (identification, or statistical) has a strong impact on NLOS mitigation approaches but in varying degrees depending on the efficiency of the method.

3.8.6. Summary

For the ULOSTECH node position estimation based on time delay, the use of LOS TOAs is sufficient to achieve the same performance as that obtained by use of a combination of both the LOS and the NLOS TOAs. This thus implies that *ULOSTECH* reduces estimation computation time and complexity while also addressing the inadequacies of NLOS UWB propagation.

<u>CHAPTER FOUR</u>

ULOSTECH D2D-BASED LOCALIZATION FOR ULTRA-DENSE NETWORKS

4.0. Chapter Overview.

4.1. Prospects of ULOSTECH D2D-based localization.

4.2. ULOSTECH IR-UWB D2D WWAN.

4.3. ULOSTECH D2D Cluster formation Scheme.

4.4. ULOSTECH Adjacent Cluster Cooperation.

4.5. Performance Evaluation of ULOSTECH IR-UWB D2D Cluster.

4.5.1. <u>SIMULATION EXPERIMENT 4.1</u> – Performance Evaluation of ULOSTECH Cluster Lifetime Relative to Available Cluster Members.

4.5.2. <u>SIMULATION EXPERIMENT 4.2</u> – Comparative analysis of ULOSTECH system throughput with standard cellular and wi-fi networks.

4.6. ULOSTECH D2D-propagation-based combined localization and communication scheme for ultra-dense networks.

4.7. <u>SIMULATION EXPERIMENT 4.3</u> – Comparative Performance Assessment of Mean Distance Error for Trilateration, ULOSTECH UD-CLOCS and MDS methods.

4.8. Summary

ULOSTECH D2D-BASED LOCALIZATION FOR ULTRA-DENSE NETWORKS

4.0. Chapter Overview

This Chapter discusses the *ULOSTECH* D2D-based localization for ultra-dense networks. It proposes an IR-UWB D2D WWAN along with its cluster formation scheme. This is followed with performance evaluation of the cluster lifetime and system throughput. Also proposed is a D2D-propagation-based combined localization and communication scheme (UD-CLOCS). The chapter concludes with results of related UD-CLOCS performance assessment experiments.

4.1. Prospects of ULOSTECH D2D-based Localization

The concept of positioning with its techniques was discussed in Section 2.3 while modelling of ULOSTECH and LOS sufficient related experiments were presented in Chapter 3. It could be deduced that provision of high accuracy positioning information that offers wider coverage will be a challenging task in the 5G setting. This is all the more difficult for the envisioned ultra-dense environments of above 1000 devices per square kilometre due to attendant of multi-user interference, multipath and NLOS propagation drawbacks that contribute to degrade positioning performance. ULOSTECH addresses the problems of NLOS propagation amongst others with the LOS sufficient model presented in Chapter 3. However, the probability of receiving signals under LOS conditions decreases with increasing distance between BS, RS and network devices [127]. Although the current 2G, 3G and 4G standards specify positioning methods that infer position information from received signals, but as highlighted in section 2.3.2. What all these methods have in common is that they require signals from at least 3 different BSs in order to calculate their position. This could be very difficult to achieve especially in dense urban scenarios. Additionally, the devices operate independent from each other without any cooperation for positioning services. There is thus the need to ensure seamless positioning whereby cognitive network devices collaborate to help each other to determine their own positions in the upcoming ultra-dense 5G setting.

CHAPTER FOUR (4): - ULOSTECH D2D-BASED LOCALIZATION FOR ULTRA-DENSE NETWORKS

From the foregoing, the ULOSTECH UD-CLOCS is proposed for ultra-dense networks. This is intended to address key 5G prospects like smaller cells, higher device densities and the capability of D2D communication to enable cooperative positioning in an ultra-dense setting. The scheme features a low system-load network where each device adaptively joins a cluster of neighbouring devices, updates its position estimate by minimizing a local cost-function, and then passes this updated position to the cluster head (CH) as well as its neighbours. Simulation results suggest that this update process utilizes a D2D distribution that has the capacity to support high density of devices per square meter of urban environments as the envisaged large-scale 5G networks. The concept is enabled with design of an IR-UWB D2D-based wireless wide area network (WWAN) tailored along the concept of piconet as its most basic component. It is uniquely characterized with the discrete micro-channel slots (DMCS). The rest of this chapter discusses the ULOSTECH IR-UWB D2D WWAN along with related simulation experiments as well as the ULOSTECH UD-CLOCS and reports of its performance assessment experiments.

4.2. ULOSTECH IR-UWB D2D WWAN

The ULOSTECH IR-UWB WWAN piconet agrees with IEEE 802.15.3 [128] that suggests that piconet consists of a piconet coordinator (PNC) and several devices. The PNC provides the basic timing with beacon and manages network resources for the piconet; and the devices transfer data with each other in a peer-to-peer manner under the administration of the PNC. All devices in a piconet communicate with each other through the rules defined in MAC protocol. However, in the ULOSTECH D2D WWAN, the piconet is IR-UWB-based which on the one hand frees-up the licensed spectrums while the ULOSTECH MAC protocol is modified such that the channel time is partitioned into DMCSs. Each DMCS acts as a distinct channel that is specific to a unique set of 2 devices engaged in a D2D interchange. The compartmentalized DMCS is composed of three parts which are the beacon period (BP), the channel access period (CAP) and the channel time allocation period (CTAP) as shown in Figure4.1. The BP is used to set the timing and to communicate management information for the ULOSTECH IR-UWB D2D piconet. The CAP is used to communicate commands and asynchronous data when available in the DMCS and this slot utilizes the ALOHA scheme [129]. The CTAP is composed of several smaller portions covering $CTAP_1$, $CTAP_2$ $CTAP_3$………$CTAP_N$ as well as feedback channel time allocations (FECTA). The

CTAPs are used for user data transmissions while FECTAs are used for feedback of acknowledgements and channel state indications. It should be noted that the difference between the IEEE 802.15.3 [130] super-frames and the ULOSTECH DCMCS lies majorly in combined communication and localization transmission services as well as the design of the FECTA. The ULOSTECH FECTA slot is designed as sub-micro channels with enough bandwidth that is capable of not only addressing the problem of in-band concurrent user interference but also increases channel throughput in comparison with Bluetooth and Wi-Fi standards as observed during simulation experiments. The ULOSTECH FECTA utilizes the advantages of IR-UWB that makes it possible for location information and identification details to be transmitted and resolved along with other traditional communication data flow.

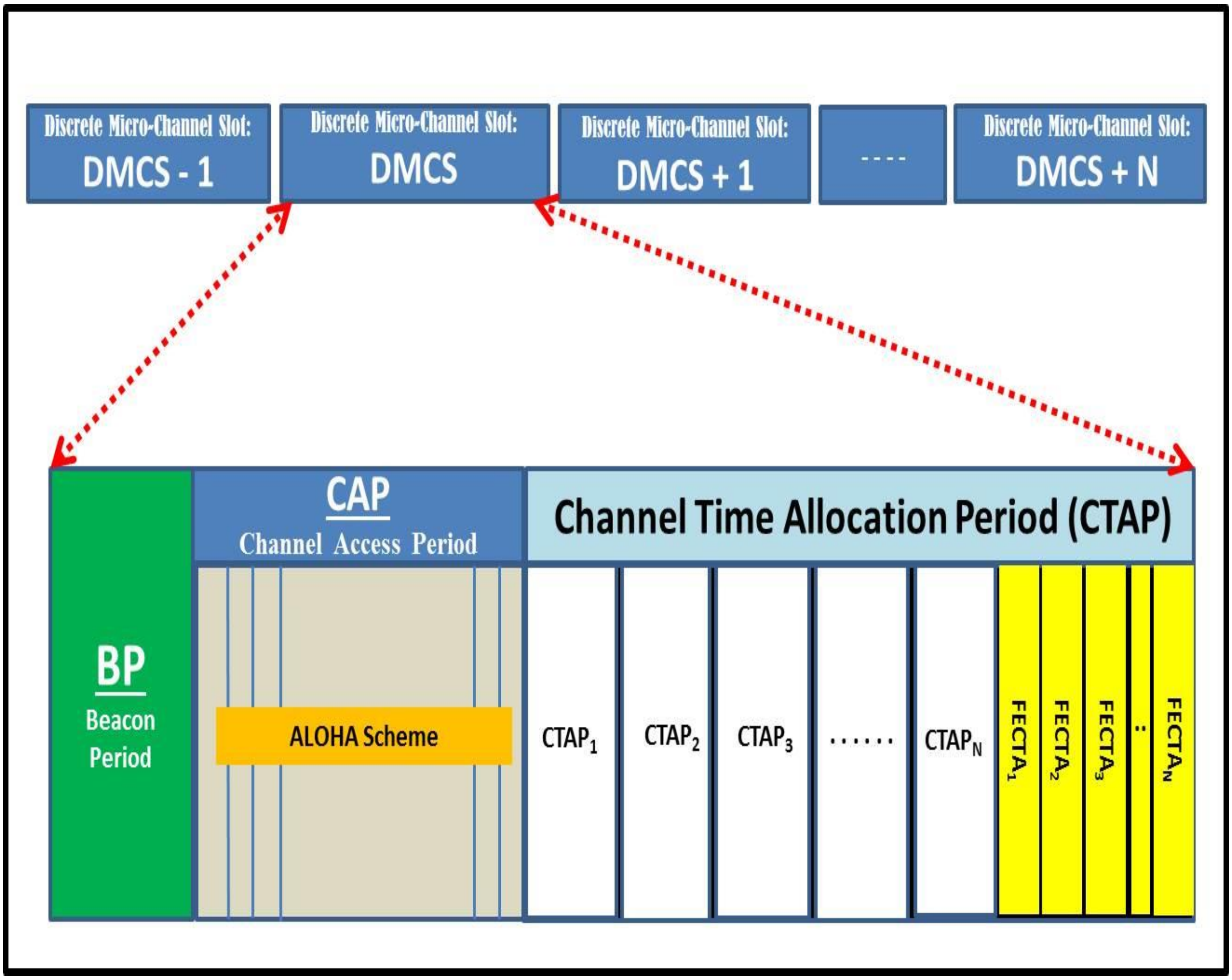

Figure 4.1. ULOSTECH IR-UWB WWAN D2D discrete micro-channel slots (DMCS) structure

4.3. ULOSTECH WWAN D2D Cluster formation Scheme

This section presents the ULOSTECH WWAN D2D cluster formation model along with the performance analysis based on simulations in MATLAB platform where a comparison is drawn with Wifi-direct hybrid D2D cluster formation. It is believed that D2D communication could reduce the burden on the cellular infrastructure and also increase the spectral efficiency in 5G setting. Earlier attempts to implement D2D communication in cellular network using OFDM technologies and distributed scheduling include [131], IEEE 802.11 protocol stack [132] and Wifi-Direct (also called Wifi-P2P) that enables efficient D2D connections in unlicensed bands without using wireless access points [133] along with Bluetooth with focus on short range, low power, low cost wireless communication that uses radio technology [134]. Figure 4.2 depicts a traditional hybrid transmission wifi-direct D2D cluster formation layout. The observed drawback in this instance regards its hybrid nature that utilizes two sets of different transmissions for the inband and outband communication whereas ULOSTECH WWAN D2D features the IR-UWB full–duplex communication within the same UWB band that covers both communication and localization data transfers with a unique signal band allocated to each D2D link.

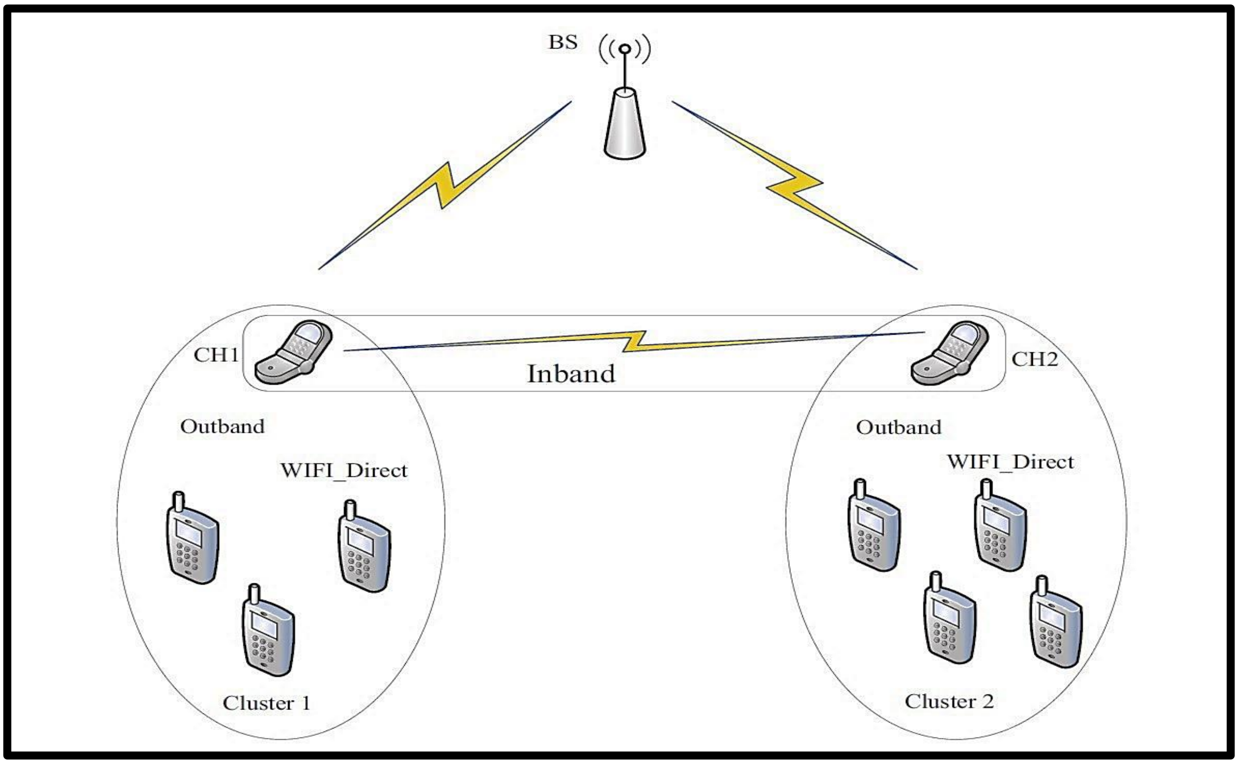

Figure 4.2. Traditional hybrid transmission wifi-direct D2D cluster formation layout [135]

4.3.1. The Cluster formation Structure

As illustrated in Figure 4.3, the hypothetic ULOSTECH D2D cluster formation scenario includes a BS, high density of RS deployments represented by $RS_{a,}$ RS_b, and RS_c s(but could go on to RS_{n+1}).as well as two clusters of many devices (D_a, D_b, D_c…… D_n, D_{n+1}. Inside each specific cluster, all the devices transfer traffic to each other directly via the IR-UWB interface. Moreover, each cluster has its own CH which carries out the D2D communications in both the in-band and the out-band modes respectively. This is unlike the hybrid architecture in Figure 4.2 where different channels are used. Moreover, it could be observed that today's mobile devices are usually driven by considerably finite battery power. This makes it essential to devise an effective scheme that reduces power consumption. Therefore, the low-power ULOSTECH IR-UWB WWAN is proposed for use as the primary option to make cluster formation with each D2D link on a separate DMCS. It agrees with standard requirements regarding cluster, CH and cluster normal member (CNM) as defined in [135]. The considered devices are able to measure their residual charge and signal-to-interference-plus-noise ratio (SINR) along with embedded cellular network WiFi and IR-UWB interfaces respectively. It also proposes each cluster to have a CH which is capable of calculating all of the CNMs' intent value (IV) which are time-synchronized with the CH via the ULOSTECH IR-UWB interface.

The flow diagram in Figure 4.4 details the procedure for ULOSTECH WWAN D2D IR-UWB cluster formation scheme. When a new user or device denoted T_{new} intends to initiate a D2D communication, it starts to scan, detect and analyse the joining instructions that is periodically broadcasted by a CH. If T_{new} detects the joining information transmitted intermittently by the CH in an existing cluster within the maximum time interval (t_{max}), it means that there exists a cluster nearby; T_{new} could then initiate the process to join. Otherwise, if no cluster is within range at the said instance, T_{new} forms a cluster itself. When there is a cluster around, the device sends a request message to the CH to enable it join the cluster. After receiving the request, the CH makes a response to the T_{new}. If the T_{new} is permitted to join the cluster, it will broadcast acceptance message to the cluster upon receipt of CH's confirmation code. Finally, the CH will add the new joining T_{new}

information to its list and also update the nearest RS. Otherwise, if the T_{new} receives the declined response, it will send request again after time interval T + 1. Nevertheless, if there is no cluster around, then T_{new} will not detect the broadcast message within the given time interval T , and it will set itself as the CH and send broadcast message periodically.

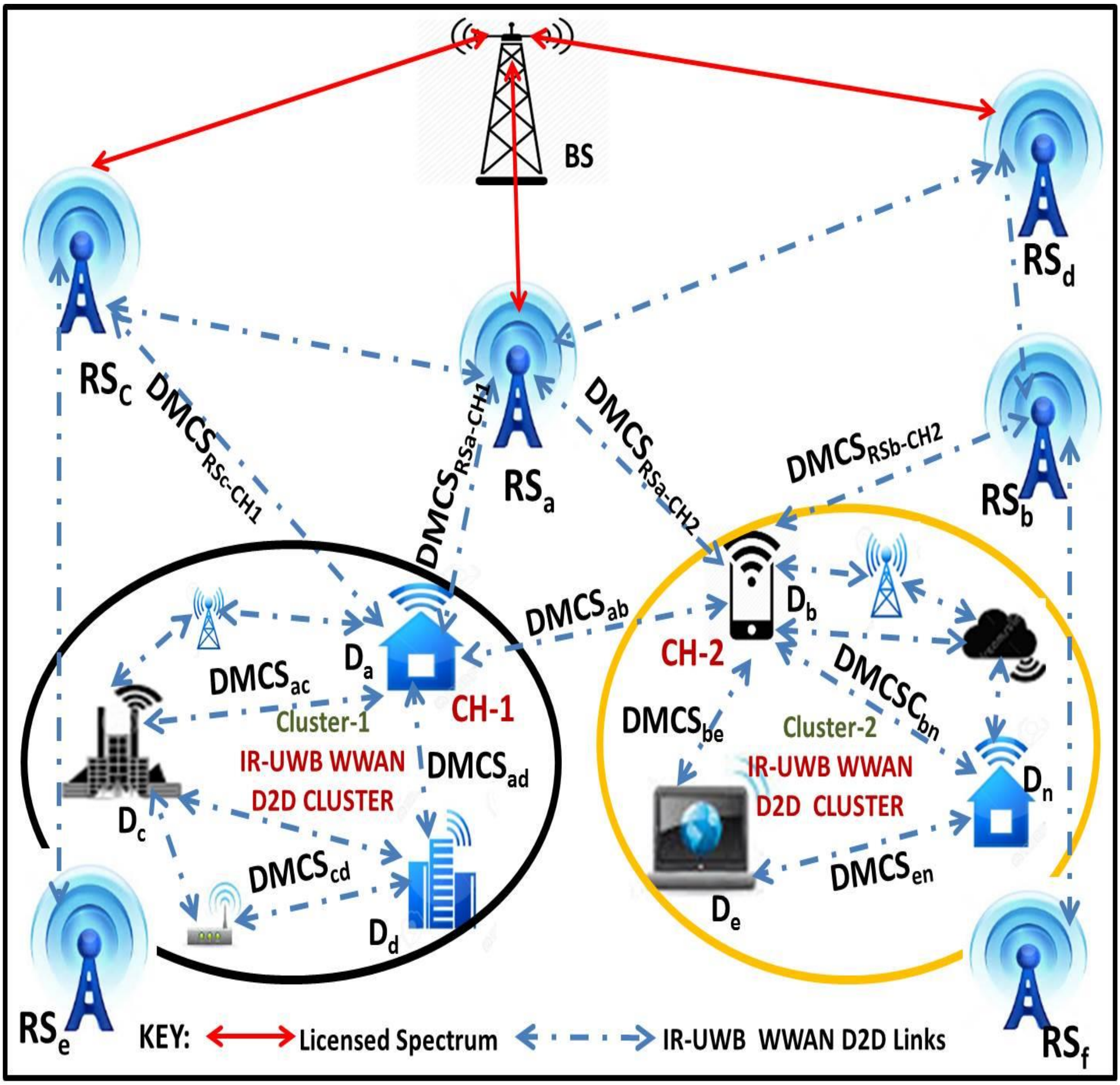

Figure 4.3. ULOSTECH IR-UWB WWAN D2D cluster formation layout

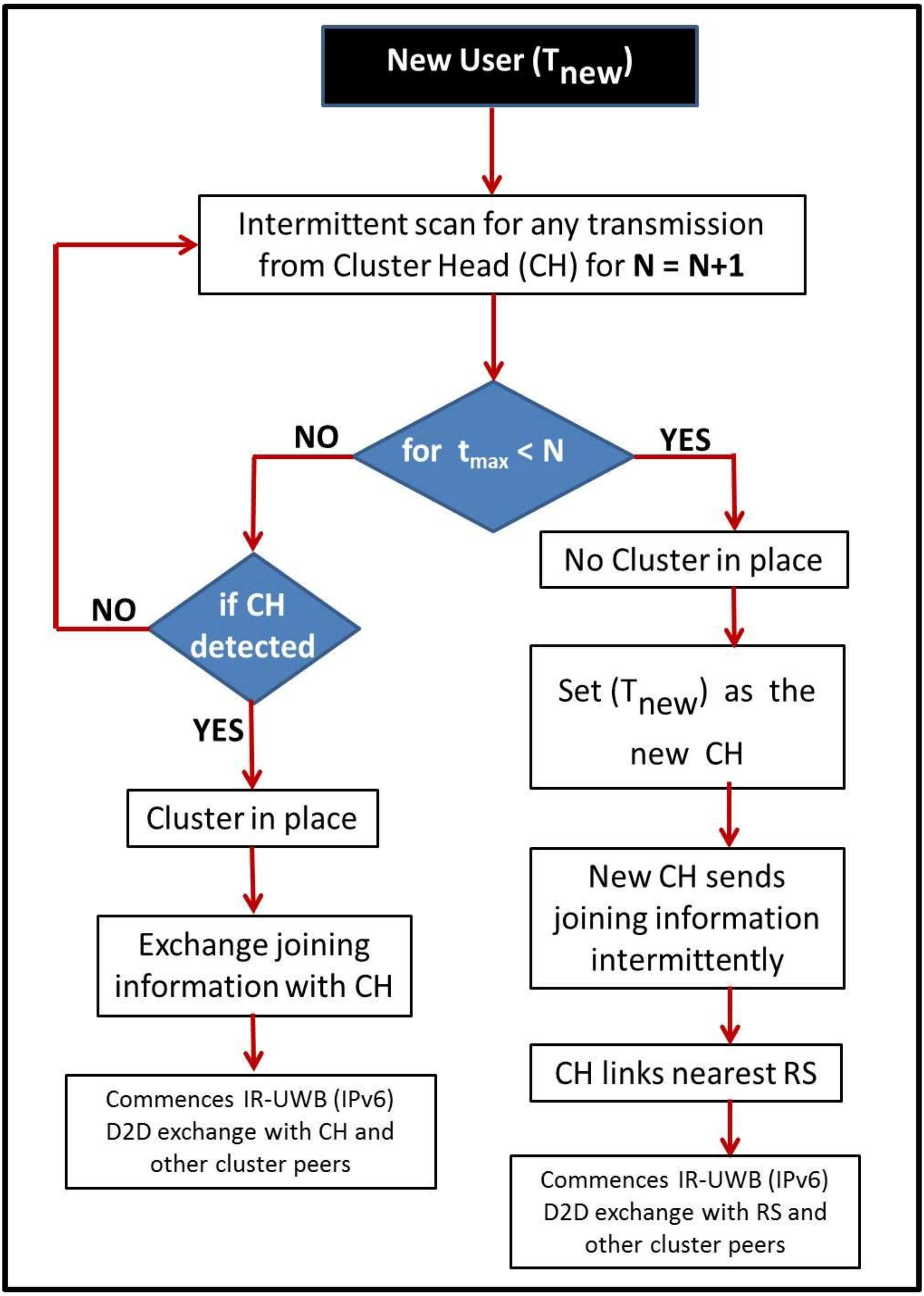

Figure 4.4. Flow diagram for the ULOSTECH IR-UWB D2D cluster formation Scheme

4.3.2. Cluster Head Transfer Scheme

Considering that the cluster lifetime and system capacity are finite, a CH selection and transfer method is proposed. This combines normalized SINR denoted as S_{Nom} with the normalized residual charge of each CNM denoted as R-CHG_{Nom}. For ULOSTECH IR-UWB WWAN D2D cluster CH transfer purposes, the following are defined:

I. IV is defined as the variable of the CH updating rank.
II. α is defined as a weight factor to the S_{Nom}.
III. R-CHG_{Nom}-1 as the residual charge of CNM when it becomes a CH.
IV. R-CHG_{Nom}-2 as the current residual charge of the CH and
V. IVCH as the intent value of the current CH such that Equation 4.1 is true.
VI. T_{xpt}-max is the maximum throughput of ULOSTECH IR-UWB WWAN D2D cluster.
VII. B represents the cumulative channel bandwidth of all DMCSs used for D2D interchange by cluster members.

Therefore, regarding the cluster members, there exist a maximum SINR denoted as $SINR_{max}$. Therefore, according to Shannon's theorem Tx-max could be expressed as equation 4.2. For this purpose, each CNM sends its SINR and residual charge to the CH at the given slot. After that, the CH compares all of the received SINR with $SINR_{max}$.and selects α based on set simulation parameters and according to Equation 4.3, the CH calculates all the CNMs' IV and the biggest IV denoted as IV_{max} will be obtained. Going by equation 4.4, the CNM with IV_{max} will be selected as the CH at the next step. Otherwise, the CH continues to be itself and do the above procedures again which thus prolongs the cluster lifetime. Simulation results suggest that this does not degrade the WWAN throughput.

$$IV = \alpha \times S_{Nom} + (1 - \alpha) \times \text{R-}CHG_{Nom} \tag{4.1}$$

$$T_{xpt}\text{-max} = B\log_2(1+SINR_{max}) \tag{4.2}$$

$$\alpha \in [0, 1],\ S_{Nom} \in [0, 1],\ \text{R-}CHG_{Nom} \in [0, 1] \tag{4.3}$$

$$IVCH \leq IV_{max} \tag{4.4}$$

4.4. ULOSTECH IR-UWB D2D WWAN Adjacent Cluster Cooperation

One of the most significant ULOSTECH applicability to the 5G setting is the concept of WWAN D2D adjacent cluster cooperation. This has the potential to seamless expand the coverage of an ultra-dense 5G network along with a reduced E2E latency below 5ns. In a Wi-fi-based D2D, transmission between CH and CNMs are carried out with a synchronized time reference via the WiFi-Direct interface [136]. If a CNM requires D2D communication, it opens the WiFi-Direct interface and sends data packets at the given slot. When the CH receives and analyses the packet headers, the data packets will be retransferred back inside the cluster by the CH via the WiFi-Direct interface provided that the receiver is within the same cluster with the transmitter. If not, the data packets will be retransferred to other CHs using a licensed cellular spectrum. However, the approach of ULOSTECH IR-UWB D2D WWAN to adjacent cluster cooperation is different as all transmission is contained within the allotted UWB band. For instance, as earlier illustrated in Figure 4.3, where 2 IR-UWB WWAN clusters (CH-1 and CH-2) are considered. Given that CH-1 has already downloaded several high capacity multimedia data that consist of videos, graphics, simulations and other bandwidth intensive on-demand data from RS_a as obtained from the BS. If a situation arises that one or more CNMs from cluster 2 require(s) to download or utilize the multimedia data, then RS_a will intimate CH-1 and CH-2 to establish D2D communication for the purpose of sharing the multimedia information as may be required. It is also given that CH-1 must have long distributed the same multimedia data to its CNMs as may be required and thereafter to CH-2.

Before the ULOSTECH IR-UWB WWAN D2D traffic transmission between CH-1 and CH-2, the link setup has to be completed in line with the procedure outlined in section 4.3.1. Upon completion of the D2D link setup, CH-1 and CH-2 will the commence transfer of data packets through the established $DMCS_{ab}$ link. In could be observed that most of the previous works about in-Band D2D communication in the cellular and wifi setup focused on the resource allocation and interference from D2D users to the cellular networks [137]. Here in-Band D2D communication can reuse the uplink (UL) or downlink (DL) resource to transfer data packets. However, adjacent cluster cooperation in ULOSTECH IR-UWB D2D WWAN focuses on the improvement of system performance. This procedure decreases workload of the RS_a since it does not have to satisfy all the individual CNMs from the 2 clusters. Ultimately this will on the one hand reduce work load on the BS while at the same time freeing up license spectrums. Moreover, the method also increases the system throughput while it also minimizes transmission delays. This could potentially enhance E2E latency by bringing it down to desirable figures envisioned for 5G setting of about 5ms. Results of simulations conducted are presented in Sections 4.5.1 and 4.5.2 respectively.

4.5. Performance Evaluation of ULOSTECH IR-UWB Cluster

In this section, we evaluate the performance of ULOSTECH IR-UWB D2D WWAN cluster lifetime as against number of cluster members as well as comparative analysis of system throughput via simulations in MATLAB environment.

4.5.1 SIMULATION EXPERIMENT 4.1 - Performance Evaluation of ULOSTECH Cluster Lifetime Relative to Available Number of Active Cluster Members

In this simulation, it is assumed that all the cluster members have the same charge and the SINR follows random distribution. It is further assumed that did not change for a long time, that is, the SINR is constant for each CNM during the whole simulation period. As results in figure 4.5 indicates, the relationship between the cluster lifetime and the number of members under the premise of different α is provided. It could be observed that the mean lifetime of the cluster increases as the number of CNMs is increasing. Comparing the curves with each other, we can find that a different α makes the various cluster lifetime. Moreover, the longest cluster lifetime is indicated at $\alpha = 0$, it means only the residual charge is considered except the SINR. If there exists a few CNMs with full charge but in a very poor channel condition, these CNMs will be selected as the CHs so that the cluster lifetime will be the longest. Nevertheless, the system performance will be degraded for the lower SINR according to Shannon's theorem. Similarly, when $\alpha = 1$, the operation of transferring the CH only depends on SINR. Under the premise of the unchangeable channel condition for each CNM, the CH with highest SINR will not transfer to other CNMs so that the cluster will breakup when the CH's battery power is exhausted. It could therefore be inferred that the cluster lifetime remains a constant value notwithstanding the growing number of CNMs. Nevertheless, ULOSTECH IR-UWB D2D WWAN cluster scheme addresses this scenario by specifically utilizing the inequality in equation 4.5 which takes this case into consideration. As Figure 4.5 shows, the cluster lifetime increases as the number of cluster members increase no matter what α is. This is very significant for ultra-dense setting expected in 5G environment.

$$2\,(\text{R-CHG}_{\text{Nom}}\text{-}2) \leq (\text{R-CHG}_{\text{Nom}}\text{-}1) \qquad (4.5)$$

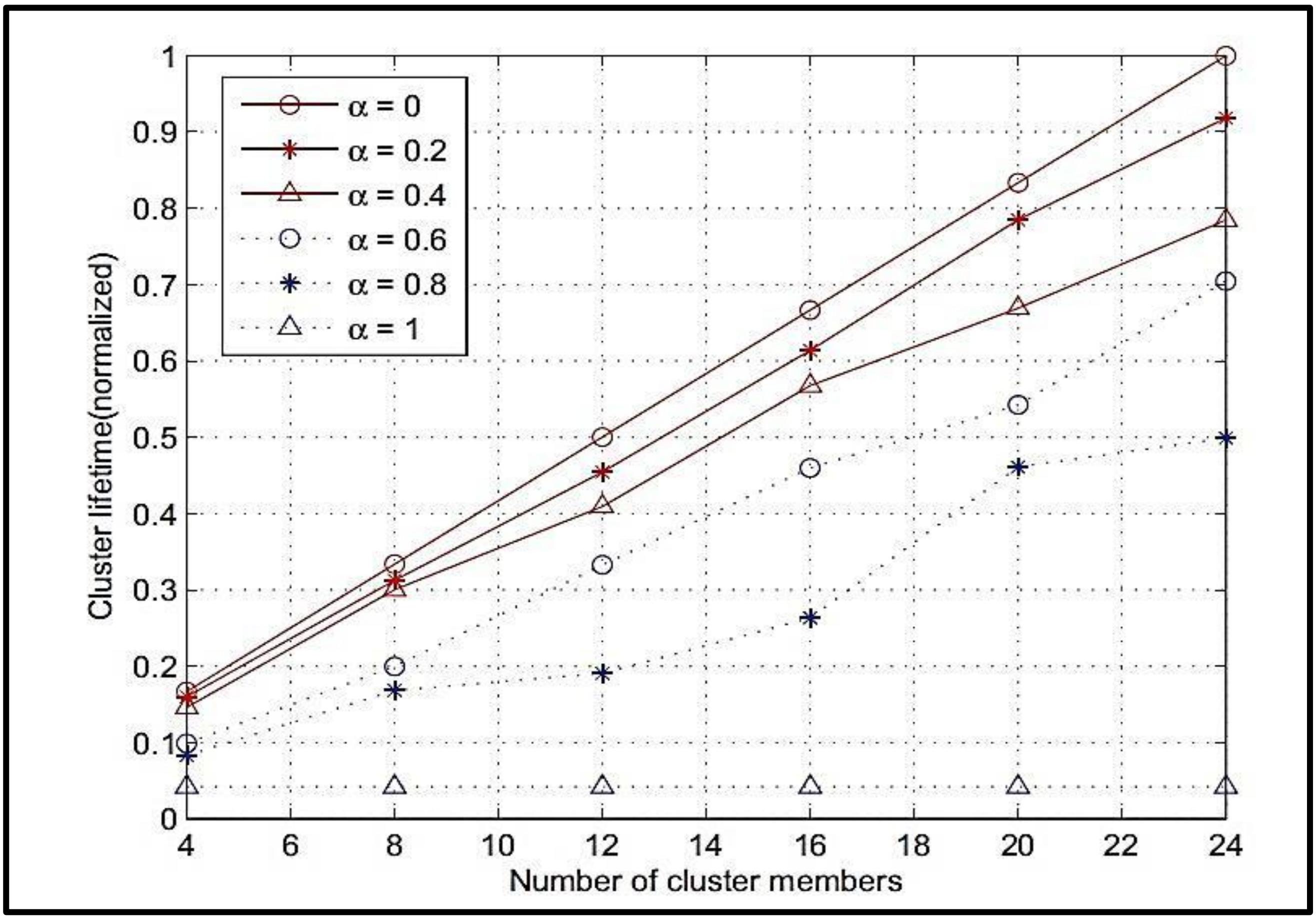

Figure 4.5. Evaluation of ULOSTECH D2D WWAN cluster lifetime against number of cluster memebers

4.5.2. SIMULATION EXPERIMENT 4.2 - Comparative Analysis of ULOSTECH System Throughput with Standard Cellular and Wi-fi Networks

For the second performance analysis, ULOSTECH IR-UWB D2D WWAN throughput is compared with existing cellular and wifi network standards. For this simulation, the cellular cell is assumed to utilize the frequency division duplexing (FDD) mode with 20 MHz system bandwidth which can be divided into 2 downlink and the cell is able to accommodate 2 cellular users at most to transmit data to the BS directly and one cell can accommodate 34 devices at most while one CH can connect with 7 CNMs at most. For the wifi simulation, this thesis is in agreement with [138] [139] that put the maximum throughput of WiFi- Direct network at 250 Mbps. Throughout this simulation, the CHs were assumed to broadcast data traffic to their own clusters at 20 Mbps. Simulation results presented in Figure 4.6 show that the ULOSTECH IR-UWB D2D WWAN cluster cooperation scheme increases the system throughput significantly by a factor of about 0.75 as the number of cluster devices increases. This suggests the suitability of the ULOSTECH approach to 5G setting.

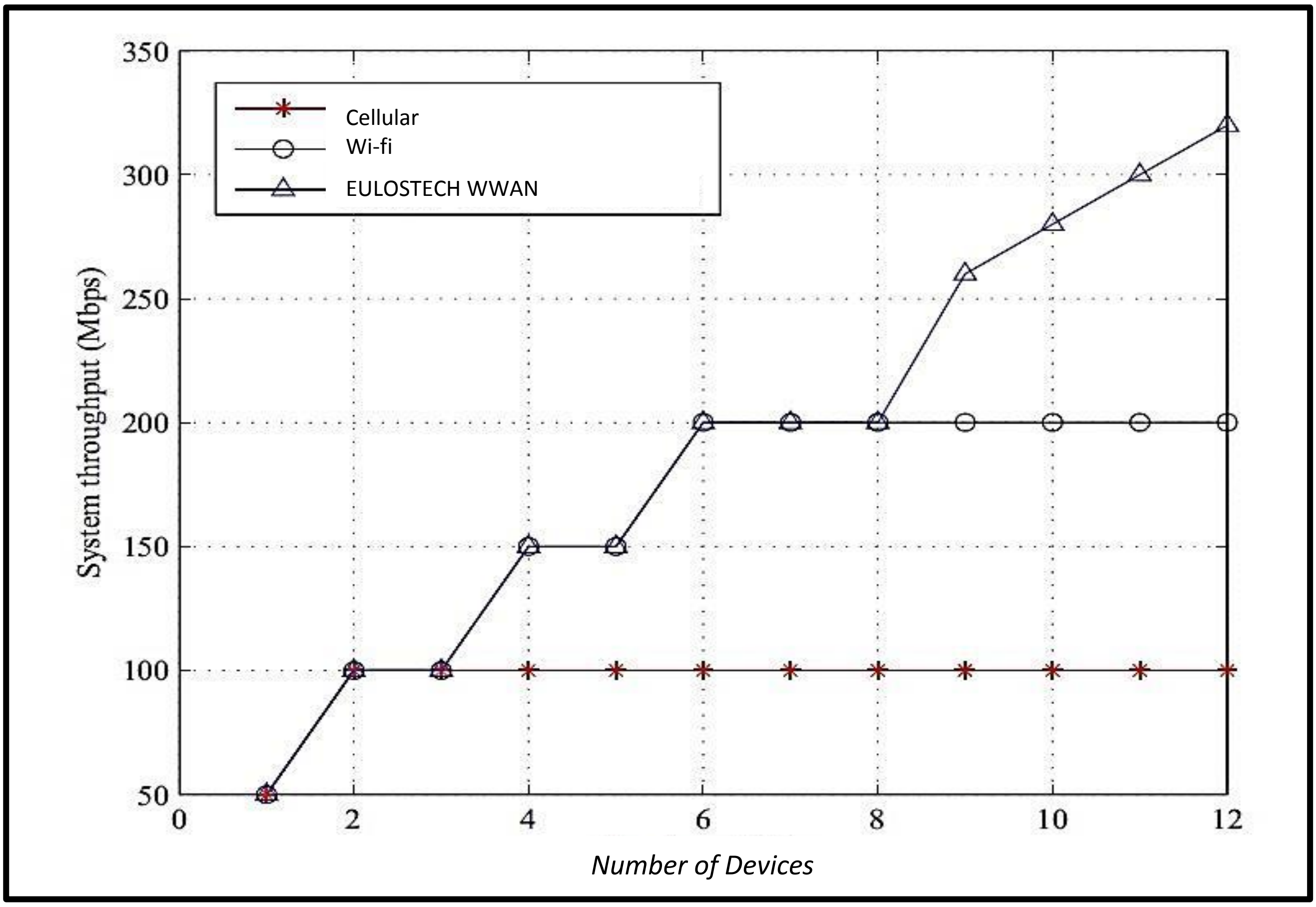

Figure 4.6. Comparison of ULOSTECH WWAN D2D system throughput with Cellular and Wi-fi Networks

4.6. ULOSTECH D2D-propagation-based combined localization and communication Scheme (ULOSTECH UD-CLOCS) for Ultra-Dense Networks

4.6.1. UD-CLOCS Considerations.

The concept of ubiquitous communication was highlighted in section 2.2.3 and it is believed that its implementation requires seamless connectivity and high-definition localization before any other services can be implemented. Moreover, traditional localization services consume system resources. It is believed that system load is a significant factor that must be carefully considered especially in an ultra-dense scenario envisaged for the 5G environment. This section therefore presents ULOSTECH UD-CLOCS; a D2D-propagation-based combined localization and communication scheme that features cognitive cooperation amongst devices in spatial proximity of clusters as defined in the preceding sections 4.2 and 4.3 respectively. Figure 4.7 shows an hypothetic UD-CLOCS network structure proposed in this section that comprises a large-scale network designed to satisfy the above 1,000,000 device density per square kilometre envisaged for the 5G setting. Each device can be classified as either 'pre-localized', 'un-localized' or 'to-be-localized'. The pre-localized devices serve as anchors for which information regarding their positions are known and readily available. Al the RSs fall into this category as well as fixed devices like cognitive factory machines and high capacity equipments like WLAN APs. It is assumed that

I. All the devices under consideration are operating in an ULOSTECH IR-UWB network overlay scenario.
II. The distribution of all the devices is uniform such that it can be modelled as an ultra-dense WWAN of a nearly uniform semi-grid structure.
III. D2D communication and localization links amongst devices will be via ULOSTECH D2D WWAN DMCS.
IV. The pre-localized devices are ULOSTECH IR-UWB enabled RS along with IR-UWB machine in within range.
V. There are fewer pre-localized devices compared to the number of un-localized devices.

VI. The devices to be localized would estimate their positions through distance estimation that utilizes D2D-propagation from pre-localized devices.

VII. RSS estimation techniques are used for distance computations using IR-UWB ray decay determination concepts; as discussed and experimented in section 3.3.

VIII. The IR-UWB threshold-based estimation update method is employed in UD-CLOCS

For a successful UD-CLOCS estimation, a threshold is set for which a measured RSS that exceeds the threshold is assumed to be imprecise. Therefore, the ULOSTECH UD-CLOCS threshold was set at 50m. When a distance exceeds the 50m threshold, it can be estimated using a UD-CLOCS D2D-propagation scheme via intermediate devices in spatial proximity between the source and destination devices. To mitigate estimation errors inherent in network distance measurements like Trilateration and multi-dimensional scaling (MDS) amongst a variety of other localization techniques as discussed in section 2.7, ULOSTECH UD-CLOCS is presents an estimation that is more accurate than trilateration and less complex than MDS methods.

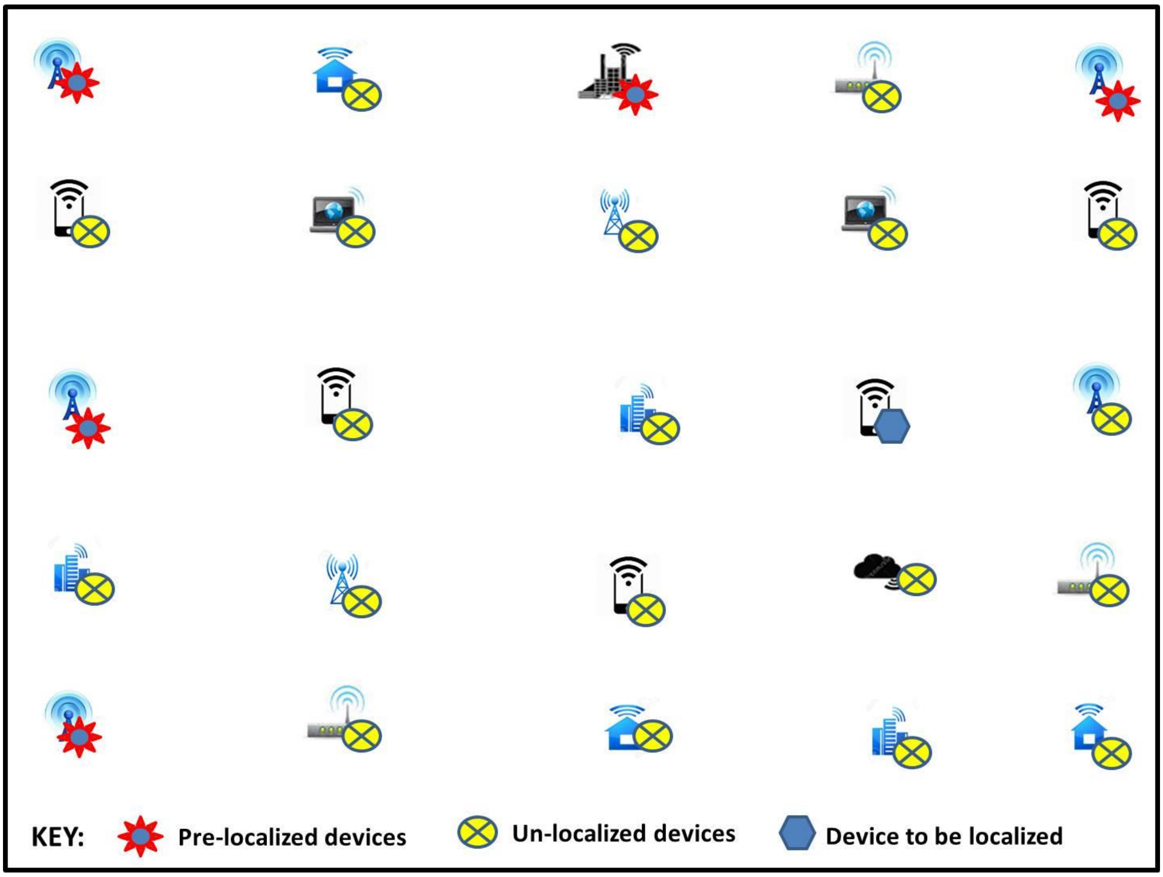

Figure 4.7. Hypothetic UD-CLOCS ultra-dense network device distribution structure

4.6.2. The ULOSTECH UD-CLOCS Algorithm Details

This section details the UCLOCS; an efficient D2D localization algorithm, that overcomes the negative aspects of both the trilateration and MDS algorithms. The proposed algorithm utilizes the envisioned dense geographical distribution of devices in a 5G network setting with evenly distributed number of devices. To account for randomness in the distance between each device and its neighbouring devices, the algorithm models distance as a Gaussian random variable and identifies the position at which the maximum likelihood of all neighbour devices are optimized. The procedures of the algorithm are as follows:

I. Cluster discovery, cluster joining/formation and D2D peer selection as presented in sections 4.3 and 4.4.

II. Average distance estimation.

III. Hop counts from pre-localized devices, via unlocalized devices to devices to be localized.

IV. Estimation of initial positional coordinates.

V. ULOSTECH UD-CLOCS estimation updates that utilizes threshold estimation modelled in section 4.6.3.

4.6.3. The ULOSTECH UD-CLOCS threshold Modelling

To model the ULOSTECH UD-CLOCS, let the received IR-UWB multipath signal be represented as equation 4.6.[140]

$$r(t) = \sum_{j=-\infty}^{\infty} d_j \omega_{mp}(t - jT_f - c_j T_c - \tau_{toa}) + n(t) \tag{4.6}$$

The frame index and frame duration are denoted by j and T_f, N_s represents the number of pulses per symbol, T_c is the pulse duration, Ts is the symbol duration, τtoa is the TOA of the received signal, If we take ω(t) as the received UWB pulse with unit energy, **E** as the pulse energy, and αl and τl are the fading coefficients and delays of the multipath components, respectively. It is further given that the additive white Gaussian noise (AWGN) with zero-mean and double-sided power spectral density $N_0/2$ and variance σ^2 is denoted by n(t) while no modulation is considered for the ranging process. Moreover, in order to avoid catastrophic collisions, and smooth the power spectral density of the transmitted signal, time-hopping codes as expressed in equation 4.7 are assigned to different users together with random-polarity codes $d_j \in \pm 1$; which are used to introduce additional processing gain for the detection of desired signal, and smooth the signal spectrum.

$$c_j^{(k)} \in \{0,1,\ldots,N_h-1\} \tag{4.7}$$

The number of samples (or blocks) is denoted by equation 4.8 and this corresponds to the sample index with respect to the starting point of the uncertainty region. At a sampling interval of t_s (which is same as block length T_b); therefore the sample value at the output is given by equation 4.9.

$$N_b = \frac{3}{2}\frac{T_f}{T_b}, \text{ and } n \in \{1,2,\ldots,N_b\} \tag{4.8}$$

$$z[n] = \sum_{j=1}^{N_s} \int_{(j-1)T_f+(c_j+n-1)T_b}^{(j-1)T_f+(c_j+n)T_b} |r(t)|^2 dt \tag{4.9}$$

From Equation 4.9, the received samples are compared to an appropriate threshold, and the first threshold-exceeding sample index can be corresponded as the desired estimate in accordance with equation 4.10; where ξ is the ULOSTECH UD-CLOCS estimation threshold that must be set based on the received signal statistics. Given the minimum and maximum energy sample values, equation 4.11 is then used to estimate the normalized threshold.

$$t_{TC} = [\min\{n|z[n] > \xi\} - 0.5]\, T_b \tag{4.10}$$

$$\xi_{norm} = \frac{\xi - \min\{z[n]\}}{\max\{z[n]\} - \min\{z[n]\}}. \tag{4.11}$$

To mitigate the expected estimation error, mean absolute error (MAE) assumes that the delay of the leading-edge energy block is fixed. It is also given that n_{toa} denotes the first arriving energy block index, n^ denotes the estimated block index, and n=1,2,⋯,NB denote the block indices where the energy block is being searched. Considering the ULOSTECH UD-CLOCS estimation threshold ξ, the probability of detecting an arbitrary block n_{hyp} to be the energy block is as expressed in equation 4.12.

$$\begin{aligned} P_D(n_{hyp}) &= P(\hat{n} = n_{hyp}) \\ &= \left[\prod_{n=1}^{n_{hyp}-1} P(z[n] < \xi)\right] \times P(z[n_{hyp}] > \xi) \end{aligned} \tag{4.12}$$

4.6.4. The ULOSTECH UD-CLOCS Locational Device Discovery

Figure 4.8, shows typical preliminary paths explored for discovery of a device to be localized while cluster discovery, joining/formation follows the earlier discussed ULOSTECH cluster schemes in section 4.3.1 and 4.3.2. Each device selects neighbours by determining which of the surrounding devices are within a measurable distance while devices outside this measurable range are not included in the micro-cluster group of neighbouring devices. Comparative performance experiments indicates that that the mean distance error of UD-CLOCS fares better in comparison with trilateration and MDS methods as presented in Experiment 4.3. Simulation results suggest that the ULOSTECH UD-CLOCS algorithm performs simple D2D-propagation with few resources of the ultra-dense network such that reduces estimation errors while it facilitates efficient device locations with pre-localized devices.

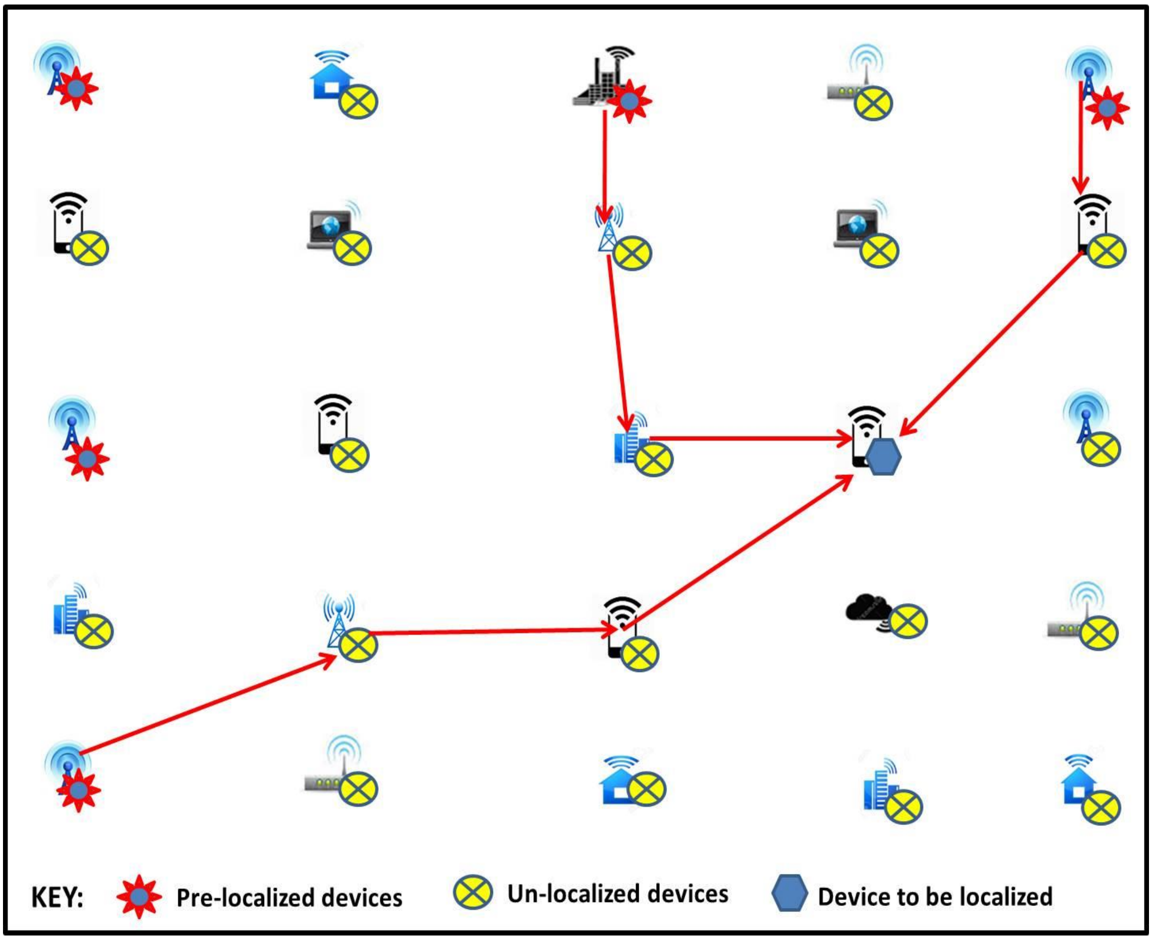

Figure 4.8. Device distribution structure of ULOSTECH UD-CLOCS ultra-dense network.

4.7. SIMULATION EXPERIMENT 4.3 - Comparative Performance Assessment of ULOSTECH UD-CLOCS mean Distance Error

4.7.1. Deployment Scenario

These simulations were conducted to determine the comparative performance of ULOSTECH UD-CLOCS mean distance errors as against that of 2 other methods – trilateration and MDS using simulation in MATLAB environment. Devices were deployed in a simulation scenario of an 100m by 100m square semi-grid condition. Moreover, pre-localized devices were semi-randomly positioned at the grid edges while the number of un-localized devices was set to 60 along with a minimum inter-device distance set to 25m. This indicates that each device detects all devices within range as neighbouring devices. Additionally, only one device is designated as 'device to be localized' for the purpose of the simulation.

4.7.2. D2D Localization Estimation Simulation Process

The simulations were conducted such that each phase entails using three different methods of trilateration, ULOSTECH UD-CLOCS and MDS in conditions of no errors and 50% errors for emi-rig, grid and random deployment scenarios. First the initial coordinates are obtained from trilateration, the ULOSTECH UD-CLOCS and finally MDS. In these steps, each device calculates distance from each pre-localized device. Here, a given device to be localized discovers routing to each pre-localized device by establishing the shortest path. Here the routing D2D devices detect neighbouring devices in spatial measurable proximity below 50m and manages them as neighbouring devices. Then the device to be localized builds transition matrix by referring the information of its neighbouring devices finds a path to each pre-localized device as earlier illustrated in Figure 4.8. Thus, un-localized devices in the process have their own transition matrices so that they set themselves as transition source devices from a route originating at the pre-localized devices on to the device to be localized. In addition, the hop counts from the pre-localized devices to the device to be localized are computed. Finally, distances to Pre-localized devices are calculated by multiplying the hop counts and the average distances. This method may bring a large error unless the devices between the pre-localized devices and the device to be localized are pre-positioned in a straight line which is not realistic. Therefore, refinement process is adopted such that the initial errors do not affect the performance of the localization algorithm, while the required time this initial step in the simulation is noted. It should be noted also that this initial time does not include.

4.7.3. Simulation Results

Simulation results obtained from running the various cycles of simulation are presented in Table 4.1. This indicates the results of three different localization al methods that were simulated for the performance comparison, including UD-CLOCS . During the simulation, each device is configured to refine its the initial coordinates by referring to position information from its neighbouring devices in the following three ways entailing

I. **Trilateration:** each device performs trilateration with its neighbouring devices.

II. **UD-CLOCS** : each device runs the UD-CLOCS algorithm to update its coordinate.

III. **MDS:** each device runs the MDS estimation update method.

The duration of the each process is then noted with which the elapsed iteration time was recorded for the three methods utilized in the simulation process. A timeline was maintained throughout the simulation process that accumulated the running time in seconds. It should be noted that by observing elapsed time, we can evaluate how the algorithms affect network system load amongst other parameter as indicted in Figures 4.9, 4.10 and 4.11 respectively that features the comparative performance under grid, semi-grid and random deployment at various non error and 50 per cent.

Table 4.1:- Comparative Mean Distance Error Estimation Refinement Data for trilateration, ULOSTECH UD-CLOCS and MDS Estimation Methods.

Simulation Configuration	Algorithm running time (s)	Method	Mean Distance Error
No error Grid setting	8.02	TRLN	6.88
		UD-CLOCS	1.75
		MDS	4.01
No error semi-Grid setting	29.60	TRLN	9.31
		UD-CLOCS	3.66
		MDS	4.93
50% error Grid setting	19.35	TRLN	9.16
		UD-CLOCS	5.18
		MDS	8.32
50% error semi-Grid setting	35.61	TRLN	15.55
		UD-CLOCS	5.92
		MDS	11.66
No error random setting	38.18	TRLN	13.13
		UD-CLOCS	5.76
		MDS	9.11
50% error random setting	30.50	TRLN	15.51
		UD-CLOCS	11.12
		MDS	12.41
No error random setting	3950.6	TRLN	39.79
		UD-CLOCS	13.71
		MDS	28.31

4.7.4. Analysis of the Simulation Results

The mean distance error, which is equal to the sum of all estimation errors divided by the number of devices, is plotted against elapsed time. Here, each symbol denotes mean distance error after each iteration cycle. In Figure 4.9, no refinement compensation was used for trilateration because the distance error was assumed to be zero. Thus, the trilateration scheme completed localization in one cycle. Note that even though the performance of the UD-CLOCS algorithm was worse than that of the MDS algorithm after refinement, the UD-CLOCS algorithm ran much faster, thereby reducing localization error. Therefore, when the system limits time and memory resources for localization, for example within 1 min, the performance of the UD-CLOCS algorithm is much better than that of MDS. Similarly, when 50% distance measurement errors exist as shown in Fig 4.10, while Figure 4.11 is the results of the position estimation for a random deployment at 50% distance errors.

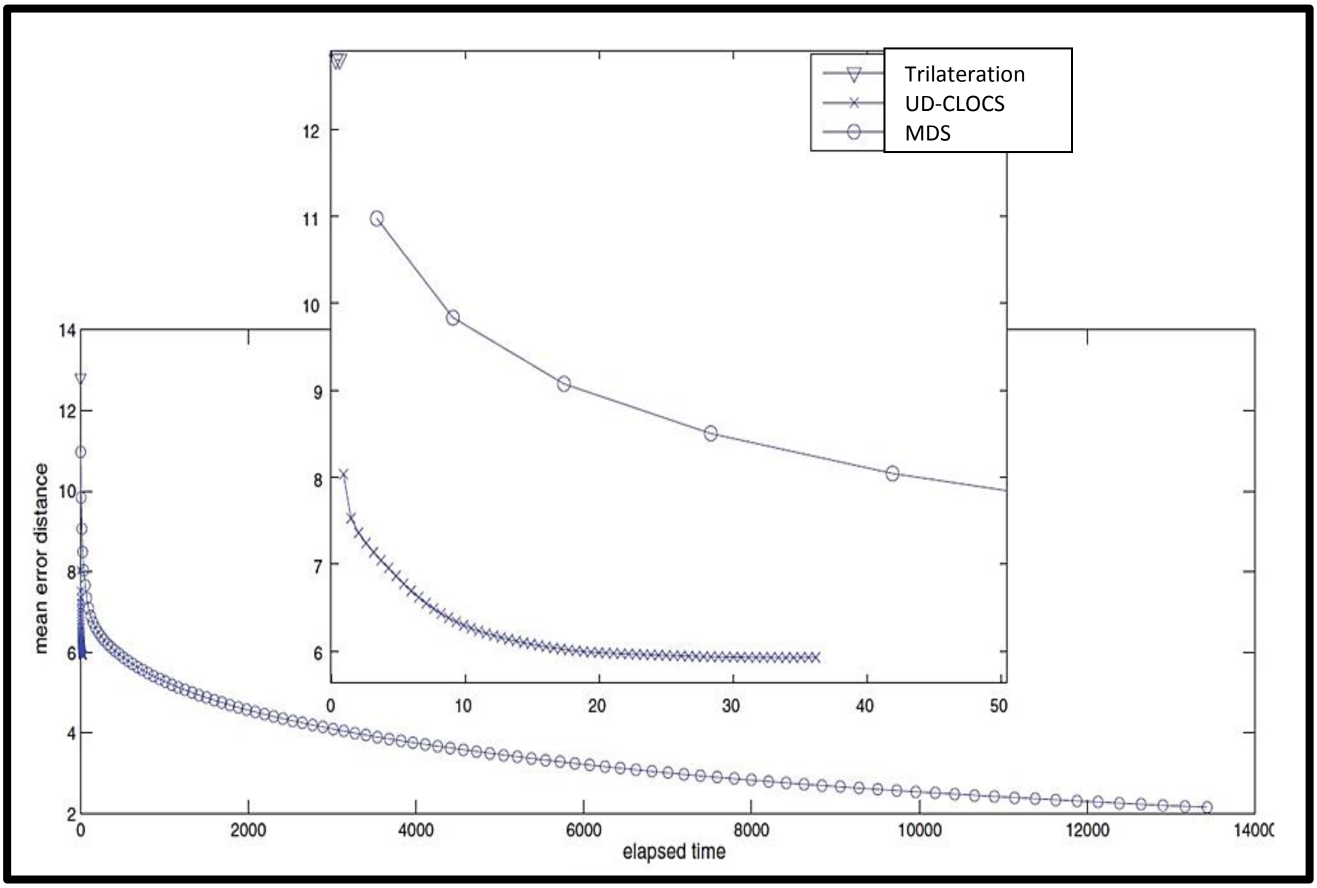

Figure 4.9. Comparative Localization Errors for trilateration, ULOSTECH UD-CLOCS and MDS Estimation Methods in a Semi-grid deployment with no distance errors.

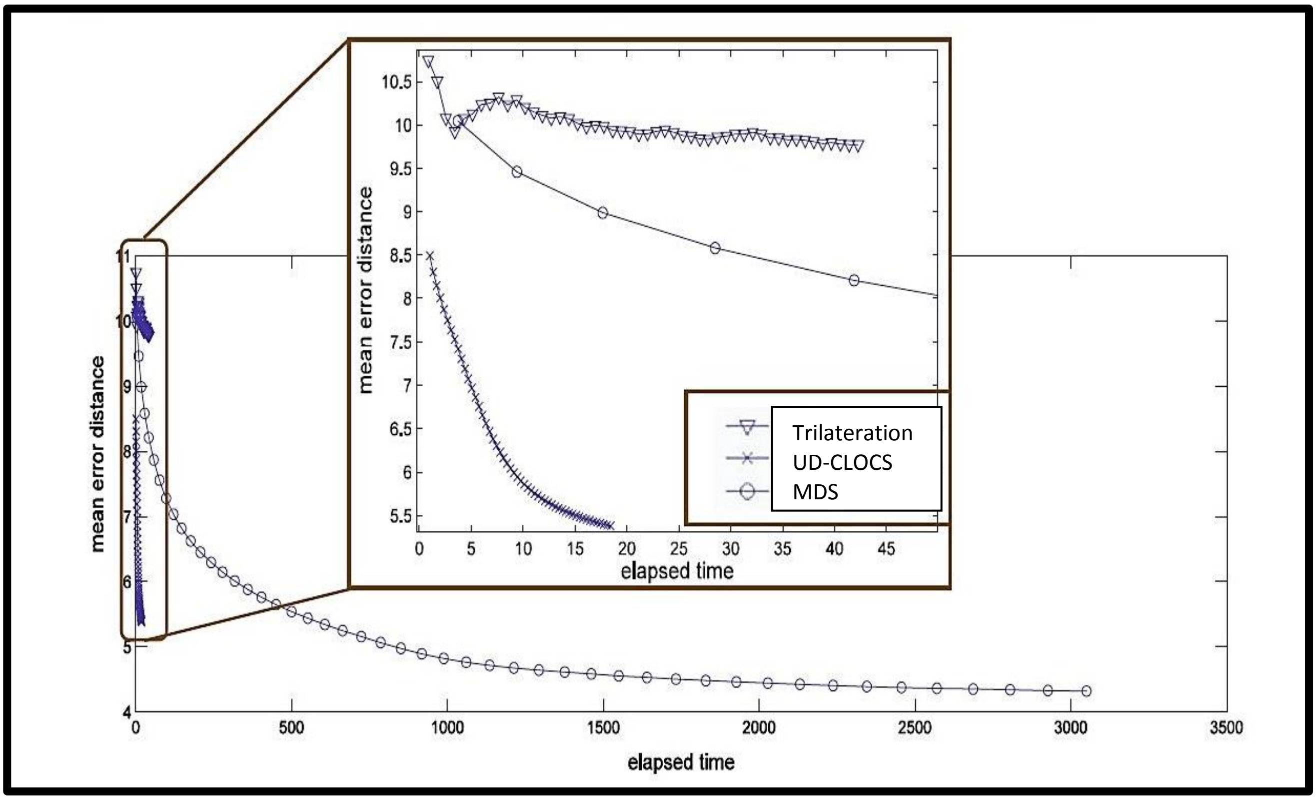

Figure 4.10. Comparative Localization Errors for trilateration, ULOSTECH UD-CLOCS and MDS Estimation Methods in a grid deployment with 50 per cent distance errors.

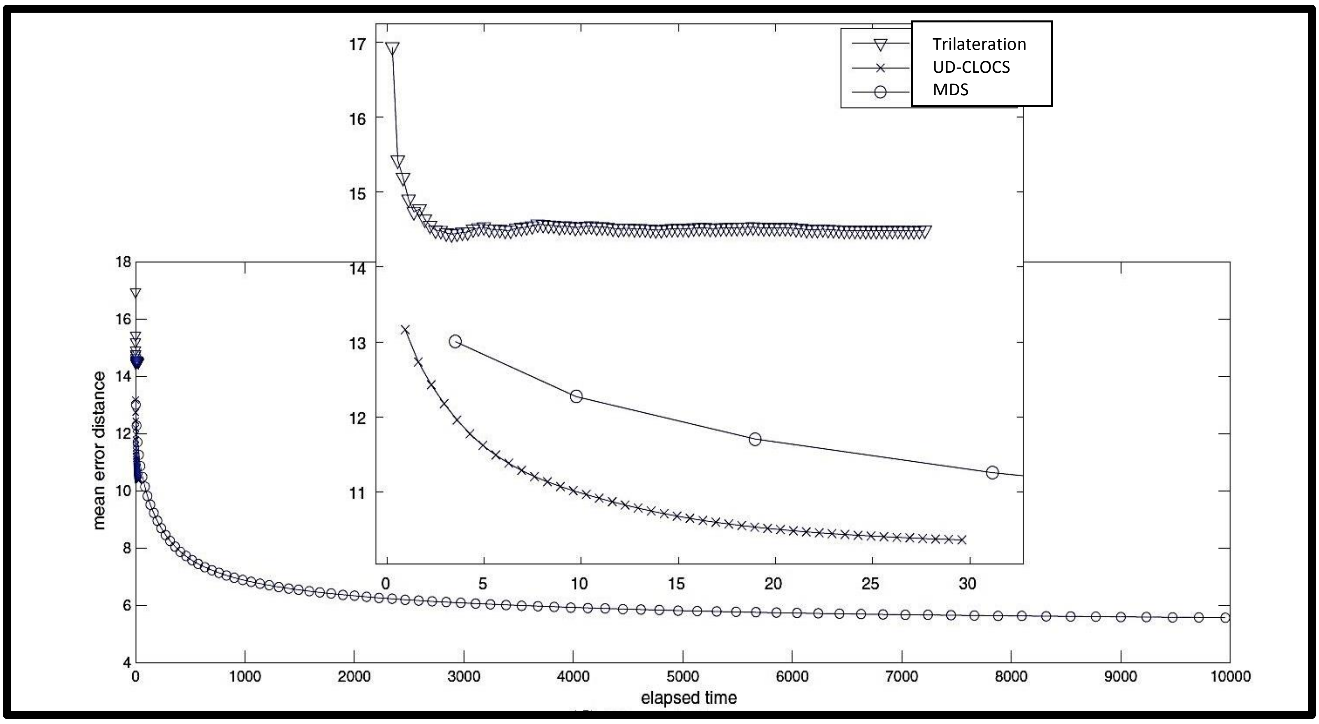

Figure 4.11. Comparative Localization Errors for trilateration, ULOSTECH UD-CLOCS and MDS Estimation Methods in a random deployment with 50 per cent distance errors.

4.8. Summary

This ULOSTECH IR-UWB D2D WWAN presents a cluster formation scheme whose performance evaluation suggest a cluster lifetime and system throughput that are suitable for the envisaged 5G setting. Also the ULOSTECH UD-CLOCS is a promising prospect for the 5G environment.

CHAPTER FIVE

5G-COMUSA: A Concurrent Super-core IR-UWB Overlay Network Architecture for the 5G Setting

5G-COMUSA: A Concurrent Super-core IR-UWB Overlay Network Architecture for the 5G Setting

5.0. Chapter Overview

This Chapter discusses 5G-COMUSA; the multi-layered, concurrent, all-IP super-core IR-UWB WWAN D2D overlay network that features cognitive self-tuneable adapters to accommodate various access networks. The 5G-COMUSA network layout is presented along with envisaged scenarios for the 5G setting. It covers the global structure for the IR-UWB WWAN D2D setting covering the overlay network, the super-core network connection as well as the multi-tier network connection.

5.1. Considerations for the 5G-COMUSA

5.1.1. 5G Design Requirements and Design Issues

As earlier discussed in section 2.9, it is understood that the 5G mobile networks must address the challenges that are not adequately addressed by the current state of-the-art access network technologies. These amongst others include ultra-dense massive device connectivity of about one million devices per metre square, higher data rate of between 1 – 10 Gbps, lower E2E latency of below 5ms as well as consistent provisioning with spectral efficiency in the range of 4.5 $bs^{-1}Hz^{-1}$. It is further opined that 5G should not be an incremental advance on the 4G but rather a major paradigm shift with massive bandwidths, extreme base and relay stations along with unprecedented numbers of antennas [141]. These proposed key requirements are summarized in Table 5.1. This Author is however of the view that considering the investments already made on current access networks, the 5G environment should be highly integrative such that would tie any new air interface and spectrum together with current terrestrial and satellite access networks. This would provide universal high-rate coverage and a seamless user experience. To support this, the core network should have to reach unprecedented levels of flexibility, intelligence and improved spectrum utilization together with energy efficiencies and cost benefits. It is further suggested that 5G requirements and key performance indicators (KPI) should be primarily related to end users. The KPIs taken as a basis for assessment of the radio link related requirements from the end-user perspective have been considered in literature to include: traffic volume and density, experienced end-user throughput, latency, reliability, availability, and retainability [142]. The technical objective of this approach to 5G requirements is to develop technical solutions toward a system concept that supports a more robust network that is better than currently obtains.

Table 5.1. Proposed key 5G requirements and respective applications [143]

Requirements	Performance expectation	Applications
Data volume	• 10 Gbph in busy period per user • 500 Gbph per month per subscriber	Dense urban information utilization centres
Data rate	1 to 10 Gbps	Virtual reality office
Connected devices	500,000 devices per AP	Massive deployment of sensors and actuators
Latency	Less than 5ms	Targets 1ms for M2M, safety and security
Spectral efficiency	$4.5 bs^{-1}Hz^{-1}$	Ultra-dense network
Dependability	99.99%	Tele-protection, traffic efficiency, safety and security

5.1.2. The 5G-COMUSA Concept

The core goals of the 5G vision include coverage expansion, backhaul offload; provision of fall-back connectivity, increase spectrum utilization and capacity per area [143]. It is suggested that the resulting 5G architecture should provide a consistent framework that integrates different access technologies. Moreover, it should be such that entails a centralized seamless all-IP super-core with flexibility of decentralized D2D service approaches. This is the central theme of the 5G-COMUSA concept. The rest of this chapter therefore lays-out various facets of the 5G-COMUSA overall network scenarios and structure proposals for the 5G setting. The proposals cover the 5G network structure which features an IR-UWB WWAN D2D overlay network with seamless connectivity for all access technologies and capability for WWAN D2D communication so that user-plane traffic does not pass-through any licensed network infrastructure. This is expected to free-up the licensed spectrums in the 5G environment.

5.2. The 5G-COMUSA Overlay Structure

In order for objects and devices to usefully become part of a wider intelligent and information sharing network such as envisioned for the 5G setting, it is vital that each one has a unique identity. The ability of objects and devices to have location information adds another important level of intelligence that allows discovery of people, objects, and resources while it also enables location-based tools, solutions and services. RFID tags constitute the most important technology used to provide network based identity. It is however believed that new approaches are required for a more secure passive RFIDs that are not cryptography-based. It is suggested that ULOSTECH solutions earlier proposed in this thesis will be suitable for high definition location and identification services in the 5G environment. Asides from 5G network architecture earlier discussed in section 2.9.5 and 2.9.6, other earlier works like [144] also highlights a UWB method based on time-hopped pulse-position modulation (TH-PPM) while the ubiquitous Networking Laboratory also proposes an active tag based on IR-UWB which realizes ultra-low-power consumption, highly accurate positioning to within 30cm, and a communication speed of 10 Mbps at a distance of 10m and 250 kbps at a distance of 30m [145].

Considering that IR-UWB technology provides an excellent means for wireless positioning due to its high resolution capability in the time domain along with capability for combined wireless communication and location positioning utilizing portable positioning algorithms [146], this research explores IR-UWB techniques in its proposal for 5G implementation architecture. Earlier thoughts along this path include investigation of the positioning problem from a UWB perspective that aims at a performance bounds and estimation algorithms for UWB ranging positioning [147]. The Authors in [148] also introduced a model for the estimated distance obtained from TOA of the first path in a multipath environment used for WPAN applications. In [149] [150] and [151] authors investigated several position estimation approaches employing UWB technology high-accuracy, low-cost IR-UWB wireless location system based on the quasi TDOA method. However, the entire aforementioned directions still had to contend with NLOS issues on the one hand while also contending with inband interference issues on two planes with co-channel users and cluster peers since different transmission technologies are utilized for communication and localization activities. The 5G-COMUSA approaches the 5G structure as shown in Figure 5.1 with facets of ULOSTECH solutions in order to address the inadequacies observed in earlier proposals in literature.

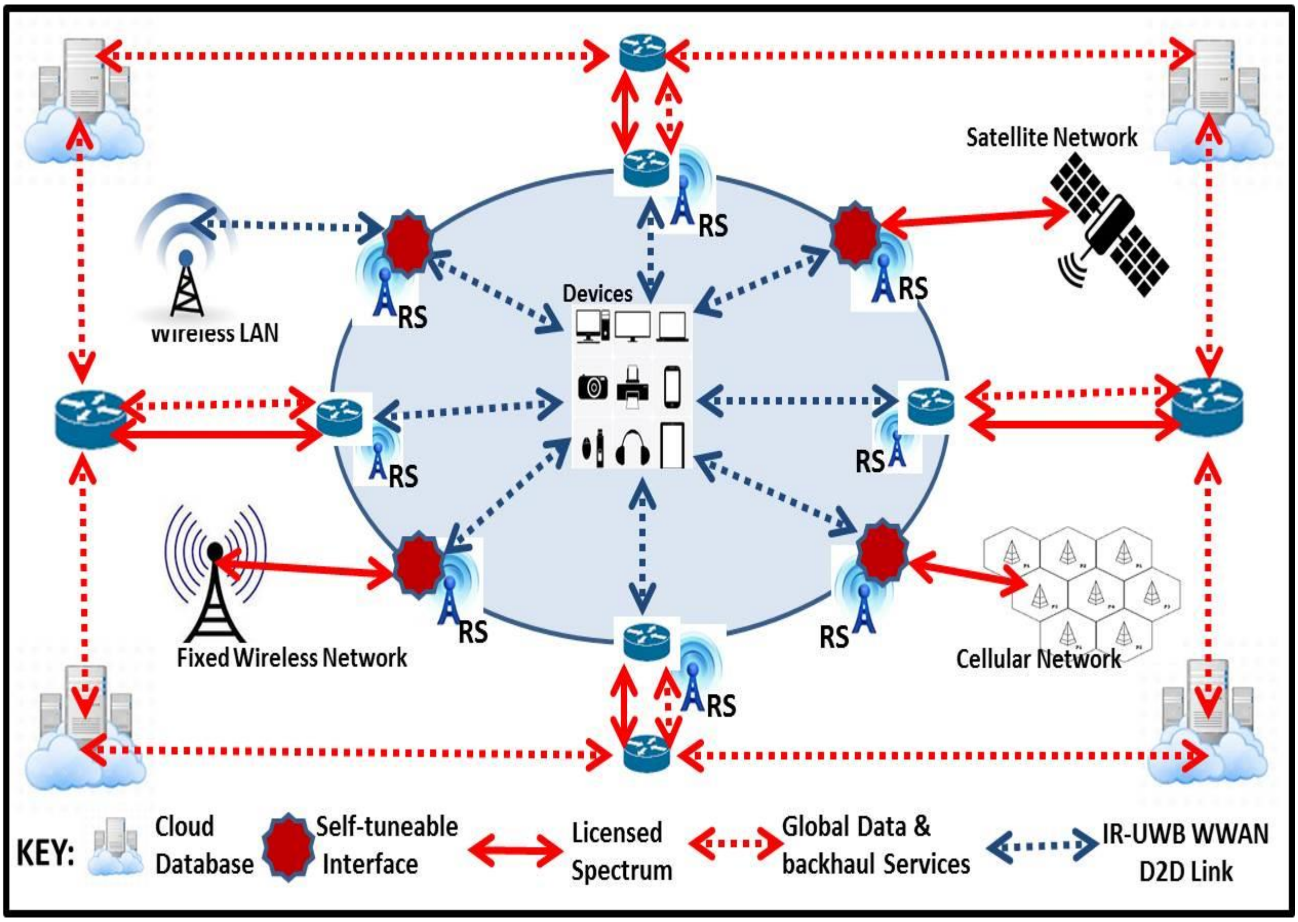

Figure 5.1. Architecture of 5G-COMUSA IR-UWB WWAN D2D overlay network.

The network structure presented in Figure 5.1 gives a global view of the 5G-COMUSA overlay network structure as well as the interplay of the various components. The 5G-COMUSA employs an IR-UWB WWAN overlay network for both terrestrial and satellite connections through self-tuneable single protocol IR-UWB adapters for a robust combined D2D communications and localization. This employs an IR-UWB RSS threshold estimation technique discussed in sections 4.6.2 and 4.6.3 respectively for location services. It features WWAN D2D devices that are linked in consonance with the unique IR-UWB DMCS as presented in section 4.2. The structure also spots a cluster formation and a cluster cooperation scheme as described in sections 4.3 and 4.4 respectively. Also featured is the UD-CLOCS scheme that is expected to support ultra-dense network scenarios in the 5G setting. The layout also features a cloud-based network databases to house critical data and information with access through licence spectrums at the various RS locations. Also included is provision for backhaul services on licensed spectrums. The 5G-COMUSA is expected to foster a very reliable and robust network for the 5G setting.

5.3. The Proposed 5G-COMUSA Scenarios.

Many scenarios have been projected in literature for the upcoming 5G environment based on the challenges, requirements, and approaches as identified in section 2.9. In the estimation of this thesis, four scenarios would most probably playout in the 5G setting. These are the ubiquitous D2D communication of assets (U-D2D-CA), unlimited always-with-you boundless service in a crowd (UABSC), always-on best experience follows you (ABEFY) and excellent real-time and reliable M2M connections (ERR-M2M-C) as highlighted in paragraphs 5.3.1, 5.3.2, 5.3.3 and 5.3.4 respectively.

5.3.1. 5G-COMUSA Scenario-1: -

Ubiquitous D2D Communication of Assets (U-D2D-CA).

The U-D2D-CA scenario focuses on the efficient handling of a very large number of ubiquitous devices; including machine-type devices and sensors, with widely varying requirements as depicted in Figure 5.2. The scenario addresses the communication needs of ubiquitous low-complexity devices like sensors and actuators along with more advanced ones like cognitive medical devices and smart industrial machinery. The resulting requirements vary widely in terms of payload size, frequency of transmission, complexity, energy consumption, transmission power and latency. For instance, massive deployment of sensors and actuators envisages massive number of small sensors and actuators to be mounted on stationary and movable objects around the world to enable a wide range of applications connected to monitoring, alerting and/or actuating. Also envisaged is provision of connectivity for about 500,000 devices within one cell along with low cost device implementations in order to support billions of connected devices expected in 5G. These novel requirements cannot be fully met by today's cellular networks. It is believed that ULOSTECH schemes presented in chapter 3 and 4 respectively point the way forward for an overall 5G architecture that will enable U-D2D-CA to thrive in the 5G setting.

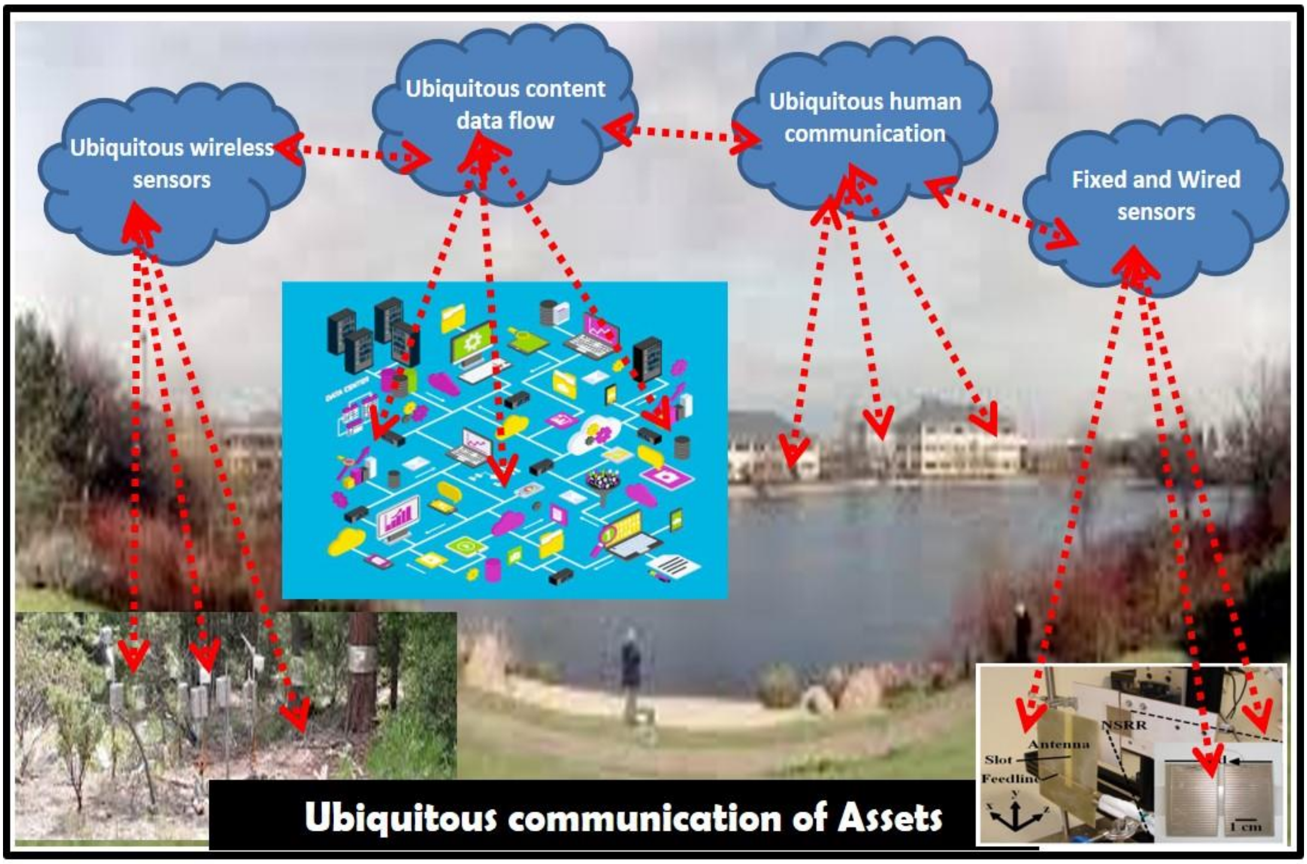

Figure 5.2. Schematic of proposed 5G scenario for ubiquitous D2D communication of assets

5.3.2. 5G-COMUSA Scenario-2: -

Unlimited always-with-you boundless service in a crowd (UABSC).

The proposed UABSC scenario outlined in Figure 5.3 focuses on provision of reasonable mobile broadband experiences in crowded areas while it addresses end-user needs for connectivity even in such ultra-dense very crowded places. These include amongst others areas such as stadia, concerts, shopping malls, open air festivals, unexpected traffic jams and other public events that attract lots of people. It is expected that cloud service providers, local content providers as well as traditional operators and other emerging service operators will be major players in the provision of UABSC solutions. Again, UWB technology is considered probably most effective for implementation of this service scenario. ULOSTECH UD-CLOCS is very suited for this scenario.

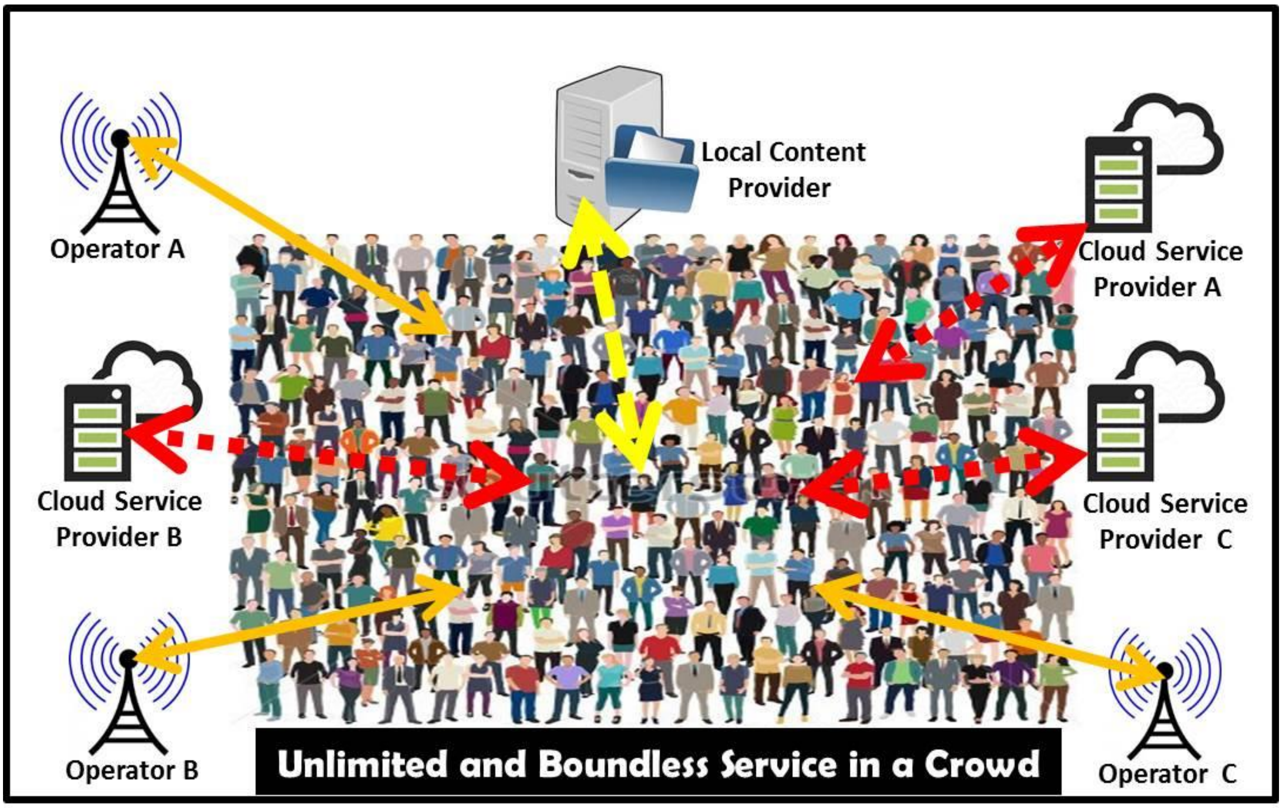

Figure 5.3. Schematic of the proposed 5G scenario for unlimited, always-with-you and boundless service in a crowd

5.3.3. 5G-COMUSA Scenario-3: -

Always-on Best Experience Follows You (ABEFY).

The proposed ABEFY 5G scenario as depicted in Figure 5.4, focuses on providing end users on the move (e.g. pedestrians, people in cars and trains) with high levels of service experience. BEFY envisages the same good user experience for an end user on the move just like the ones at home or in the office. Users on the move would have the impression that the network infrastructure "follows them" in situations that are known to currently suffer from poor coverage. High data rate services such as video streaming and file downloads in "blind spots" are typical applications for this scenario and it is expected at every location of the service area, even in remote rural areas. The end users should be able to experience a data rate of above 1 Gbps while maintaining end-to-end (E2E) latencies below 5ms. The ULOSTECH UD-CLOS WWAN cluster to cluster cooperation is expected to foster seamless transitions as users move around in the 5G environment.

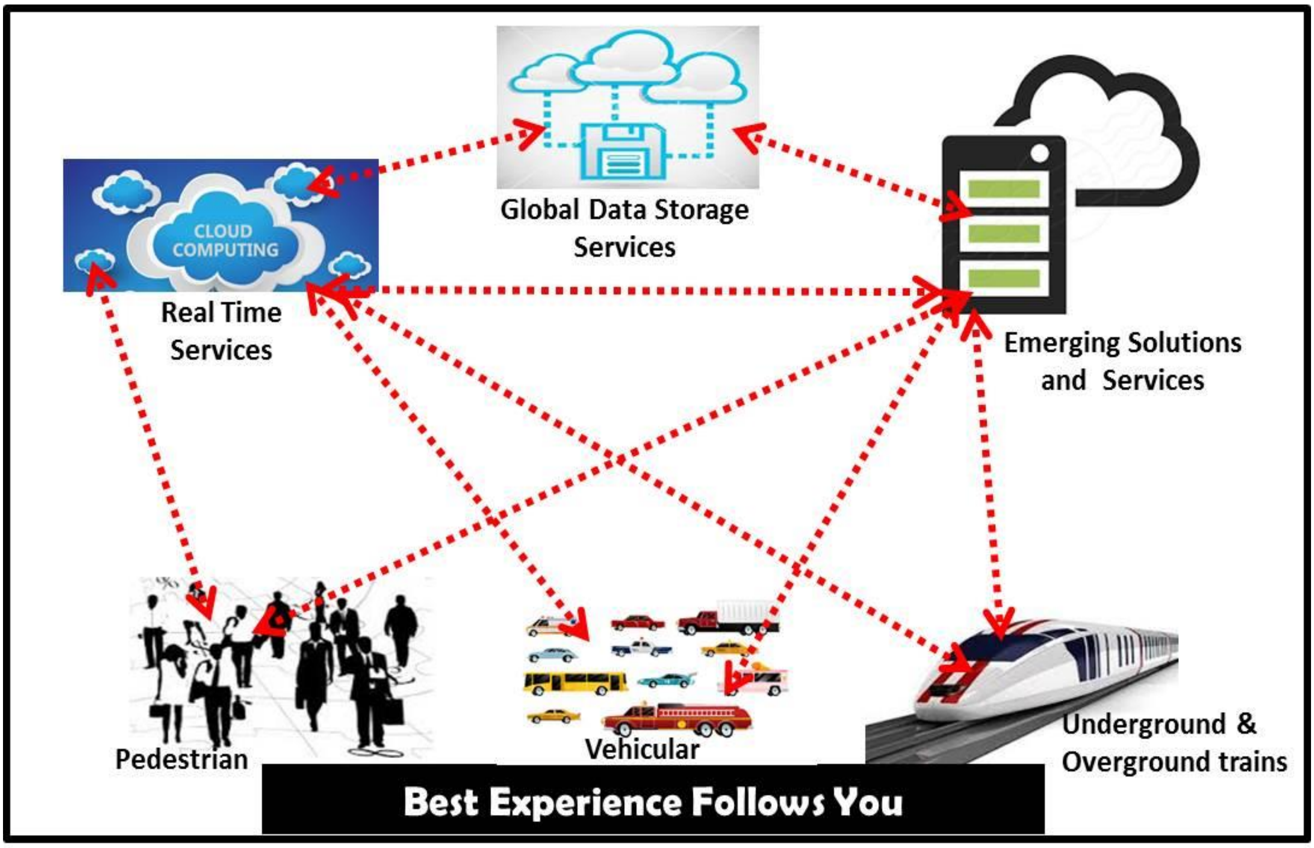

Figure 5.4. Schematic of proposed 5G scenario for always-on best experience follows you.

5.3.4. 5G-COMUSA Scenario-4: -

Excellent real-time and reliable M2M connections (ERR-M2M-C).

The ERR-M2M-C 5G scenario as depicted in Figure 5.5; focuses on new applications and use-cases with very strict requirements on latency and reliability. The reliability and latency in today's communication systems have been designed with the human user in mind. ERR-M2M-C is envisioned to have new applications based on M2M communication with real-time constraints that enable new functionalities for traffic safety and mission-critical control for industrial applications. These new applications will require much higher reliability and lower latency than today's communication systems. A typical application is super real-time and reliable connections for timely and reliable exchange of information with less than 5ms E2E latency requirement in Tele-protection smart grid networks that demands reliable information transfer between power grid substations within a few milliseconds.

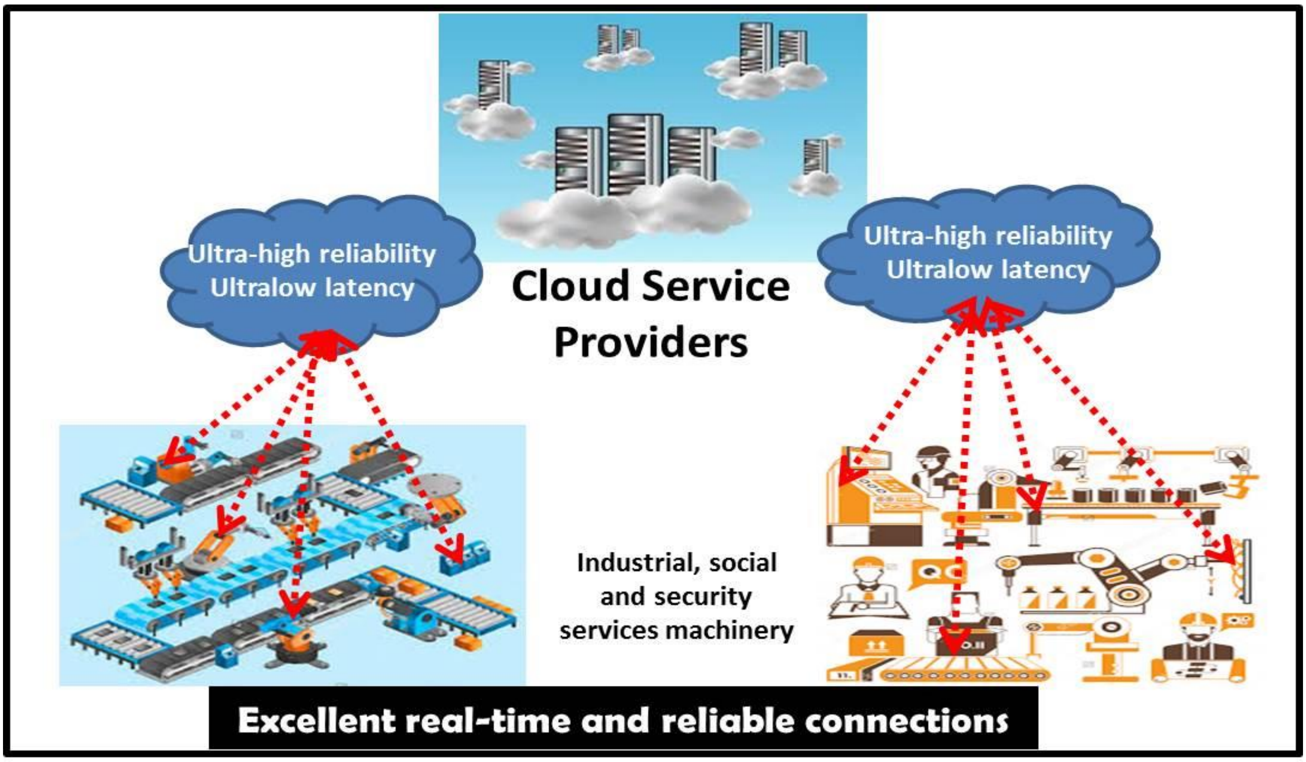

Figure 5.5. Schematic of proposed excellent real-time and reliable connections 5G scenario

5.4. 5G-COMUSA Core Network Connection Setup

Existing telecom networks are fashioned in hierarchical way, where subscriber traffic is aggregated at designated points and then routed to gateways as shown in current network connection setup in Figure 5.6. It is however believed that a flat IP architecture will lessen burden on aggregation point and traffic will directly move from BS to RS and on to IR-UWB WWAN overlay network and then to the devices. It is suggested that legacy platforms should transition to a common all-IP platform on a super-core; based on IPv6 platform. It is suggested that the shift be evolved to a complete packet core for the future 5G system such that leverages on the economy of scale of software-based ICT technologies, namely software defined networking and cloud computing. The research thus proposes a hierarchical 5G mobile network that is cloud-enabled. In particular the new architecture focuses on mobility, proposing low latency Layer 2 solutions for the access network, while exploiting aggregating Layer 3 mobility functionalities in the regional and national clouds. Here, all network operators (GSM,CDMA, Wimax, Wireline) could be connected to one Super core with massive capacity. The realization of this single network infrastructure is depicted in the proposed 5G-COMUSA connection setup in Figure 5.7. The concept of software defined super core is expected to eliminate all interconnecting charges and complexities that network operators are facing right now. It could also reduce number of network entities in end to end connection, thus reducing latency considerably.

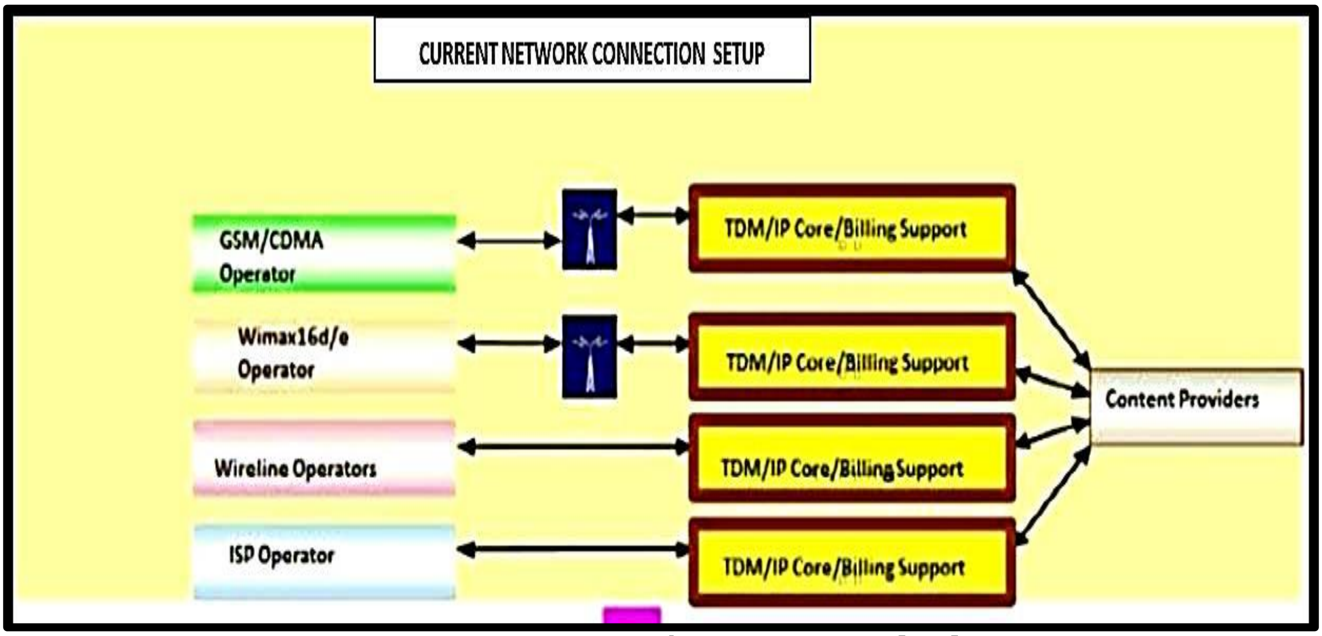

Figure 5.6. Current network connection setup.[143]

5.5. 5G-COMUSA multi-tier network setup.

It is expected that in the 5G wireless systems ecosystem, legacy RAT will co-exist with new access technologies, as well as very dense multi-layer networks consisting of cells of very different sizes. Both aspects raise challenges of interference and mobility management. For instance, the very dense deployments expected beyond 2020 will lead to massive users per cell with attendant high traffic. The 5G-COMUSA multi-tier network setup as laid-out in Figure 5.8 is believed to be adequate to make makes identification and mitigation of interference to be easily implemented. It is expected to afford highly centralized super core concept discussed in 5.4 as well as a distributed, fully decentralized WWAN D2D overlay networks. This will allow for easy access and necessary trade-offs between system performance, minimized infrastructure, signalling overhead, as well as scalability. The expected ultra-dense networks and a more prominent role of WWAN D2D communication lead to new mobility management challenges. It is believed that the ULOSTECH solutions have schemes that are tailored specifically for mobile and machine-type devices. 5G-

COMUSA multi-tier network setup caters for a wide range of approaches including user autonomous, network assisted, or fully network driven service connectivity management.

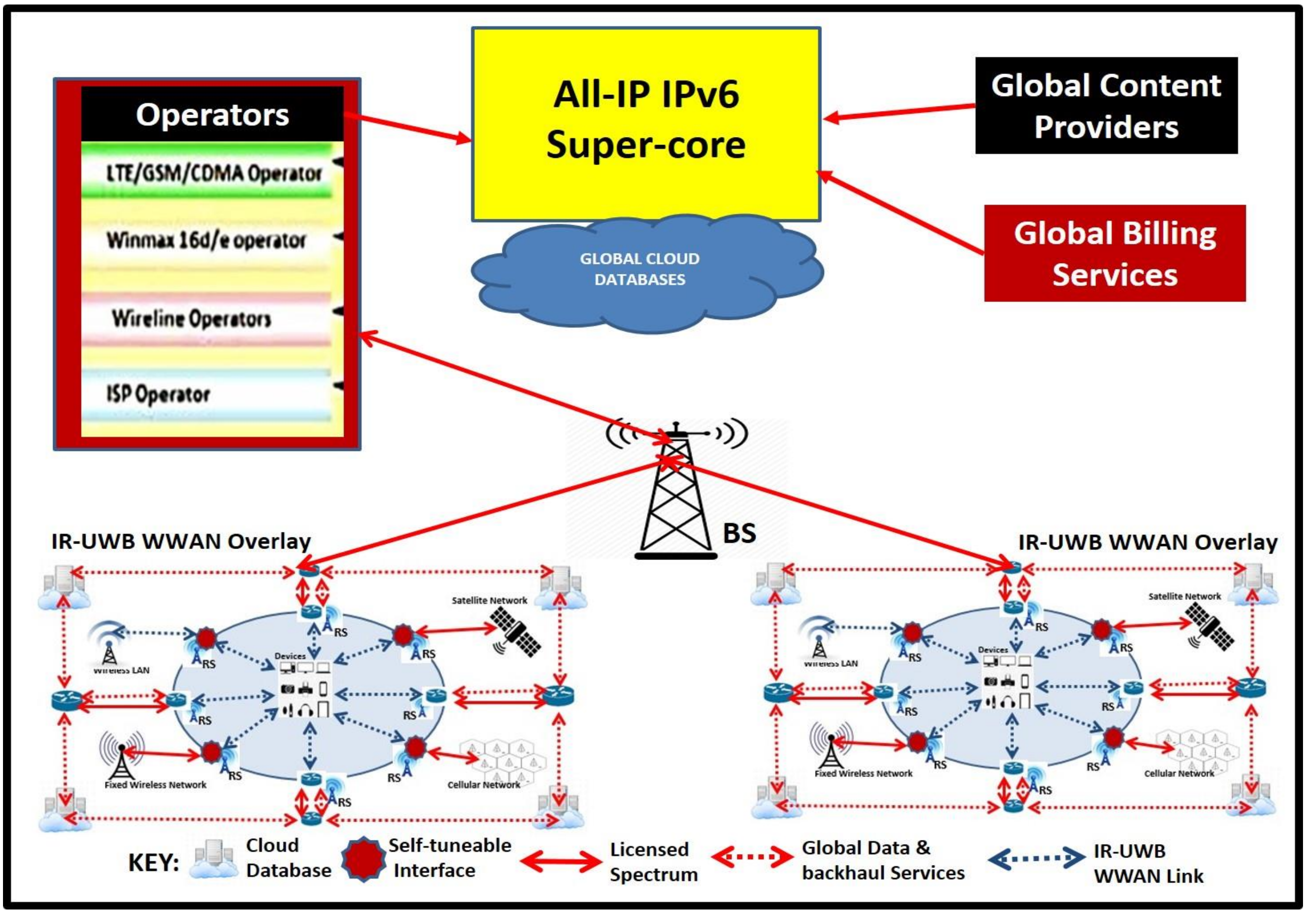

Figure 5.7. 5G-COMUSA super-core network infrastructure connection setup

To address both interference and mobility management aspects in 5G in one holistic framework, 5G-COMUSA multi-tier network setup considers a complete redesign of control and user plane functionality, and novel cell concepts built around IR-UWB WWAN picocells and RS. For example, phantom or virtual cells that are fully or partially transparent to the device are proposed. One clear differentiator between the 5G-COMUSA and earlier generations therefore would be that one will move toward proactive management of demand, mobility, and interference instead of simply reacting to instantaneous channel, demand, and network conditions. Ultimately, 5G-COMUSA multi-tier network setup addresses the fundamental questions regarding interference and mobility management in a 5G setting.

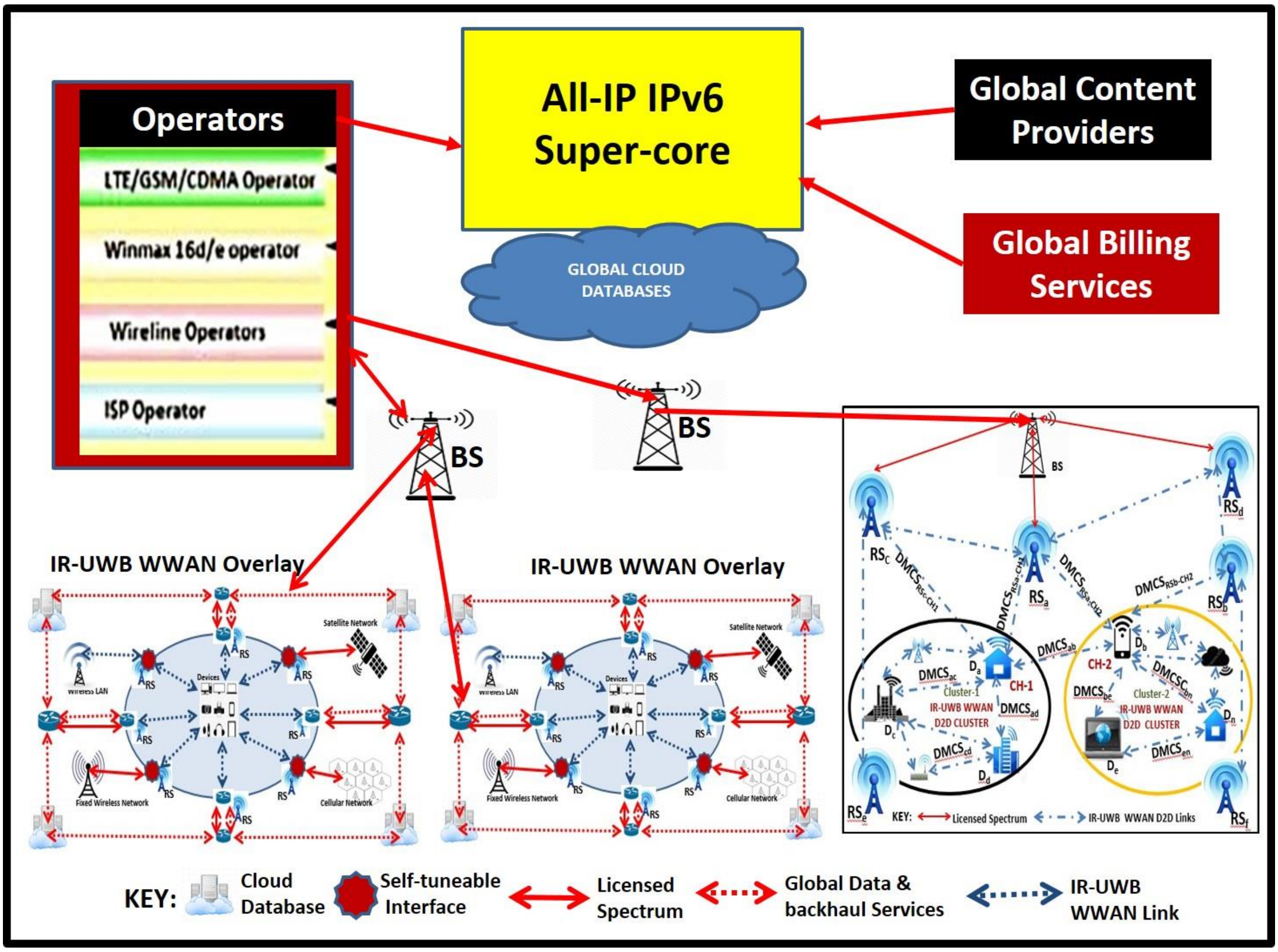

Figure 5.8. 5G-COMUSA multi-tier network setup

5.6. SUMMARY

It is believed that the concurrent vision is the most appropriate path to 5G/Future wireless implementation. This should be such that would encompass all legacy networks and access technologies currently deployed across the world in a single all-IP global platform with a single protocol for seamless integration. 5G-COMUSA embodies this view as outlined in this chapter with a single protocol device capable of automatically switching between networks such that will make it possible for wireless networks to support a common protocol to access satellite-based networks and terrestrial networks. This requires amongst other features, a high definition positioning technique for which ULOSTECH solutions are capable.

<u>CHAPTER SIX</u>

Conclusion and Future Plans

6.0. Conclusion

6.1. Future plans

Conclusion and Future Plans

6.0. Conclusion

This thesis describes the research effort on UWB IEEE802.15.4a cognitive localization methods for the 5G environment. The research presented has been very focused on identifying issues arising from the utilization of IR-UWB for combined localization and communication in a 5G setting that utilized WWAN D2D solutions. This thesis in its entirety provides a thorough review of the state of the art literature, detailed description of proposed methods and eventually exhaustive simulation experimental results. In order to provide fair evaluations, all simulation experiments were performed repeatedly in MATLAB environment using different scenario to arrive at envisaged 5G network parameters. In chapter 3 for instance it was established that ULOSTECH sampling variance and the RMSE are within tolerable limits of UWB IEEE802.15.4a standards with improvement ratio of about 0.36 above traditional RSS cellular standards. ULOSTECH also addresses the dominant challenges of NLOS in positioning propagations by modelling an algorithm that is able to accurately localize target devices irrespective of LOS or NLOS condition through a scheme that makes the presence of NLOS irrelevant to accuracy of the positioning service.

It was observed that the ULOSTECH channel has an exponentially decaying PDP with the last tap being about 20dB weaker than the first tap which shows that the estimator can achieve a higher diversity gain in comparison with narrow band signals. The implication is that ULOSTECH can achieve a diversity gain which is proportional to the number of sub-bands and the channel diversity. This is very significant since it is a low complexity estimation scheme which makes it applicable in the 5G environment with ease of data transfer. It is also novel in that simulation could be conducted with different values of the parameters concurrently with a number of signal sub-bands. It is believed that the concurrent use of signal sub-bands ensures the efficient use of complete bandwidth as channels for data exchange with no in-band interference due to separation by frequency.

The resulting shadowing variance from sampling of the transmitted ULOSTECH IR-UWB signal in both LOS and NLOS scenarios was observed to consist of evenly distributed phases despite random variables generated by MATLAB functions used. This confirms that the same shadowing variance is experienced throughout the sampling period for any given range of SNR either in LOS or NLOS condition. It was however observed that the performance in NLOS condition varies from 0.05 variance for ML, to 0.07 for WLS and 0.1 for LS simulations. This could be detrimental if the NLOS component is not effectively mitigated. It is of particular note that under LOS condition, the shadowing variance remains relatively the same for LS, WLS and ML simulations. The significance of this is that the ULOSTECH performs within acceptable parameters under many scenarios and gives optimal performance irrespective of the bounds parameters in those given scenarios as the accuracy of its localization would not be degraded at a peak variance of 0.03. It could thus be deduced that ULOSTECH is a promising proposition for the 5G setting.

In chapter 4, results of performance analysis on ULOSTECH IR-UWB D2D WWAN throughput compared with cellular and wifi network standards was presented. Simulation results show that the ULOSTECH IR-UWB D2D WWAN cluster cooperation scheme increases the system throughput significantly by a factor of about 0.75 as the number of cluster devices increases. This suggests the suitability of the ULOSTECH approach for the envisaged ultra-dense scenario in 5G setting. Indeed, it was observed that the mean lifetime of the cluster increases as the number of CNMs is increasing. Moreover, the 5G-COMUSA IR-UWB WWAN overlay network was presented for both terrestrial and satellite connections through self-tuneable single protocol The solution employs an IR-UWB RSS threshold estimation technique for location services that features WWAN D2D devices that are linked with the IR-UWB DMCS. The structure features a cluster formation and a cluster cooperation scheme along with the UD-CLOCS scheme that is expected to support ultra-dense network scenarios in the 5G setting. The layout also features a cloud-based network databases to house critical data and information with access through licence spectrums at the various RS locations.

Chapter 5 presents four scenarios that would most probably playout in the 5G setting. These are the ubiquitous D2D communication of assets (U-D2D-CA), unlimited always-with-you boundless service in a crowd (UABSC), always-on best experience follows you (ABEFY) and excellent real-time and reliable M2M connections (ERR-M2M-C). It is expected that in the 5G wireless systems ecosystem, legacy RAT will co-exist with new access technologies, as well as very dense multi-layer networks consisting of cells of very different sizes. Both aspects raise challenges of interference and mobility management. To address both interference and mobility management aspects in 5G in one holistic framework, 5G-COMUSA multi-tier network setup considers a complete redesign of control and user plane functionality, and novel cell concepts built around IR-UWB WWAN picocells and RS. For example, phantom or virtual cells that are fully or partially transparent to the device are proposed. One clear differentiator between the 5G-COMUSA and earlier generations therefore would be that one will move toward proactive management of demand, mobility, and interference instead of simply reacting to instantaneous channel, demand, and network conditions. Ultimately, 5G-COMUSA multi-tier network setup addresses the fundamental questions regarding interference and mobility management in a 5G setting.

6.1. Future Plans

Although this thesis presents hopefully, solutions that have been tested rigorously, and many interesting results were obtained, there is still room for future work on IR-UWB localization for 5G environment since it is still at its nascent stage. With the near future implementation of the 5G solutions, an extension of the research is to consider more investigation on the effective performance bounds for the developed algorithm with further simulation using MATLAB. Thereafter to compare all simulation results with real life scenario using WWAN UWB radios which to the best knowledge of the Author must be ordered factory produced specifically since they are not yet in production. Another plan is to take the multiple access interference mitigation further; possibly during post-doctoral research. It might also be worthwhile to consider improvements of RRS localization threshold estimation algorithm.

It is worthy of mention, that feedback from various conferences attended to present results of this research though posits encouraging future for 5G, it could however be observed that there was a new thinking in both academia and industry that 5G might not after all present the desired global network that was initially envisaged and conceived. 5G is increasingly viewed as a mere upgrade of 4G. Therefore, there are preliminary discussions towards the possibility of a 6G in the horizon. Therefore, and extension of this research will consider early specification and threshold works on 6G standards.

References:

[1] Frodigh, M., et al., "Future-generation wireless networks. Personal Communications", IEEE, 2001. 8(5): p. 10-17.

[2] Chih-Lin, I. et al. "Toward green and soft: a 5G perspective." IEEE Communications Magazine 52.2 (2014): 66-73.

[3] Yusof, K. Mohamad, John Woods, and Steve Fitz. "Frequency Scanning using Software Defined Radio for Localised Range Estimation." Sensor Technologies and Applications, 2009. SENSORCOMM'09. Third International Conference on. IEEE, 2009.

[4] Roh, W. "5G mobile communications for 2020 and beyond-vision and key enabling technologies." Key note: at IEEE WCNC (2014).

[5] Gavrilovska, L. Valentin, R. and Vladimir, Atanasovski. "Visions towards 5G: Technical requirements and potential enablers." Wireless Personal Communications 87.3 (2016): 731-757.

[6] Cisco Inc. "Internet of everything: A $4.6 trillion public-sector opportunity" Technical Report (2013).

[7] Osseiran, Afif, Federico Boccardi, Volker Braun, Katsutoshi Kusume, Patrick Marsch, Michal Maternia, Olav Queseth et al. "Scenarios for 5G mobile and wireless communications: the vision of the METIS project." IEEE Communications Magazine 52, no. 5 (2014): 26-35.

[8] Clarke, Richard N. "Expanding mobile wireless capacity: The challenges presented by technology and economics." Telecommunications Policy 38.8 (2014): 693-708.

[9] Li, Qian Clara, Huaning Niu, Apostolos Tolis Papathanassiou, and Geng Wu. "5G network capacity: key elements and technologies." IEEE Vehicular Technology Magazine 9, no. 1 (2014): 71-78.

[10] Gupta, P. and P. Patil, 4G - A NEW ERA IN WIRELESS TELECOMMUNICATION.

[11] Porcino, Domenico, and Walter Hirt. "Ultra-wideband radio technology: potential and challenges ahead." IEEE communications magazine 41, no. 7 (2003): 66-74.

[12] Reed, J.H., et al., An overview of the challenges and progress in meeting the E-911 requirement for location service. Communications Magazine, IEEE, 1998. 36(4): p. 30-37.

[13] Guo, Nan, et al. "60-GHz millimeter-wave radio: Principle, technology, and new results." EURASIP Journal on Wireless Communications and Networking 2007.1 (2007): 48-48.

[14] Sahinoglu, Zafer, Sinan Gezici, and Ismail Guvenc. "Ultra-wideband positioning systems." Cambridge, New York (2008).

[15] Karapistoli, Eirini, et al. "An overview of the IEEE802.15.4a standard." IEEE Communications Magazine 48.1 (2010): 47-53.

[16] Grewal, M.S., L.R. Weill, and A.P. Andrews, Global positioning systems, inertial navigation, and integration. 2007: John Wiley & Sons.

[17] Park, Cheolhee, and Theordore S. Rappaport. "Short-range wireless communications for next-generation networks: UWB, 60 GHz millimeter-wave WPAN, and ZigBee." IEEE Wireless Communications 14.4 (2007): 70-78.

[18] Kraemer, Rolf, and Marcos Katz, eds. Short-range wireless communications: Emerging technologies and applications. John Wiley & Sons, 2009.

[19] WWRF. URL: http://www.wirelss-world-research.org:

[20] Pottie, Gregory J., and William J. Kaiser. "Wireless integrated network sensors." Communications of the ACM 43.5 (2000): 51-58.

[21] Yasuda, Mitsuyoshi, et al. "Short range wireless communication system, portable terminal apparatus, and wireless communication apparatus." U.S. Patent No. 7,336,929. 26 Feb. 2008.

[22] Kopetz, Hermann. "Internet of things." Real-time systems. Springer US, 2011. 307-323.

[23] Weiser M (1993) Ubiquitous computing. IEEE Comput 26:71–72
[24] Li, Mingyan, et al. "Swing & swap: user-centric approaches towards maximizing location privacy." Proceedings of the 5th ACM workshop on Privacy in electronic society. ACM, 2006.
[25] Yelmo, Juan C., et al. "A user-centric service creation approach for Next Generation Networks." Innovations in NGN: Future Network and Services, 2008. K-INGN 2008. First ITU-T Kaleidoscope Academic Conference. IEEE, 2008.
[26] Fitzek, Frank HP, and Marcos D. Katz. Cooperation in wireless networks: principles and applications. New York: Springer, 2006.
[27] https://www.britannica.com/topic/cognition-thought-process
[28] Fitzek, F.H. and M.D. Katz, Cognitive wireless networks: concepts, methodologies and visions inspiring the age of enlightenment of wireless communications. 2007: Springer Publishing Company, Incorporated.
[29] Devroye, Natasha, et al. "Cooperation and cognition in wireless networks." SK Telecom Review, special issue on 4G Spectrum and System Engineering issues (2007): 990-1005.
[30] Vossiek, M., et al. Wireless local positioning-concepts, solutions, applications. in Radio and Wireless Conference, 2003. RAWCON'03. Proceedings. 2003. IEEE.
[31] Warehouse, M. Hyperbola graph:- http://www.mathwarehouse.com/hyperbola/graph-equation-of-a-hyperbola.php.
[32] Glisic, Savo, and Beatriz Lorenzo. Advanced wireless networks: cognitive, cooperative & opportunistic 4G technology. John Wiley & Sons, 2009.
[33] Ferraro, Richard, and Murat Aktihanoglu. Location-aware applications. Manning Publications Co., 2011.
[34] Wymeersch, Henk, Jaime Lien, and Moe Z. Win. "Cooperative localization in wireless networks." Proceedings of the IEEE 97.2 (2009): 427-450.
[35] Patwari, Neal, et al. "Locating the nodes: cooperative localization in wireless sensor networks." IEEE Signal processing magazine 22.4 (2005): 54-69.
[36] Gezici, Sinan, et al. "Localization via ultra-wideband radios: a look at positioning aspects for future sensor networks." IEEE signal processing magazine 22.4 (2005): 70-84.
[37] Win MZ, Scholtz RA (1998) Impulse radio: how it works. IEEE Comms Letter 2:36–38.
[38] ISO/IEC_26907 (2007) High rate ultra wideband PHY and MAC standard. International Organization for Standardization.
[39] ISO/IEC_26908 (2007) MAC_PHY interface for ISO/IEC 26907.International Organization for Standardization.
[40] Rappaport, T.S., J.H. Reed, and B.D. Woerner, Position location using wireless communications on highways of the future. Communications Magazine, IEEE, 1996. 34(10): p. 33-41.
[41] Wymeersch, H., J. Lien, and M.Z. Win, Cooperative Localization in Wireless Networks. Proceedings of the IEEE, 2009. 97(2): p. 427-450.
[42] Glisic, Savo, and Beatriz Lorenzo. Advanced wireless networks: cognitive, cooperative & opportunistic 4G technology. John Wiley & Sons, 2009.
[43] Conti, Andrea, et al. "Network experimentation for cooperative localization." IEEE Journal on Selected Areas in Communications 30.2 (2012): 467-475.
[44] Molisch, Andreas F., Jeffrey R. Foerster, and Marcus Pendergrass. "Channel models for ultrawideband personal area networks." IEEE wireless communications 10.6 (2003): 14-21.
[45] Gutierrez, Jose A., et al. "IEEE 802.15.4: a developing standard for low-power low-cost wireless personal area networks." IEEE network 15.5 (2001): 12-19.
[46] Becker, Philipp, Reinhard Gotzhein, and Thomas Kuhn. "MacZ-a quality-of-service mac layer for ad-hoc networks." 7th International Conference on Hybrid Intelligent Systems (HIS 2007). IEEE, 2007.
[47] Molisch, Andreas F. "Ultrawideband propagation channels-theory, measurement, and modeling." IEEE Transactions on Vehicular Technology 54.5 (2005): 1528-1545.

[48] Commission, F.C., Revision of Part 15 of the Commissions Rules Regarding Ultra-Wideband Transmission Systems. First Report and Order, ET Docket 98-153, FCC 02-48; Adopted: February 14, 2002; Released: April 22, 2002. 2002, April.
[49] Lu, K., et al. On medium access control for high data rate ultra-wideband ad hoc networks. in Wireless Communications and Networking Conference, 2005 IEEE. 2005. IEEE.
[50] Molisch, A.F., J.R. Foerster, and M. Pendergrass, Channel models for ultrawideband personal area networks. Wireless Communications, IEEE, 2003. 10(6): p. 14-21.
[51] Ye, Z., et al. A low-complexity synchronization design for MB-OFDM ultra-Wideband systems. in Communications, 2008. ICC'08. IEEE International Conference on. 2008. IEEE.
[52] Qi, Y., H. Kobayashi, and H. Suda, On time-of-arrival positioning in a multipath environment. Vehicular Technology, IEEE Transactions on, 2006. 55(5): p. 1516-1526.
[53] Weiss, A.J., Direct position determination of narrowband radio frequency transmitters. Signal Processing Letters, IEEE, 2004. 11(5): p. 513-516.
[54] Rui, Y. and D. Florencio. New direct approaches to robust sound source localization. in Multimedia and Expo, 2003. ICME'03. Proceedings. 2003 International Conference on. 2003. IEEE.
[55] Guvenc, I., C.-C. Chong, and F. Watanabe. Joint TOA estimation and localization technique for UWB sensor network applications. in Vehicular Technology Conference, 2007. VTC2007-Spring. IEEE 65th. 2007. IEEE.
[56] Reggiani, L., et al. Adapting the Ranging Algorithm to the Positioning Technique in UWB Sensor Networks. in Proceedings 4th COST289 workshop. 2007.
[57] Whitehouse, K., et al. The effects of ranging noise on multihop localization: an empirical study. in Proceedings of the 4th international symposium on Information processing in sensor networks. 2005. IEEE Press.
[58] Denis, B., J.-B. Pierrot, and C. Abou-Rjeily, Joint distributed synchronization and positioning in UWB ad hoc networks using TOA. Microwave Theory and Techniques, IEEE Transactions on, 2006. 54(4): p. 1896-1911.
[59] Alavi, B. and K. Pahlavan, Modeling of the TOA-based distance measurement error using UWB indoor radio measurements. Communications Letters, IEEE, 2006. 10(4): p. 275-277.
[60] Savarese, C., J.M. Rabaey, and J. Beutel. Location in distributed ad-hoc wireless sensor networks. in Acoustics, Speech, and Signal Processing, 2001. Proceedings.(ICASSP'01). 2001 IEEE International Conference on. 2001. IEEE.
[61] Savvides, A., C.-C. Han, and M.B. Strivastava. Dynamic fine-grained localization in ad-hoc networks of sensors. in Proceedings of the 7th annual international conference on Mobile computing and networking. 2001. ACM.
[62] Caffery, J.J. and G.L. Stuber, Overview of radiolocation in CDMA cellular systems. Communications Magazine, IEEE, 1998. 36(4): p. 38-45.
[63] Wylie-Green, M.P. and S. Wang. Robust range estimation in the presence of the non-line-of-sight error. in Vehicular Technology Conference, 2001. VTC 2001 Fall. IEEE VTS 54th. 2001. IEEE.
[64] Al-Jazzar, S., J. Caffery Jr, and H.-R. You. A scattering model based approach to NLOS mitigation in TOA location systems. in Vehicular Technology Conference, 2002. VTC Spring 2002. IEEE 55th. 2002. IEEE.
[65] Riba, J. and A. Urruela. A robust multipath mitigation technique for time-of-arrival estimation. in Vehicular Technology Conference, 2002. Proceedings. VTC 2002-Fall. 2002 IEEE 56th. 2002. IEEE.
[66] Patwari, N., et al., Relative location estimation in wireless sensor networks. Signal Processing, IEEE Transactions on, 2003. 51(8): p. 2137-2148.
[67] Riba, J. and A. Urruela. A non-line-of-sight mitigation technique based on ML-detection. in Acoustics, Speech, and Signal Processing, 2004. Proceedings.(ICASSP'04). IEEE International Conference on. 2004. IEEE.

[68] Cong, L. and W. Zhuang. Non-line-of-sight error mitigation in TDOA mobile location. in Global Telecommunications Conference, 2001. GLOBECOM'01. IEEE. 2001. IEEE.
[69] Liao, J.-F. and B.-S. Chen, Robust mobile location estimator with NLOS mitigation using interacting multiple model algorithm. Wireless Communications, IEEE Transactions on, 2006. 5(11): p. 3002-3006.
[70] Venkatesh, S. and R.M. Buehrer, NLOS mitigation using linear programming in ultrawideband location-aware networks. Vehicular Technology, IEEE Transactions on, 2007. 56(5): p. 3182-3198.
[71] Wylie, M.P. and J. Holtzman. The non-line of sight problem in mobile location estimation. in Universal Personal Communications, 1996. Record., 1996 5th IEEE International Conference on. 1996. IEEE.
[72] Borras, J., P. Hatrack, and N.B. Mandayam. Decision theoretic framework for NLOS identification. in Vehicular Technology Conference, 1998. VTC 98. 48th IEEE. 1998. IEEE.
[73] Venkatraman, S. and J. Caffery Jr. Statistical approach to non-line-of-sight BS identification. in Wireless Personal Multimedia Communications, 2002. The 5th International Symposium on. 2002. IEEE.
[74] Gezici, S., H. Kobayashi, and H.V. Poor. Nonparametric nonline-of-sight identification. in Vehicular Technology Conference, 2003. VTC 2003-Fall. 2003 IEEE 58th. 2003. IEEE.
[75] Lakhzouri, A., et al., Extended Kalman filter channel estimation for line-of-sight detection in WCDMA mobile positioning. EURASIP Journal on Advances in Signal Processing, 1900. 2003(13): p. 1268-1278.
[76] Al-Jazzar, S. and J. Caffery Jr. New algorithms for NLOS identification. in Proceedings of the 14th IST Mobile and Wireless Communications Summit. 2005.
[77] Schroeder, J., et al. NLOS detection algorithms for ultra-wideband localization. in Positioning, Navigation and Communication, 2007. WPNC'07. 4th Workshop on. 2007. IEEE.
[78] Van Trees, H.L., Classical detection and estimation theory. Detection, Estimation, and Modulation Theory: Detection, Estimation, and Linear Modulation Theory: p. 19-165.
[79] Chan, Y.-T., et al., Time-of-arrival based localization under NLOS conditions. Vehicular Technology, IEEE Transactions on, 2006. 55(1): p. 17-24.
[80] Wang, X., Z. Wang, and B. O'Dea, A TOA-based location algorithm reducing the errors due to non-line-of-sight (NLOS) propagation. Vehicular Technology, IEEE Transactions on, 2003. 52(1): p. 112-116.
[81] Venkatesh, S. and R.M. Buehrer. A linear programming approach to NLOS error mitigation in sensor networks. in Proceedings of the 5th international conference on Information processing in sensor networks. 2006. ACM.
[82] Guvenc, I., C.-C. Chong, and F. Watanabe. NLOS identification and mitigation for UWB localization systems. in Wireless Communications and Networking Conference, 2007. WCNC 2007. IEEE. 2007. IEEE.
[83] Li, B., et al. A database method to mitigate the NLOS error in mobile phone positioning. in Proceedings of IEEE Position, Location, and Navigation Symposium (PLANS'06). 2006. Citeseer.
[84] Venkatesh, S. and R.M. Buehrer. Multiple-access design for ad hoc UWB position-location networks. in Wireless Communications and Networking Conference, 2006. WCNC 2006. IEEE. 2006. IEEE.
[85] Kim, S., et al., Geolocation in ad hoc networks using DS-CDMA and generalized successive interference cancellation. Selected Areas in Communications, IEEE Journal on, 2005. 23(5): p. 984-998.
[86] Sahinoglu, Z. and I. Guvenc, Multiuser interference mitigation in noncoherent UWB ranging via nonlinear filtering. EURASIP Journal on Wireless Communications and Networking, 2006. 2006(2): p. 67-67.

[87] Sahinoglu, Z., et al. Interference suppression in non-coherent time-hopping IR-UWB ranging. in Ultra-Wideband, The 2006 IEEE 2006 International Conference on. 2006. IEEE.

[88] Dardari, D., A. Giorgetti, and M.Z. Win. Time-of-arrival estimation of UWB signals in the presence of narrowband and wideband interference. in Ultra-Wideband, 2007. ICUWB 2007. IEEE International Conference on. 2007. IEEE

[89] Taha, Ali, and Keith M. Chugg. "A theoretical study on the effects of interference UWB multiple access impulse radio." Signals, Systems and Computers, 2002. Conference Record of the Thirty-Sixth Asilomar Conference on. Vol. 1. IEEE, 2002.

[90] Somayazulu, V. Srinivasa. "Multiple access performance in UWB systems using time hopping vs. direct sequence spreading." Wireless Communications and Networking Conference, 2002. WCNC2002. 2002 IEEE. Vol. 2. IEEE, 2002.

[91] Zhang, Hongyuan, and Huaiyu Dai. "Cochannel interference mitigation and cooperative processing in downlink multicell multiuser MIMO networks." EURASIP Journal on Wireless Communications and Networking 2004.2 (2004): 222-235.

[92] Baccarelli, E., Mauro Biagi, and L. Taglione. "A novel approach to in-band interference mitigation in ultra wideband radio systems." Ultra Wideband Systems and Technologies, 2002. Digest of Papers. 2002 IEEE Conference on. IEEE, 2002.

[93] Molisch, Andreas F. "Adaptive frame durations for time-hopped impulse radio systems." U.S. Patent No. 7,403,746. 22 Jul. 2008.

[94] Viani, Federico, et al. "Localization, tracking, and imaging of targets in wireless sensor networks: An invited review." Radio Science 46.5 (2011).

[95] Venkatesh, Swaroop, and R. Michael Buehrer. "Power control in UWB position-location networks." 2006 IEEE International Conference on Communications. Vol. 9. IEEE, 2006.

[96] Thiele, Lars, Michael Peter, and Volker Jungnickel. "Statistics of the Ricean k-factor at 5.2 GHz in an urban macro-cell scenario." 2006 IEEE 17th International Symposium on Personal, Indoor and Mobile Radio Communications. IEEE, 2006.

[97] R. Baldemair et al., ``Evolving wireless communications: Addressing the challenges and expectations of the future," IEEE Veh. Technol. Mag., vol. 8, no. 1, pp. 2430, Mar. 2013.

[98] Goldsmith, A., Wireless communications. 2005: Cambridge university press.

[99] Glisic, S. and J.-P. Makela. Advanced wireless networks: 4G technologies. in Spread Spectrum Techniques and Applications, 2006 IEEE Ninth International Symposium on. 2006. IEEE.

[100] Vossiek, M., et al. Wireless local positioning-concepts, solutions, applications. in Radio and Wireless Conference, 2003. RAWCON'03. Proceedings. 2003. IEEE.

[101] Wang, Cheng-Xiang, et al. "Cellular architecture and key technologies for 5G wireless communication networks." IEEE Communications Magazine 52.2 (2014): 122-130.

[102] Chin, Woon Hau, Zhong Fan, and Russell Haines. "Emerging technologies and research challenges for 5G wireless networks." IEEE Wireless Communications 21.2 (2014): 106-112.

[103] Ge, Xiaohu, et al. "5G wireless backhaul networks: challenges and research advances." IEEE Network 28.6 (2014): 6-11.

[104] Chen, Shanzhi, and Jian Zhao. "The requirements, challenges, and technologies for 5G of terrestrial mobile telecommunication." IEEE Communications Magazine 52.5 (2014): 36-43.

[105] Tehrani, Mohsen Nader, Murat Uysal, and Halim Yanikomeroglu. "Device-to-device communication in 5G cellular networks: challenges, solutions, and future directions." IEEE Communications Magazine 52.5 (2014): 86-92.

[106] Kumar, Vashu, and Vipin Kumar. "A New Generation Wireless Mobile Network-5G." International Journal of Computer Applications 70.20 (2013).

[107] Demestichas, Panagiotis, Andreas Georgakopoulos, Dimitrios Karvounas, Kostas Tsagkaris, Vera Stavroulaki, Jianmin Lu, Chunshan Xiong, and Jing Yao. "5G on the horizon: key challenges for the radio-access network." IEEE Vehicular Technology Magazine 8, no. 3 (2013): 47-53.

[108] Tafazolli, Rahim, ed. Technologies for the Wireless Future: Wireless World Research Forum (WWRF). John Wiley & Sons, 2006.

[109] Gubbi, Jayavardhana, et al. "Internet of Things (IoT): A vision, architectural elements, and future directions." Future Generation Computer Systems 29.7 (2013): 1645-1660.

[110] Janevski, Toni. "5G mobile phone concept." 2009 6th IEEE Consumer Communications and Networking Conference. IEEE, 2009.

[111] Gohil, Asvin, Hardik Modi, and Shobhit K. Patel. "5G technology of mobile communication: A survey." Intelligent Systems and Signal Processing (ISSP), 2013 International Conference on. IEEE, 2013.

[112] Agyapong, Patrick Kwadwo, et al. "Design considerations for a 5G network architecture." IEEE Communications Magazine 52.11 (2014): 65-75.

[113] Cattoni, Andrea F., et al. "Ethernet-based mobility architecture for 5G." Cloud Networking (CloudNet), 2014 IEEE 3rd International Conference on. IEEE, 2014.

[114] Cattoni, Andrea Fabio, et al. "Ethernet-based mobility architecture for 5G: An architectural vision for the future 5G cloudified packet core." Third IEEE International Conference on Cloud Networking.

[115] Sezer, Sakir, et al. "Are we ready for SDN? Implementation challenges for software-defined networks." IEEE Communications Magazine 51.7 (2013): 36-43.

[116] Monserrat, Jose F., et al. "Rethinking the mobile and wireless network architecture: the METIS research into 5G." Networks and Communications (EuCNC), 2014 European Conference on. IEEE, 2014.

[117] Tudzarov, Aleksandar, and Toni Janevski. "Functional architecture for 5G mobile networks." International Journal of Advanced Science and Technology 32 (2011): 65-78.

[118] Yeh, Shu-Ping, et al. "Capacity and coverage enhancement in heterogeneous networks." IEEE Wireless Communications 18.3 (2011): 32-38.

[119] Dardari, Davide, Andrea Giorgetti, and Moe Z. Win. "Time-of-arrival estimation of UWB signals in the presence of narrowband and wideband interference." 2007 IEEE International Conference on Ultra-Wideband. IEEE, 2007.

[120] Markus, Ots. "Method and apparatus for planning a cellular radio network by creating a model on a digital map adding properties and optimizing parameters, based on statistical simulation results." U.S. Patent No. 5,561,841. 1 Oct. 1996.

[121] A. Rabbachin and I. Oppermann, "Synchronization analysis for UWB systems with a low-complexity energy collection receiver," in Proc. IEEE Conf. Ultrawideband Syst. Technol. (UWBST), Kyoto, Japan, May 2004, pp. 288–292.

[122] Fleming, C. Kushner, G. Roberts, and U. Nandiwada, "Rapid acquisition for ultra-wideband localizers," in Proc. IEEE Conf. Ultrawideband Syst. Technol. (UWBST), Baltimore, MD, May 2002, pp. 245–249.

[123] Guvenc and Z. Sahinoglu, "TOA estimation with different IR-UWB transceiver types," IEEE Int. Conf. UWB (ICU), Zurich, Switzerland, Sept. 2005, accepted for publication.

[124] J.-Y. Lee and R. A. Scholtz, "Ranging in a dense multipath environment using an UWB radio link," IEEE J. Select. Areas Commun., vol. 20, no. 9, Dec. 2002, pp. 1677–1683,

[125] C. Mazzucco, U. Spagnolini, and G. Mulas, "A ranging technique for UWB indoor channel based on power delay profile analysis," in Proc. IEEE Vehic. Technol. Conf. (VTC), Los Angeles, CA, Sep. 2004, pp. 2595–2599.

[126] Ye, Zhenzhen, et al. "A low-complexity synchronization design for MB-OFDM ultra-wideband systems." 2008 IEEE International Conference on Communications. IEEE, 2008.

[127] Coll-Perales et al. "Empirical performance models for P2P and two hops multi-hop cellular networks with mobile relays." Proceedings of the 8th ACM workshop on Performance monitoring and measurement of heterogeneous wireless and wired networks. ACM, 2013.

[128] Li Y et al (2007) A frequency synchronization method for IRUWB system. In: IEEE WiCOM 2007

[129] Bonuccelli, Maurizio A. et al. "Tree slotted ALOHA: a new protocol for tag identification in RFID networks." Proceedings of the 2006 International Symposium on on World of Wireless, Mobile and Multimedia Networks. IEEE Computer Society, 2006.

[130] IEEE_802.15b (2005) Part 15.3b: wireless medium access control (MAC) and physical layer (PHY) specifications for high rate wireless personal area networks (WPAN): amendment to MAC sublayer. IEEE P802-15-3-DF8 draft Amendment, 2005.

[131] Xinzhou W, Tavildar S, Shakkottai S, Richardson T, Junyi L,Laroia R, Jovicic A (2010) FlashLinQ: A synchronous distributed scheduler for peer-to-peer ad hoc networks. In: 48th annual Allerton conference on communication, control, and computing (Allerton), Allerton. pp 514–521

[132] IEEE, Std 802.11-2012: Wireless LAN Medium Access Control (MAC) and Physical Layer (PHY) Specifications, (2012).

[133] Huang J, Qian F, Gerber A, Mao ZM, Sen S, Spatscheck O (2012) A close examination of performance and power characteristics of 4g lte networks. pp 225–238

[134] McDermott-Wells P (2005) What is Bluetooth? Potentials. IEEE 23(5):33–35.

[135] Asadi A, Mancuso V (2013) WiFi Direct and LTE D2D in actionWireless Days (WD), 2013 IFIP, Valencia. pp 1–8.

[136] Asadi, Arash, and Vincenzo M. "WiFi Direct and LTE D2D in action." Wireless Days (WD), 2013 IFIP. IEEE, 2013.

[137] Tang, Huan, et al. "Enabling D2D communications through neighbor discovery in LTE cellular networks." IEEE Transactions on Signal Processing 62.19 (2014): 5157-5170.

[138] Conti, Marco, et al. "Experimenting opportunistic networks with WiFi Direct." Wireless Days (WD), 2013 IFIP. IEEE, 2013.

[139] Musaloiu-E, Razvan, and Andreas Terzis. "Minimising the effect of wifi interference in 802.15. 4 wireless sensor networks." International Journal of Sensor Networks 3.1 (2008): 43-54.

[140] P. Baldi, L. De Nardis and M. Di Benedetto, Modeling and optimization of uwb communication networks through a flexible cost function, IEEE Journal on Selected Areas in Communications (2002) 1733–1743.

[141] Andrews, Jeffrey G., et al. "What will 5G be?." IEEE Journal on Selected Areas in Communications 32.6 (2014): 1065-1082.

[142] Wang, Cheng-Xiang, et al. "Cellular architecture and key technologies for 5G wireless communication networks." IEEE Communications Magazine 52.2 (2014): 122-130.

[143] Osseiran, Afif, et al. "Scenarios for 5G mobile and wireless communications: the vision of the METIS project." IEEE Communications Magazine 52.5 (2014): 26-35.

[144] Ha DS, Schaumont PR (2007) Replacing cryptography with ultrawideband (UWB) modulation in secure RFID. In: IEEE international conference on RFID.

[145] YRP Ubiquitous Networking Laboratory (2006) The world's first & smallest UWB active tag of 10 mm square.

[146] Baghaei-Nejad M et al (2007) Enabling ubiquitous wireless sensing by a novel RFID-based UWB module. In: RFID.

[147] Gezici S et al (2005) Localization via ultra-wideband radios: a look at positioning aspects for future sensor networks. IEEE Signal Process Mag 22:70–84

[148] Alavi B, Pahlavan K (2006) Modeling of the TOA-based distance measurement error using UWB indoor radio measurements. In: IEEE Commun Lett 10

[149] Yu K (2007) 3-D localization error analysis in wireless networks. IEEE Transaction Wireless Communications 6.

[150] Jourdan DB et al (2008) Position error bound for UWB localization in dense cluttered environments. IEEE Trans Aerosp Electron Syst 44:613–628

[151] Mizugaki K et al (2007) Accurate wireless location/communication system with 22-cm error using UWB-IR. In: Radio and Wireless Symposium, IEEE, 2007, pp 455–458.

Appendixes:

APPENDIX 1

MATLAB Codes: Channel realization of IEE802.15.4a channel

```
% Matlab codes to generate PDP for S-V channel
Lmbd = 1/200; % Cluster arrival rate
lmbd = 1/5; % Ray arrival rate
Gmm = 60; % Cluster decay rate
gmm = 20; % Ray decy rate
Th = 300; % Maximum channel delay
T(1) = 0; % Cluster arrival time 'T'
num_cluster = 1; % Number of clusters
while 1
% Generate next cluster arrival time
temp_T = T(num_cluster) + exprnd(1/Lmbd);

% Maximum channel delay < Th
if temp_T < Th
num_cluster = num_cluster + 1;
T(num_cluster) = temp_T;
else
break;
end
end

        B_pp_given_gamma =  c^2 * (1 / ( 8 * pi^2 * beta_bar^2 * SNR)) *
inv(Phi_bar* diag(alpha_true(M+1:B))^2 * (eye(B-M) +
...
                        (1/(16 * pi^2 * beta_bar^2)) *
diag(gamma_true(M+1:B))^2 * inv( diag(tau_true(M+1:B))^2 ) ) * Phi_bar');
        bias_p_LS(n_SNR) = mean(sqrt( error_p_LS(1,:).^2 + error_p_LS(2,:).^2 ));
        bias_p_WLS_known_gamma(n_SNR) =
mean(sqrt(error_p_WLS_known_gamma(1,:).^2 + error_p_WLS_known_gamma(2,:).^2 ));
        bias_p_ML_known_gamma(n_SNR) = mean(sqrt( error_p_ML_known_gamma(1,:).^2
+ error_p_ML_known_gamma(2,:).^2 ));
        CRB_p_given_gamma(n_SNR) = sqrt(trace(B_pp_given_gamma));

end
end

 figure
 hold on
 %subplot(2,1,1);
 grid
on
 plot(SNR_range,RMSE_p_LS,
'r*','LineWidth',.5,'MarkerEdgeColor','r','MarkerSize',5
)
 plot(SNR_range,RMSE_p_LS_theory,
':r','LineWidth',.5,'MarkerEdgeColor','r','Marker
Size',5)
```

```
plot(SNR_range,RMSE_p_WLS_known_gamma,
'mo','LineWidth',.5,'MarkerEdgeColor','m','
MarkerSize'
,5)

plot(SNR_range,RMSE_p_ML_known_gamma,
'bs','LineWidth',.5,'MarkerEdgeColor','b','M
arkerSize'
,5)
 plot(SNR_range,CRB_p_given_gamma,
'-
k'
,'LineWidth',.5,'MarkerEdgeColor','k','MarkerSize',5)
 legend(
'LS: simulation','LS: analysis','WLS: simulation','ML: simulation','CRB')
 h = findobj(gcf,'type','axes','tag','legend');
 Pos = get(h,
'position');
 Pos(3) = 1.9 * Pos(3); % Double the length
 Pos(4) = 3 * Pos(4);
% Double the length
 set(h,
'position',Pos) % Implement it
 title('RMSE as a function of SNR ($M=0$, $N_R=1{,}000$)')
 ylabel(
'Root Mean Square Error (m)')%,'FontSize',10,'FontName','Times New
Roman')
 xlabel(
'Transmitted SNR $\frac{E_{\mathrm{s}}}{\sigma^2_{\mathrm{n}}}$
(dB)'
)%,'FontSize',10,'FontName','Times New Roman')
 %axis([min(xi_range) max(xi_range) min(varepsilon_CRB(4,:))
max(varepsilon_CRB(3,:))])

 hold off

 figure
 hold
on

%subplot(2,1,2);
 grid
on

plot(SNR_range,bias_p_LS,
'r*','LineWidth',.5,'MarkerEdgeColor','r','MarkerSize',5
)
 plot(SNR_range,bias_p_WLS_known_gamma,
'mo','LineWidth',.5,'MarkerEdgeColor','m','
MarkerSize',5)
plot(SNR_range,bias_p_ML_known_gamma,
'bs','LineWidth',.5,'MarkerEdgeColor','b','M
```

```
arkerSize',5)
 legend(
'LS: simulation','WLS: simulation','ML: simulation','CRB')
 h = findobj(gcf,'type','axes','tag','legend');
 Pos = get(h,
'position');
 Pos(3) = 1.9 * Pos(3);
% Double the length
 Pos(4) = 3 * Pos(4); % Double the length
 set(h,
'position',Pos) % Implement it
 title('Bias as a function of SNR ($M=0$, $N_R=1{,}000$)')
 ylabel(
'Bias (m)')%,'FontSize',10,'FontName','Times New Roman')
 xlabel(
'Transmitted SNR $\frac{E_{\mathrm{s}}}{\sigma^2_{\mathrm{n}}}$
(dB)')%,'FontSize',10,'FontName','Times New Roman')

%axis([min(xi_range) max(xi_range) min(varepsilon_CRB(4,:))
max(varepsilon_CRB(3,:))])

 hold
off

 set(0,
'defaulttextinterpreter','none')%laprint
end
  end
```

APPENDIX 2

MATLAB Codes: Probability of mis-timing as a function of SNR

```
% clear screen
clc;
% clear worksapce
clear;
% L: number of channel taps
L = 12;
% Lmt: number of purse noise samples
Lmt = 5;
% Td: channel delay spread
Td = 70;
% N: Simulation number
N = 20000;
% Nb: number of subbands
Nb = 6;
% m: Nakagami-m parameter
m = 1;
% snr: signal to noise ratio
snr = 0:2:30;
SNR = 10.^((snr/10));
% t: tap delays of the discrete time channel
t = linspace(0, Td, L);
% decay_factor: last tap energy / first tap energy
```

```
decay_factor = 100.0;
% factor_a: PDP fading factor
factor_a = log(decay_factor)/Td;
% hpw: exponential PDP
hpw = exp(-factor_a*t);
hwind = zeros(2*Lmt+1);
Pe = zeros(size(snr));
Pe_ub = zeros(L, length(snr));
% channel paths
h = zeros(Nb,L+2*Lmt);
% n0: noise samples
n0 = zeros(Nb,L+2*Lmt);
for ln = 1:N
% print the progress of simulation
if mod(ln, 1000) == 0
ln
end
% lb: index of subband
for lb = 1:Nb
% thta: channel tap phases
thta = 2*pi*rand(1,L);
% h: Nakagami-m channel taps
A = m;
B = hpw/m;
dlt = gamrnd(A, B, 1, L);
h(lb,:) = [zeros(1,Lmt), sqrt(dlt).*exp(sqrt(-1)*thta), zeros(1,Lmt)];
end
% noise with unity variance
n0 = sqrt(1/2)*randn(size(h))+sqrt(-1/2)*randn(size(h));
% lsnr: index of snr
for lsnr = 1:length(snr)
% add noise to channel taps
h1 = h*sqrt(SNR(lsnr)) + n0;
h1 = h1.*conj(h1);
% noncoherent combining of subbands
h2 = sum(h1, 1);
% calculate energy for L samples
for lw = 1:length(h1)-L+1
hwind(lw) = sum(h2(lw:lw+L-1));
end
% union bound of the mistiming probability
for lw = 1:Lmt
if (hwind(lw)>hwind(Lmt+1))
Pe_ub(lw, lsnr) = Pe_ub(lw, lsnr) + 1;
end
if (hwind(lw+Lmt+1)>hwind(Lmt+1))
Pe_ub(lw, lsnr) = Pe_ub(lw, lsnr) + 1;
end
end
% I: estimated TOA
[C,I] = max(hwind);
% Pe: number of timing errors
if (I~=Lmt+1)
Pe(lsnr) = Pe(lsnr) + 1;
end
end
end
% output result
```

```
figure;
semilogy(snr, Pe/N);
hold on;
```

APPENDIX 3

MATLAB Codes: Shadowing Variance

```
%Shadowing variance
sigma1=[4,6,8];
%The variance of K is the sum of shadowing variance and penetration loss
variance
sigma0=sqrt(12.4^2+sigma1.^2);
%the range of K pdfs
x=-3*sigma0:0.1:3*sigma0;
%Initialize K pdf array for NLOS and LOS
kdb_nlos=zeros(length(sigma1),length(x));
kdb_los=kdb_nlos;
%Mean of K of LOS
u1=12;
%Mean of K of NLOS
u0=u1-16.2;
%Compute pdfs of K
for index=1:length(sigma1)
kdb_nlos(index,:)=1/sqrt(2*pi)/sigma0(index)*exp(-(x-
u0).^2/sigma0(index)^2);
kdb_los(index,:)=1/sqrt(2*pi)/sigma1(index)*exp(-(x-
u1).^2/sigma1(index)^2);
end
figure
plot(x,kdb_nlos(1,:),'b--',x,kdb_nlos(2,:),'g-',x,kdb_nlos(3,:),'r-
      .',x,kdb_los(1,:),'b--',x,kdb_los(2,:),'g-',x,kdb_los(3,:),'r-
      ','linewidth',2)
grid on

xlabel('K(dB)','fontsize',12)
legend(['\sigma_[18]=',num2str(sigma1(1)),'dB'],['\sigma_[18]=',num2str(sig
ma1(2)),'dB'],['\sigma_[18]=',num2str(sigma1(3)),'dB']);
%Compute the threshold
kth=((sigma0.^2*u1-sigma1.^2*u0)-...
sqrt((sigma0.^2*u1-sigma1.^2*u0).^2-(sigma0.^2-sigma1.^2).*(sigma0.^2*u1^2-
sigma1.^2*u0^2-sigma1.^2.*sigma0.^2.*log(sigma0./sigma1)))./(sigma0.^2-
sigma1.^2)
%Compute the probability of detection
PD=1-(0.5-0.5*erf((kth-u0)./sigma0/sqrt(2)))
%Compute the probability of false alarm
PF=1-(0.5-0.5*erf((kth-u1)./sigma1/sqrt(2)))
sh}=',num2str(sigma1(1)),'dB'],['\sigma_[18]=',num2str(sigma1(2)),'dB'],['\
sigma_[18]=',num2str(sigma1(3)),'dB']);
%Compute the threshold
kth=((sigma0.^2*u1-sigma1.^2*u0)-...
sqrt((sigma0.^2*u1-sigma1.^2*u0).^2-(sigma0.^2-sigma
```

APPENDIX 4

MATLAB Codes: - Root mean square error (RMSE) of position estimate as a function of the transmitted SNR

```
% RMSE of the position estimate as a function of the transmitted SNR
clc
clear all
c = 3 * 10^8;
beta_bar = 2 * pi * (1/sqrt(3)) * 5 * 10^6;
r = 2000; %4000/sqrt(3);
p = (1/2) * r * cos(pi/6)* [cos(pi/6);sin(pi/6)];
B = 7;
M = 0; % base stations receiving NLOS
a_range = [4.6 4.0 3.6];
b_range = [0.0075 0.0065 0.0050];
c_range = [12.6 17.1 20.0];
scenario_range = [1:length(a_range)];
p_true = p;
h_b = 45; % (80+10)/2c
f = 1.9 * 10^9;
d_0 = 100;
kappa = c^2 / (16 * pi^2 * f^2 * d_0^2);
P = r * [0,3/2,0,-3/2,-3/2,0,3/2;0,sqrt(3)/2,sqrt(3),sqrt(3)/2,-sqrt(3)/2,-
sqrt(3),-sqrt(3)/2].';
P_diff = P - repmat(p',B,1);
phi = atan2(P_diff(:,2),P_diff(:,1));
Phi = [cos(phi).';sin(phi).'];
Phi_tilde = Phi(:,1:M);
Phi_bar = Phi(:,M+1:B);
n_scenario = 0;
N_R = 10000;
SNR_range = [50:10:230]; %dB
n_SNR = 0;
for SNR_dB = SNR_range;
n_SNR = n_SNR + 1;
SNR = 10^(SNR_dB/10);
for scenario = 1 %scenario_range
n_scenario = n_scenario + 1;
gamma_gen = a_range(scenario) - b_range(scenario)*h_b +
c_range(scenario)/h_b;
gamma_true = ones(B,1)*gamma_gen;
bar_gamma = gamma_true(M+1:B,1);
for b = 1 : B
x_tilde(b) = P(b,1) - p_true(1);
y_tilde(b) = P(b,2) - p_true(2);
if b <= M
tau_true(b) = (1/c) * (sqrt(x_tilde(b)^2 + y_tilde(b)^2) + l_true(b));
else
tau_true(b) = (1/c) * (sqrt(x_tilde(b)^2 + y_tilde(b)^2));
end
d_true(b) = c * tau_true(b);
alpha_true(b) = sqrt( kappa * ( d_0/d_true(b) )^(gamma_true(b)) );
frac(b) = 1 + (gamma_true(b)^2)/(8 * pi^2 * beta_bar^2 * tau_true(b)^2);
sigma2_true(b) = 1 / ( 8 * pi^2 * SNR * alpha_true(b)^2 * beta_bar^2 *
frac(b));
end % b
bar_sigma2 = sigma2_true(M+1:B)';
for n_R = 1 : N_R
```

```
for b = 1 : B
u_1(b) = randn;
hat_tau_gen(b) = tau_true(b) + sqrt(sigma2_true(b)) * u_1(b);
end
hat_bar_tau = hat_tau_gen(M+1:B)';
p_in = p_true + randn(1,1);
bar_eta_in = [p_in;gamma_true(M+1,1)] + randn(3,1);
hat_p_LS = fminsearch('LS_quick_search',p_in,[],hat_bar_tau,P,M,B,c);
hat_p_WLS_known_gamma =
fminsearch('WLS_known_gamma_original_search',p_in,[],hat_bar_tau,bar_gamma,
beta_bar,d_0,SNR,P,M,B,c,kappa);
hat_p_ML_known_gamma =
fminsearch('ML_known_gamma_original_search',p_in,[],hat_bar_tau,bar_gamma,b
eta_bar,d_0,SNR,P,M,B,c,kappa);
SE_p_LS(n_SNR,n_R) = sum((hat_p_LS - p_true).^2);
SE_p_WLS_known_gamma(n_SNR,n_R) = sum((hat_p_WLS_known_gamma - p_true).^2);
SE_p_ML_known_gamma(n_SNR,n_R) = sum((hat_p_ML_known_gamma - p_true).^2);
error_p_LS(:,n_R) = hat_p_LS - p_true;
error_p_WLS_known_gamma(:,n_R) = hat_p_WLS_known_gamma - p_true;
error_p_ML_known_gamma(:,n_R) = hat_p_ML_known_gamma - p_true;
end
RMSE_p_LS(n_SNR) = sqrt(mean(SE_p_LS(n_SNR,:)))
RMSE_p_WLS_known_gamma(n_SNR) = sqrt(mean(SE_p_WLS_known_gamma(n_SNR,:)))
B_LS_theory = c^2 * inv(Phi_bar * Phi_bar') * Phi_bar * diag(
sigma2_true(M+1:B) ) * Phi_bar' * inv(Phi_bar * Phi_bar');
RMSE_p_LS_theory(n_SNR) = sqrt( trace( B_LS_theory ) );
RMSE_p_ML_known_gamma(n_SNR) = sqrt(mean(SE_p_ML_known_gamma(n_SNR,:)))
B_pp_given_gamma = c^2 * (1 / ( 8 * pi^2 * beta_bar^2 * SNR)) *
inv(Phi_bar* diag(alpha_true(M+1:B))^2 * (eye(B-M) + ...
(1/(16 * pi^2 * beta_bar^2)) * diag(gamma_true(M+1:B))^2 * inv(
diag(tau_true(M+1:B))^2 ) ) * Phi_bar');
bias_p_LS(n_SNR) = mean(sqrt( error_p_LS(1,:).^2 + error_p_LS(2,:).^2 ));
bias_p_WLS_known_gamma(n_SNR) = mean(sqrt(error_p_WLS_known_gamma(1,:).^2 +
error_p_WLS_known_gamma(2,:).^2 ));
bias_p_ML_known_gamma(n_SNR) = mean(sqrt( error_p_ML_known_gamma(1,:).^2 +
error_p_ML_known_gamma(2,:).^2 ));
CRB_p_given_gamma(n_SNR) = sqrt(trace(B_pp_given_gamma));
end
end
figure
hold on
%subplot(2,1,1);
grid on
plot(SNR_range,RMSE_p_LS,'r*','LineWidth',.5,'MarkerEdgeColor','r','MarkerS
ize',5)
plot(SNR_range,RMSE_p_LS_theory,':r','LineWidth',.5,'MarkerEdgeColor','r','
MarkerSize',5)
plot(SNR_range,RMSE_p_WLS_known_gamma,'mo','LineWidth',.5,'MarkerEdgeColor'
,'m','MarkerSize',5)
plot(SNR_range,RMSE_p_ML_known_gamma,'bs','LineWidth',.5,'MarkerEdgeColor',
'b','MarkerSize',5)
plot(SNR_range,CRB_p_given_gamma,'-
k','LineWidth',.5,'MarkerEdgeColor','k','MarkerSize',5)
legend('LS: simulation','LS: analysis','WLS: simulation','ML:
simulation','CRB')
h = findobj(gcf,'type','axes','tag','legend');
Pos = get(h,'position');
Pos(3) = 1.9 * Pos(3); % Double the length
```

```
Pos(4) = 3 * Pos(4); % Double the length
set(h,'position',Pos) % Implement it
title('RMSE as a function of SNR ($M=0$, $N_R=1{,}000$)')
ylabel('Root Mean Square Error (m)')%,'FontSize',10,'FontName','Times New
Roman')
xlabel('Transmitted SNR $\frac{E_{\mathrm{s}}}{\sigma^2_{\mathrm{n}}}$
(dB)')%,'FontSize',10,'FontName','Times New Roman')
%axis([min(xi_range) max(xi_range) min(varepsilon_CRB(4,:))
max(varepsilon_CRB(3,:))])
hold off
figure
hold on
%subplot(2,1,2);
grid on
plot(SNR_range,bias_p_LS,'r*','LineWidth',.5,'MarkerEdgeColor','r','MarkerS
ize',5)
plot(SNR_range,bias_p_WLS_known_gamma,'mo','LineWidth',.5,'MarkerEdgeColor'
      ,'m','MarkerSize',5)
plot(SNR_range,bias_p_ML_known_gamma,'bs','LineWidth',.5,'MarkerEdgeColor',
'b','MarkerSize',5)
legend('LS: simulation','WLS: simulation','ML: simulation','CRB')
h = findobj(gcf,'type','axes','tag','legend');
Pos = get(h,'position');
Pos(3) = 1.9 * Pos(3); % Double the length
Pos(4) = 3 * Pos(4); % Double the length
set(h,'position',Pos) % Implement it
title('Bias as a function of SNR ($M=0$, $N_R=1{,}000$)')
ylabel('Bias (m)')%,'FontSize',10,'FontName','Times New Roman')
xlabel('Transmitted SNR $\frac{E_{\mathrm{s}}}{\sigma^2_{\mathrm{n}}}$
(dB)')%,'FontSize',10,'FontName','Times New Roman')
%axis([min(xi_range) max(xi_range) min(varepsilon_CRB(4,:))
max(varepsilon_CRB(3,:))])
hold off
set(0,'defaulttextinterpreter','none')%laprint
```

APPENDIX 5

MATLAB Codes: - Weighted Least Square estimator of Gaussian measurement error

```
% main
rng = [0 4.2500 6.9031 6.8031 0 0;
4.2500 0 0 0 5.1052 5.5052 ];
Anchors = [0,0; 0,10; 10,10; 10,0];
save testdata rng Anchors
[xest, error] = lsqnonlin(@squareerror, zeros(4,1));
% squareerror
function [ s ] = squareerror( x );
% determines the square error of the positions of x
N = length(x)/2;
load testdata
s = 0;
k=0;
Na = size(Anchors,1);
```